
University of Alberta

**Transverse, Vertical, and Antero-posterior changes between
Tooth-borne versus Dresden Bone-borne Rapid Maxillary
Expansion: A Randomized Controlled Clinical Trial**

by

Connie P. Ling

A thesis submitted in partial fulfillment of the requirements for the degree of

Master of Science

Medical Sciences - Orthodontics

University of Alberta

© Connie P. Ling, 2016

ABSTRACT

Objectives:

- 1) To identify accurate and easily repeatable (intra-examiner reliability) 3-D landmarks in the cranial base, maxilla, and mandible which can be used to quantify treatment changes after rapid maxillary expansion (RME).
- 2) To compare the transverse, vertical and antero-posterior, skeletal and dental post-treatment changes for the Dresden Bone-borne expander, 4-band Tooth-borne expander, and an untreated control group.

Methods:

Fifty adolescents with maxillary transverse constriction were randomly assigned into one of three groups according to type of expander: 2-point Dresden-type Bone-borne RME (B-RME; n = 17, mean age = 14.1 years), 4-band Tooth-borne RME (T-RME; n = 17, mean age = 13.7 years), or the untreated control group (n = 16, mean age = 13.3 years). The Dresden B-RME had a unique set-up where one side was anchored by a temporary anchorage device (TAD-side), and the other side was anchored to a shortened implant (implant-side). Cone-beam computed tomography (CBCT) scans were taken at 0.3-mm voxel size before treatment (T1), and 6 months later (T2). The CBCT data were coded, and then loaded into 3-D visualization software (AVIZO 8.1 software) by a blinded examiner for measurement. The transverse, vertical and sagittal changes of the maxilla was evaluated. Dental changes at the level of the pulp horn, buccal alveolar bone and root apex were evaluated on upper molars, upper premolars, upper canines, and lower molars. Repeated measures Multivariate analysis of variance (rm-MANOVA) and Bonferroni post-hoc tests were performed to identify significant differences between groups at each landmark and time-point.

Results:

Transverse

- a) T-RME group showed symmetrical maxillary premolar and molar expansion.
- b) The B-RME appliance configuration showed asymmetrical maxillary molar expansion.

- c) The TAD-anchor side of B-RME, showed greater molar crown displacement (mean 1.84 mm) than the Implant-anchor side, with statistical significance of $p < .015$.

Antero-posterior

- d) T-RME group showed anterior displacement of molar apex and premolar crown (mean < 1.5 mm), compared to other groups, with statistical significance ($p < .05$).
- e) No significant antero-posterior changes were found for B-RME group.

Vertical

- f) T-RME showed some dental vertical extrusion of premolar and molar crowns (< 1.8 mm ; $p < .05$), relative to control group.
- g) No significant dental vertical changes were found for the B-RME group. Minimal skeletal superior displacement at infra-orbital foramen (IORB) was noted for B-RME group (mean < 1.3 mm ; $p < .05$), relative to control group.
- h) Vertical changes were minimal and non-significant between the B-RME and T-RME groups.

Posterior versus Anterior transverse discrepancy

- i) T-RME group showed greater expansion between upper molars than between upper canines (1.6 mm more per side), with statistical significance ($p < .002$). No statistical significant differences were found between inter-molar and inter-premolar expansion.
- j) In the B-RME group, both the TAD- and Implant-sides showed greater inter-molar expansion than inter-canine. This difference was 1.1 mm on the Implant-side, and 1.9 mm on the TAD-side, with statistical significance ($p < .001$).
- k) In the B-RME group, only the TAD-side showed greater inter-molar expansion than inter-premolar (1.3 mm; $p < .001$). This was not statistically significant on the Implant-side.

Dental to Skeletal Ratio

- l) The B-RME group showed a smaller ratio of dental to skeletal expansion compared to T-RME group. The dental to skeletal ratio of expansion in the T-RME group, was roughly 40:60, with 42% dental expansion, 27% alveolar, 31% sutural. The dental to

skeletal ratio of expansion in the B-RME group was approximately 20:80, with 17% dental expansion, 40% alveolar, and 43% sutural.

Conclusions:

The decision to use B-RME or T-RME in adolescents depends upon operator preferences and specific dental and skeletal considerations for the patient. B-RME may be preferred in patients with missing permanent posterior teeth, or periodontal/endodontically compromised dentition, or when a lower ratio of dental to skeletal expansion is desired. Based solely on this study's sample, T-RME may be more effective for patients with similar severity of transverse maxillary constriction at the molar level and premolar levels. Meanwhile, B-RME may be more effective for patients with greater constriction at the bilateral maxillary molar level than the premolar level. In addition, the Dresden B-RME appliance configuration produced asymmetrical molar expansion. Placement of the TAD-anchor on the side of more severe maxillary transverse constriction may be helpful in cases with more pronounced maxillary arch asymmetry.

PREFACE

This thesis is an original work by Connie P. Ling.

DEDICATION

This thesis is dedicated to my wonderfully supportive and caring family, husband, my in-laws, and dear friends who have placed their trust in me.

In particular,

To my dearest mom, dad, and sister, Wendy, Raymond, Bonnie -

I am who I am because of all your tremendous efforts, sacrifices, sense of humor, nurture, boundless and unconditional love. Thank you for your faith in me, constantly motivating me to do my best, and allowing me to leave your side while pursuing my dreams. I hope to be as great a parent and role model when the time comes.

To my beloved husband, Jeffrey Woo -

I am so grateful for your endless love, practical support, encouragement, wit and wisdom. You have been my vital source of motivation throughout my amazing decade-long dentistry and orthodontic training journey. You always manage to deliver at times of greatest need. Your own self-actualizing character resonates deeply in me. I thoroughly enjoyed all the moments we spent together, and I look forward to creating many more with you in the future.

ACKNOWLEDGEMENTS

First, I wish to thank my supervisor, Professor Dr. Manuel Lagravere, for his mentorship and for granting me the opportunity to work on such a fascinating and impactful orthodontic problem. I want to thank Professor Dr. Paul Major for the invaluable insights and critical thoughts he presented to me on this piece of research. I wish to thank Professor Jason Carey for his prompt feedback and agreeing to serve on the examination panel. As well as Professor Dr. William Wiltshire who flew in from the University of Manitoba to generously take part in my defense examination as the external examiner. I also wish to thank Professor Dr. Carlos Flores-Mir for offering me the valuable opportunities to write the book chapter on maxillary expansion, and to present the works at conferences as a resident.

I want to express my deepest gratitude to Jeffrey Woo, my husband, for his critical thoughts, technical contributions, and collaboration towards key components of my research as leveraged from his computer engineering research training. His knowledge and assistance in the mathematical and engineering aspects of this work was vitally important towards the reference plane methodology including the programming for the calculations used. Due to the 15,000+ landmarks used in this research (50 patients x 50+ landmarks x 2 time points x 3 repeats), much more of my time and energy would have been consumed if it was not for his technical assistance in programming. He always helped me as much as he could, both mentally and in person. He has been here throughout the toughest and best times during my amazing decade-long dental and orthodontic training pathway.

I will never forget the invaluable inspiration and teachings from my first two orthodontic mentors: Dr. Clement Chan and Dr. Yanqi Yang, which led me into the profession of orthodontics. I am also indebted to numerous professors who have strongly encouraged me to pursue the Masters degree and orthodontic training pathway. I particularly wish to thank Professor Dr. Esmonde Corbet, Professor Dr. Coleman McGrath, and Professor May Wong for their support and faith.

My appreciation extends to all my fellow orthodontic colleagues & friends throughout this journey, including, but not limited to Drs: Humam Saltaji, Long Tieu, Jose-Roberto Pereira, Mona Afrand, Mostafa Altalibi, Neel Kaipatur, Parvaneh Badri, Ryan Edwards, Saeed Ghorashi, Zahra Najirad. I also want to mention my good friend and fellow orthodontist, Dr. Engee Ling, studying at the University College London Eastman Dental Institute. She does not

hesitate to share her knowledge and I often learn much through these interactive intellectual exchanges.

I deeply appreciated all the support, motivation and companionship from my dear friends spread across multiple cities around the world during this intense period of training. I particularly want to mention: Jean Hui, Frank Hui, Chimene Lo, Henry Yu, Eileen Ting, Mandy Poon, from Edmonton.

Last but not least, I would like to thank all the faculty staff, clinical instructors, and support staff members at the University of Alberta Edmonton Clinic Health Academy, and Kaye Edmonton Clinic, for their professional instruction, exceptional clinical guidance, and companionship on a daily basis.

Table of Contents

ABSTRACT	ii
List of Tables.....	xiii
List of Figures	xv
Chapter 1	1
1. Introduction	2
1.1 Problem Statement.....	2
1.2 Research Objectives.....	4
1.3 Research Questions.....	5
1.4 Null Hypotheses.....	5
1.5 Contributions & Outline	6
1.6 References.....	7
Chapter 2	10
2. Literature Review	11
2.1 Implications of Maxillary Transverse Constriction	11
2.2 Dental and Skeletal Expansion with T-RME	12
2.3 New Developments with Bone-borne RME.....	13
2.4 2-D Measurement Techniques.....	14
2.5 3-D Measurement Techniques.....	15
2.6 Summary	18
2.7 References.....	19
Chapter 3	26
3. Reliability and Accuracy of three-dimensional reference planes and landmarks related to maxillary expansion	27
3.1 Introduction	27

3.2	Landmark Selection	27
3.2.1	Selection Criteria.....	27
3.2.2	Mid-Sagittal Plane.....	28
3.2.3	Palatal Plane.....	29
3.2.4	Frontal Plane.....	30
3.2.5	Treatment Landmarks	30
3.3	Purpose of study	31
3.4	Materials & Methods.....	31
3.5	Plane construction.....	41
3.5.1	Mid-Sagittal plane.....	42
3.5.2	Posterior Palatal plane	43
3.5.3	Frontal plane.....	44
3.6	Finding orthogonal distances from landmark of interest to the reference plane	45
3.7	Statistical analysis.....	45
3.7.1	Accuracy for 3-D landmarks.....	45
3.7.2	Intra-examiner reliability for 3-D landmarks.....	46
3.7.3	Intra-examiner reliability for reference plane construction	46
3.8	Results.....	46
3.8.1	Intra-examiner reliability of 3-D landmarks	47
3.8.2	Accuracy of 3-D landmarks.....	47
3.8.3	Intra-examiner reliability of 3-D reference plane construction	51
3.9	Discussion	54
3.9.1	Overview	54
3.9.2	Reference landmarks used for Plane construction	54
3.9.3	Reference plane construction	59

3.9.4	Dental Landmarks for Treatment Evaluation.....	60
3.9.5	Limitations	61
3.9.6	Summary & Conclusion	62
3.10	References	64
Chapter 4	68
4.	Three-dimensional changes between tooth-borne versus bone-borne (Dresden-type) rapid maxillary expansion in adolescents: A randomized clinical trial.	69
4.1	Introduction	69
4.2	Materials & Methods.....	70
4.2.1	Subjects	70
4.2.2	RME Design and Activation Protocol	71
4.3	Identification of CBCT Landmarks.....	73
4.3.1	Orthogonal distances between landmarks to planes	74
4.4	Results.....	75
4.4.1	Measurement error.....	75
4.4.2	Statistical analysis	76
4.4.3	Treatment Changes (T2-T1)	79
4.4.4	Between-Group Comparisons (T2-T1)	80
4.4.5	Within-Group Comparisons (T2-T1).....	81
4.5	Discussion	90
4.5.1	Limitations	94
4.6	Summary & Conclusions	94
4.7	Future recommendations:	95
4.8	References.....	97
Chapter 5	99

5. Summary of findings	100
5.1 Introduction	100
5.2 Summary	101
5.3 Limitations:.....	105
5.3.1 Reliability & Accuracy chapter:	105
5.3.2 Randomized Controlled Clinical trial chapter:.....	106
5.4 Remarks	106
5.5 References.....	108
Appendices	109

List of Tables

Table 3-1: 3-D Maxilla-mandibular skeletal landmark definitions	36
Table 3-2: 3-D Cranial base skeletal landmark definitions	37
Table 3-3: 3-D Dental Root (PULP, APEX, AVBN) landmark definitions	39
Table 3-4: Portney and Watkins' ICC recommendation	46
Table 3-5: Ease of Identification of the investigated 3-D landmarks	48
Table 3-6: Accuracy of Cranial Base Landmarks, based on ICC and Mean Identification Errors	49
Table 3-7: Accuracy of Maxillo-mandibular Landmarks, based on ICC and Mean Identification Errors.....	50
Table 3-8. Accuracy of Dental Landmarks, based on ICC and Mean Identification Errors.	50
Table 3-9: Mean errors (in mm) of orthogonal distances, from 3 repeated reference plane constructions for 20 landmarks.....	53
Table 4-1. Subject Demographics	73
Table 4-2. Subject Demographics within B-RME group.....	73
Table 4-3: Mean errors (in mm) from 3 repeated reference plane constructions for the skeletal and dental landmarks.	75
Table 4-4. Baseline (T1) orthogonal distances (in mm) for all groups, from variable landmark to respective planes (Transverse (T*), Vertical (V*), and Antero-posterior (AP*) dimensions). 78	
Table 4-5. Between-Group Comparisons: Transverse treatment changes (T2-T1), based on orthogonal distances from landmark to Mid-sagittal Plane for all three groups.	83
Table 4-6. Between-Group Comparisons: Vertical treatment changes (T2-T1), based on orthogonal distances from landmark to Palatal Plane for all three groups.	85
Table 4-7. Between-Group Comparisons: Antero-posterior treatment changes (T2-T1), based on orthogonal distances from landmark to Frontal Plane for all three groups.	86
Table 4-8. Within-Group comparisons: Left- to Right-side discrepancy in treatment changes (T2-T1), based on orthogonal distances to the mid-sagittal 3-D plane, for all three groups... 87	

Table 4-9. Within-Group B-RME comparisons: transverse discrepancy in treatment changes (T2-T1) between TAD- and Implant-side.	88
Table 4-10. Within-Group B-RME comparisons: vertical discrepancy in treatment changes (T2-T1) between TAD- and Implant-side.	88
Table 4-11. Within-Group comparisons: Posterior- vs. Anterior- transverse discrepancy in treatment changes (T2-T1), based on orthogonal distances to the mid-sagittal 3-D plane, for all three groups.	89
Table 4-12. Within-Group comparisons: Crown- vs. Root-transverse discrepancy in treatment changes (T2-T1), based on orthogonal distances to the mid-sagittal 3-D plane, for all three groups.	89
Table 4-13: : Within-Group comparisons: Upper- vs. Lower- transverse discrepancy in treatment changes (T2-T1), based on orthogonal distances to the mid-sagittal 3-D plane, for all three groups.	90

List of Figures

Figure 2.1: Illustrates how Euclidean distance measurement can overestimate actual changes (Image of maxillary first molar teeth adapted from Nelson et al ⁹²).	16
Figure 3.1: Dry Skull Specimen enclosed by Plexiglass mounted on CBCT machine	32
Figure 3.2: Double-layered Plexiglass box (Left), filled with water in the external layer (Right).....	32
Figure 3.3: Example of a Dry skull with Gutta Percha markers.....	33
Figure 3.4: Dry skull with Gutta Percha markers inside Plexiglass box (Left), CBCT scan (Right).....	33
Figure 3.5: Orientation of the 3 axes: X-axis (Red, Transverse), Y-axis (Green, Anterior-posterior), Z-axis (Dark Blue, Vertical).	35
Figure 3.6: 3-D Landmarks viewed from axial, coronal, and sagittal planes (Left to Right) using the 3-D visualization software (AVIZO).....	35
Figure 3.7: 3-D Mid-sagittal Reference Plane	42
Figure 3.8: 3-D Posterior Palatal Reference Plane	43
Figure 3.9: 3-D Frontal Reference Plane.....	44
Figure 3.10: Mid-sagittal planes with 0.2 mm imposed errors in X-axis of A) MDFM and Mid.SPIN (Left Picture), B) MDFM and Mid.NPF (Right picture).	51
Figure 3.11: Posterior Palatal planes with 0.2 mm imposed error in Z-axis of GPF.L&R and Mid.NPF	52
Figure 3.12: Frontal planes with 0.2 mm imposed error in Y-axis of IORB.L&R and Mid.NPF ..	52
Figure 4.1. Clinical Photo of the A) Tooth-borne (Left), and B) Bone-borne Expander (Right) 72	
Figure 4.2. Bone-borne RME (B-RME) with Mini-Hyrax jackscrew supported by TAD on one side (TAD-anchor side), and palatal implant (Implant-anchor side) on the other.	72
Figure 4.3: Orientation of the 3 axes:.....	74

Chapter 1

1. Introduction

1.1 Problem Statement

Posterior crossbite is one of the most easily recognized clinical signs that result from a transverse constricted maxilla ¹. This is a common condition, with a prevalence of approximately 7% to 23% in the population under 18 years old ²⁻⁷. This narrow maxillary width relative to the mandible, causes a mismatch between opposing posterior teeth ^{1,8,9}. This can bring a negative cosmetic and functional impact on patients, including, but not limited to excess buccal corridor spaces when smiling, crowded anterior teeth, and uneven dental attrition ^{1,10}.

Posterior crossbites can present in a unilateral or bilateral form ¹¹. When the transverse mismatch occurs on both sides of the dental arch, it is classified as a bilateral crossbite. When it is only one side of the dental arch, it is classified as unilateral crossbite. Posterior crossbites can originate from true (narrow maxilla) or relative (abnormally wide mandible) sources ¹². Relative maxillary constriction exists when the maxillary skeleton is normal in width, but the mandibular skeleton and/or teeth are too wide. True maxillary constriction exists when the maxillary skeleton and/or teeth are narrow in width on its own. This study is interested specifically in the true maxillary constriction cases where the primary treatment is through maxillary expansion.

In orthodontics, traditionally used methods to determine the skeleto-dental extent of maxillary transverse constriction included 2-dimensional (2-D) cephalometric radiographs (postero-anterior and lateral cephalograms), occlusal radiographs, and dental models ^{13,14}. These diagnostic methods provide only limited skeleto-dental information, and subject to varying degrees of projection errors and measurement errors.

Cone-beam Computed Tomography (CBCT) 3-dimensional (3-D) imaging offer significant improvements over older 2-D imaging techniques ¹⁵⁻¹⁹. It presented negligible magnification error with a 1:1 ratio in all three dimensions ²⁰ along with the ability to generate sub-millimeter voxel-sized high-resolution images; down to the range of 0.4 mm to 0.125 mm in the three axes ^{21,22}. Furthermore, 3-D imaging allows deep visualization of internal anatomic structures that were previously overlapped in 2-D imaging ²³.

This study utilized CBCT's advantages to evaluate the various skeleto-dental components of maxillary transverse constriction as a treatment evaluation method. Nonetheless, this brought new challenges since there are no specific guidelines about how to analyze this type of images, or about how to identify stable anatomical landmarks which could be used in quantifying skeletal and dental maxillary constriction, as well as maxillary posterior arch symmetry^{24,25}. Great difficulty has been reported in using 2-D headfilms (postero-anterior, submentovertex or lateral) to evaluate 3-D facial asymmetry^{18,26,27}. Many 2-D cephalometric measurements are distorted in the presence of facial asymmetry²⁸. Problems such as patient head positioning²⁹, anatomical overlap^{26,27,30}, and magnification errors^{19,31,32} often lead to interpretation errors and misdiagnoses^{17,18}.

In 2-D imaging, transverse changes are commonly measured between two treatment landmarks (eg. between left and right molars), or from a treatment landmark to a skeletal midline. On a postero-anterior headfilm, this skeletal midline can be defined by drawing a line between the Crista galli (CG), Anterior Nasal Spine (ANS) and Menton landmarks. However, this line cannot be easily reproduced in 3-D due to several reasons. Firstly, the Menton landmark cannot be easily identified as it is located on an almost flat bony surface in 3D. Secondly, a line now becomes a plane in 3-D. Hence, the line needs to somehow be extended to the posterior region. This document proposed a measurement method to circumvent these difficulties and a more in-depth discussion is provided in later sections.

Regarding correction of maxillary constriction, this study focused specifically on comparing the traditional Tooth-borne Rapid Maxillary Expander (T-RME), with the recently developed Dresden Bone-borne Rapid Maxillary Expander (B-RME)^{33,34}. Both of these uses a hyrax jackscrew, attached to either the teeth (for T-RME) or into the palatal bone (for B-RME), that is incrementally turned (a.k.a. activated) to expand the maxilla. Due to its dental attachment, T-RME has been reported to induce greater dental than skeletal expansion (70% dental vs. 30% skeletal)³⁵ that may cause buccal tipping of the maxillary posterior teeth. Consequently, B-RME was designed to hopefully reduce this dental side-effect^{36,37}. It attempts to achieve this by performing skeletal expansion that involves separating the left and right maxillary halves at the mid-palatal suture (non-surgically for young adolescents, surgically for mature adults)³⁸.

To date, only two B-RME controlled clinical trials have been published, and they showed different results. Whereas Lin et al³³ found almost two-fold greater skeletal effects

using B-RME (57% - 77%) compared to T-RME (25% - 43%), Lagravère et al ³⁴ reported limited differences between the T-RME and B-RME group. When interpreting these results, it should be noted there were appliance design differences. In hopes to gain greater insight into this discrepancy between the studies, the present study re-defined some of the previously reported landmarks and also introduced new landmarks. The goal of re-defining landmarks was to improve the precision and accuracy for measurements. New landmarks also allowed us to measure changes in regions that were not previously covered such as the Greater Palatine Foramen (GPF) region.

Lastly, the Dresden B-RME was chosen for use in an adolescent population in this study. This appliance had been used in two previous studies on ten mature adult patients who underwent surgically-assisted rapid maxillary expansion in the study by Tausche et al ³⁹ and Hansen et al ³⁷. The Dresden B-RME has a unique design feature where it is anchored by an osteointegrated implant on one side and a mini-implant-anchor (a.k.a. Temporary Anchorage Devices, or TAD) on the other. Due to the limited resources available for this study, other expansion treatments such as Tooth-Tissue-borne and Bone-Tooth-borne expanders will not be detailed in this document ⁴⁰.

1.2 Research Objectives

- 1) To identify accurate and easily repeatable (intra-examiner reliability) 3-D landmarks in the cranial base, maxilla, and mandible which can be used to quantify treatment changes after rapid maxillary expansion (RME).
- 2) To compare the transverse, vertical and antero-posterior, skeletal and dental post-treatment changes for Dresden B-RME, 4-band T-RME, and an untreated control group.

1.3 Research Questions

Acknowledging the issues presented, two main research questions were identified:

- 1) Which skeletal and dental landmarks are the most accurate and repeatable (intra-examiner reliability) in CBCT images, and can be used to assess transverse, vertical, and antero-posterior treatment changes after maxillary expansion?
- 2) When several dento-skeletal variables are considered simultaneously over time, does age, gender, or treatment group (B-RME/T-RME/No Treatment) affect the final maxillary outcome (transverse, vertical, antero-posterior) in a selected sample of patients with maxillary transverse constriction?
 - i) Are there are significant differences in the amount of maxillary transverse expansion on the TAD-anchor side, and shortened-implant-anchor side of the Dresden B-RME group?

1.4 Null Hypotheses

Ho1: There is no difference in maxillary skeletal or dental treatment effects between T-RME and B-RME appliances.

Ho2: Treatment with T-RME appliance produces no additional maxillary skeletal or dental effects in comparison to normal growth changes among maxillary constricted untreated controls.

Ho3: Treatment with B-RME appliance produces no additional maxillary skeletal or dental effects in comparison to normal growth changes among maxillary constricted untreated controls.

Ho4: Treatment with T-RME or B-RME expansion appliances produces no difference in maxillary changes between the left and right sides.

Ho5: Treatment with B-RME appliance produces no difference in maxillary changes between the left and right sides, in comparison to normal growth changes among untreated controls.

Ho6: Treatment with T-RME appliance produces no difference in maxillary changes between the left and right sides, in comparison to normal growth changes among untreated controls.

Ho7: B-RME Treatment with the TAD-anchor side or Implant-anchor side produces no difference in maxillary changes between the left and right sides.

1.5 Contributions & Outline

A literature review was conducted on the skeletal and dental effects of expansion using conventional T-RME and the new development of B-RME appliances in Chapter 2 of this document. A review of existing 2-D and 3-D measurement techniques is also presented.

In Chapter 3 of this document, existing landmarks were re-defined, and newly defined 3-D anatomical landmarks (reference and treatment landmarks) were chosen to provide improved accuracy and reliability in all axes. Utilizing this landmark pool, this study also proposed a method for mathematically constructing 3-D reference planes for transverse, vertical, and antero-posterior measurements; its reliability is also shown.

Applying the newly defined reference planes, maxillary skeletal and dental changes were measured. A comparison is drawn between the Dresden B-RME and the 4-band T-RME at 6 months through CBCT images. Both treatment groups were compared with a group of untreated subjects as a control to account for natural growth changes. In particular, the three-dimensional skeletal and dental changes, symmetrical implications and skeletal-to-dental ratios were analyzed extensively. This is presented in Chapter 4 of this document.

Lastly, discussions on the clinical significance and implications of this research are summarized in Chapter 5 of this document.

1.6 References

1. McNamara JA. Maxillary transverse deficiency. *American Journal of Orthodontics and Dentofacial Orthopedics* 2000;117:567-570.
2. Kutin G, Hawes RR. Posterior cross-bites in the deciduous and mixed dentitions. *American journal of orthodontics* 1969;56:491-504.
3. Thilander B, Myrberg N. The prevalence of malocclusion in Swedish schoolchildren. *European Journal of Oral Sciences* 1973;81:12-20.
4. Heikinheimo K, Salmi K, Myllärniemi S. Long term evaluation of orthodontic diagnoses made at the ages of 7 and 10 years. *The European Journal of Orthodontics* 1987;9:151-159.
5. Thilander B, Pena L, Infante C, Parada SS, de Mayorga C. Prevalence of malocclusion and orthodontic treatment need in children and adolescents in Bogota, Colombia. An epidemiological study related to different stages of dental development. *The European Journal of Orthodontics* 2001;23:153-168.
6. Keski-Nisula K, Lehto R, Lusa V, Keski-Nisula L, Varrela J. Occurrence of malocclusion and need of orthodontic treatment in early mixed dentition. *American Journal of Orthodontics and Dentofacial Orthopedics* 2003;124:631-638.
7. da Silva Filho OG, Santamaria Jr M, Filho LC. Epidemiology of posterior crossbite in the primary dentition. *Journal of Clinical Pediatric Dentistry* 2007;32:73-78.
8. Bishara SE, Staley RN. Maxillary expansion: clinical implications. *American Journal of Orthodontics and Dentofacial Orthopedics* 1987;91:3-14.
9. Lagravère MO, Heo G, Major PW, Flores-Mir C. Meta-analysis of immediate changes with rapid maxillary expansion treatment. *The Journal of the American Dental Association* 2006;137:44-53.
10. Bell RA. A review of maxillary expansion in relation to rate of expansion and patient's age. *American journal of orthodontics* 1982;81:32-37.
11. Kennedy DB, Osepchok M. Unilateral posterior crossbite with mandibular shift: a review. *Journal-Canadian Dental Association* 2005;71:569.
12. Haas AJ. Long-term posttreatment evaluation of rapid palatal expansion. *Angle Orthod* 1980;50:189-217.
13. Lagravere MO, Major PW, Flores-Mir C. Long-term dental arch changes after rapid maxillary expansion treatment: a systematic review. *The Angle orthodontist* 2005;75:155-161.
14. Lagravere MO, Major PW, Flores-Mir C. Long-term skeletal changes with rapid maxillary expansion: a systematic review. *The Angle orthodontist* 2005;75:1046-1052.
15. Sievers MM, Larson BE, Gaillard PR, Wey A. Asymmetry assessment using cone beam CT: A Class I and Class II patient comparison. *The Angle Orthodontist* 2011;82:410-417.
16. Sanders DA, Rigali PH, Neace WP, Uribe F, Nanda R. Skeletal and dental asymmetries in Class II subdivision malocclusions using cone-beam computed tomography. *American Journal of Orthodontics and Dentofacial Orthopedics* 2010;138:542. e541-542. e520.

17. Katsumata A, Fujishita M, Maeda M, Ariji Y, Ariji E, Langlais RP. 3D-CT evaluation of facial asymmetry. *Oral Surgery, Oral Medicine, Oral Pathology, Oral Radiology, and Endodontology* 2005;99:212-220.
18. Baek S-H, Cho I-S, Chang Y-I, Kim M-J. Skeletodental factors affecting chin point deviation in female patients with class III malocclusion and facial asymmetry: a three-dimensional analysis using computed tomography. *Oral Surgery, Oral Medicine, Oral Pathology, Oral Radiology, and Endodontology* 2007;104:628-639.
19. Jacobson A, RL J. *Radiographic Cephalometry: From Basics to 3-D Imaging*, (Book/CD-ROM set), Chapter 23. 2007.
20. Lagravère MO, Carey J, Toogood RW, Major PW. Three-dimensional accuracy of measurements made with software on cone-beam computed tomography images. *American Journal of Orthodontics and Dentofacial Orthopedics* 2008;134:112-116.
21. Scarfe WC, Farman AG, Sukovic P. Clinical applications of cone-beam computed tomography in dental practice. *Journal-Canadian Dental Association* 2006;72:75.
22. Yajima A, Otonari-Yamamoto M, Sano T, Hayakawa Y, Otonari T, Tanabe K et al. Cone-beam CT (CB Throne) applied to dentomaxillofacial region. *The Bulletin of Tokyo Dental College* 2006;47:133-141.
23. Mah JK, Huang JC, Choo H. Practical applications of cone-beam computed tomography in orthodontics. *The Journal of the American Dental Association* 2010;141:75-135.
24. Lagravère MO, Gordon JM, Guedes IH, Flores-Mir C, Carey JP, Heo G et al. Reliability of traditional cephalometric landmarks as seen in three-dimensional analysis in maxillary expansion treatments. *The Angle orthodontist* 2009;79:1047-1056.
25. de Moraes ME, Hollender LG, Chen CS, Moraes LC, Balducci I. Evaluating craniofacial asymmetry with digital cephalometric images and cone-beam computed tomography. *Am J Orthod Dentofacial Orthop* 2011;139:e523-531.
26. Lee K-M, Hwang H-S, Cho J-H. Comparison of transverse analysis between posteroanterior cephalogram and cone-beam computed tomography. *Angle Orthodontist* 2013;84:715-719.
27. Ghafari J, Cater PE, Shofer FS. Effect of film-object distance on posteroanterior cephalometric measurements: suggestions for standardized cephalometric methods. *American Journal of Orthodontics and Dentofacial Orthopedics* 1995;108:30-37.
28. Gateno J, Xia JJ, Teichgraber JF. Effect of facial asymmetry on 2-dimensional and 3-dimensional cephalometric measurements. *Journal of Oral and Maxillofacial Surgery* 2011;69:655-662.
29. Thiesen G, Gribel BF, Freitas MPM. Facial asymmetry: a current review. *Dental press journal of orthodontics* 2015;20:110-125.
30. Betts N, Vanarsdall R, Barber H, Higgins-Barber K, Fonseca R. Diagnosis and treatment of transverse maxillary deficiency. *The International journal of adult orthodontics and orthognathic surgery* 1994;10:75-96.
31. Chien P, Parks E, Eraso F, Hartsfield J, Roberts W, Ofner S. Comparison of reliability in anatomical landmark identification using two-dimensional digital cephalometrics and three-dimensional cone beam computed tomography in vivo. *Dentomaxillofacial Radiology* 2014.

32. Oz U, Orhan K, Abe N. Comparison of linear and angular measurements using two-dimensional conventional methods and three-dimensional cone beam CT images reconstructed from a volumetric rendering program in vivo. *Dentomaxillofac Radiol* 2011;40:492-500.
33. Lin L, Ahn H-W, Kim S-J, Moon S-C, Kim S-H, Nelson G. Tooth-borne vs bone-borne rapid maxillary expanders in late adolescence. *The Angle Orthodontist* 2014;85:253-262.
34. Lagravère MO, Carey J, Heo G, Toogood RW, Major PW. Transverse, vertical, and anteroposterior changes from bone-anchored maxillary expansion vs traditional rapid maxillary expansion: A randomized clinical trial. *American Journal of Orthodontics and Dentofacial Orthopedics* 2010;137:304.e301-304.e312.
35. Krebs A. Expansion of the midpalatal suture, studied by means of metallic implants. *Acta Odontologica Scandinavica* 1959;17:491-501.
36. Wehrbein H, Göllner P. Skeletal Anchorage in Orthodontics - Basics and Clinical Application. *Journal of Orofacial Orthopedics / Fortschritte der Kieferorthopädie* 2007;68:443-461.
37. Hansen L, Tausche E, Hietschold V, Hotan T, Lagravère M, Harzer W. Skeletally-anchored Rapid Maxillary Expansion using the Dresden Distractor. *Journal of Orofacial Orthopedics / Fortschritte der Kieferorthopädie* 2007;68:148-158.
38. Baydas B, Yavuz İ, Uslu H, Dagsuyu İM, Ceylan İ. Nonsurgical rapid maxillary expansion effects on craniofacial structures in young adult females: a bone scintigraphy study. *The Angle orthodontist* 2006;76:759-767.
39. Tausche E, Hansen L, Hietschold V, Lagravère MO, Harzer W. Three-dimensional evaluation of surgically assisted implant bone-borne rapid maxillary expansion: A pilot study. *American Journal of Orthodontics and Dentofacial Orthopedics* 2007;131:S92-S99.
40. Rakosi T, Graber T. Orthodontic and Dentofacial Orthopedic Treatment, Chapter 7 2009:155-176.

Chapter 2

2. Literature Review

2.1 Implications of Maxillary Transverse Constriction

To illustrate the impact of maxillary constriction with posterior crossbite on the general population, an in-depth review showed that the prevalence of approximately 7% to 23% of the population under 18 years old ²⁻⁷. This sizable patient population all suffer from varying degree of functional and cosmetic problems, including, but not limited to excess buccal corridor spaces when smiling, crowded anterior teeth, and uneven dental attrition ^{1,10}.

Posterior crossbites can present in a unilateral or bilateral form ¹¹. Bilateral posterior crossbites result from a transverse constricted maxilla on both the left and right sides. However, the degree of skeletal maxillary constriction on the left and right halves can either be unequal (asymmetric bilateral crossbite) or equal (symmetric bilateral crossbite), relative to the mid-sagittal plane ⁴¹. Correction of symmetrical bilateral crossbite involves bilateral expansion of the maxilla. However, asymmetrical bilateral crossbite, should ideally be corrected through greater expansion on the more severe (collapsed) constricted side, in order to achieve proper arch widths on both sides as a final outcome ⁴¹.

A common feature noted in cases of unilateral posterior crossbite is a functional shift of the mandible, due to the narrow width of the maxilla and inability of the jaws to obtain stable maximum intercuspation ¹¹. The prevalence of functional shift have been reported to range between 65% to 80% in the mixed dentition ^{2,42-45}. The chances of self-correction of crossbites with functional shift are as low as 0% - 7% during transition from primary to mixed dentition ^{11,44}, and full correction is increasingly difficult beyond the early mixed dentition years ⁴⁴. Treatment is recommended as early as possible in order to minimize the development of progressive skeletal asymmetry ^{10,38,46-49}, due to compensatory temporomandibular joint changes ^{43,50} and asymmetrical masticatory muscle activity ^{51,52}. Crossbite patients have also shown smaller bite forces than non-crossbite subjects ⁵².

Functional unilateral crossbites should be corrected by expanding the maxilla and eliminating occlusal interferences. True skeletal unilateral posterior crossbites, however, should ideally receive greater skeletal maxillary expansion on the more severe (collapsed) cross-bite side in order to avoid overexpansion of the normal side into a buccal crossbite which lengthens overall treatment time and is more difficult to correct ^{41,53,54}. Unfortunately,

asymmetric dental-tipping mechanics involving unilateral cross-elastics or quad-helix appliance with differential arm lengths, are unsatisfactory in the correction of maxillary constriction with a skeletal origin ⁴¹. Correction of skeletal maxillary constriction through dental expansion methods have been reported to produce greater relapse ^{8,10,55}.

2.2 Dental and Skeletal Expansion with T-RME

To better understand the justifications for developing B-RME and this study's specific interest on B-RME, it is prudent to review T-RME's limitations. Over the past century, correction of maxillary constriction in adolescents have been accomplished through variations of T-RME appliances. The most traditional type of T-RME involves a hyrax jackscrew secured by orthodontic bands cementation to bilateral maxillary first molars and premolars, a.k.a. 4-band T-RME ⁴⁰. When only bilateral maxillary first molars are banded, it can be called 2-band T-RME ⁵⁶. In later discussions (see section 5), the 2-band T-RME is compared to the Dresden B-RME, since it also has only two points of bone contact.

The intense forces (cumulatively up to 90 N ⁵⁷) from the jackscrew are applied to molar and premolar crowns, and passed through the roots into the alveolar bone. Forces in the initial 3 to 7 days are high enough to temporarily disable dental movements within the bone (due to hyalinization and undermining resorption on the pressure side) ^{58,59}. The teeth then acts as bone anchors in the two maxillary halves ⁵⁵. This time window is the only opportunity to induce skeletal expansion (up to 30%) of the maxillary jaw in skeletally immature adolescents ^{60,55}.

Skeletal expansion is believed to produce more stable expansion outcomes (less relapse) than dental expansion ⁸. Skeletal expansion can be classified into sutural expansion versus alveolar bending ^{33,61}. Alveolar bending occurs when the expansion forces caused by RME separate the two maxillary halves in a fan-shaped pattern, centered on the frontonasal suture in the frontal plane ^{33,62,63}.

When applied to skeletally mature adults, the separation of densely interdigitated mid-sagittal and circum-maxillary sutures is nearly impossible ^{8,64}. This results in negative consequences including, but not limited to: root resorption ^{65,66}, buccal alveolar bone loss

^{67,68}, excess buccal dental tipping and bite opening ⁶⁸, relapse of the crossbite ⁶⁹, limited suture separation ⁷⁰, and buccal alveolar bending ⁶¹.

Evidently, one of the primary factors which affects the skeletal to dental expansion ratio is skeletal maturity ^{8,71}. Based on the classic metallic implant study by Krebs et al in 1958 ³⁵, 47% skeletal expansion can be achieved in patients aged 8.5 to 12 years, and only about 30% skeletal expansion for ages 13 to 19.

These limitations motivated a variety of new maxillary expander designs in hopes of minimizing dental side effects and increasing the skeletal component of transverse correction. These efforts gradually evolved into a new class of B-RME expanders.

2.3 New Developments with Bone-borne RME

B-RME attempts to minimize dental structures disturbance and maximize skeletal expansion by directly inserting either shortened palatal implants or temporary anchorage devices (TADs) ^{36,37} into the two halves of the bony maxillary palate.

Prominence of B-RME also increased as patients with multiple missing maxillary teeth, poor periodontal or coronal status, that were not able to use T-RME treatment, can now undergo B-RME treatment instead ^{34,37}. Although it should still be noted that B-RME does have its inherent risk, including possibility of infection, and the need for local anesthesia during placement ^{34,39}.

This study's literature review found two B-RME controlled clinical trials with different results. Whereas Lin et al ³³ found almost two-fold greater skeletal effects using B-RME (57% - 77%) compared to T-RME (25% - 43%), Lagravère et al ³⁴ reported both T-RME and B-RME to show similar skeletal change (a difference of only 3% - 6% between the two groups). When interpreting these results, it should be noted there were appliance design differences.

The bone anchorage used by Lin et al consisted of four TADs and a split-acrylic resin plate resting on the palate. Lagravère's design consisted of two onplants on top of two TADs. Several in vitro studies have found differences in bone-anchor appliance design, especially in anchorage site and stress distribution, can generate varying patterns of dental and skeletal displacements ^{72,73}. Nonetheless, a deeper analysis into the internal dental, alveolar and

skeletal anatomical structures between both groups is needed to provide more conclusive answers.

2.4 2-D Measurement Techniques

The literature reviewed in this section was part of the landmark selection process (see section 4.2). It serves as a reference for the landmarks that was used for dental arch and skeletal measurements, as part of the research objective.

In the past, orthodontists have used 2-D occlusograms to evaluate maxilla and mandible arch width changes ^{64,74}. This technique requires examiner to manually trace dental crown outlines from plaster stone models onto acetate tracing paper, and mapping a constructed maxillary midline to the mandible. Only limited discussion will be provided for this technique. Reader should be referred to Ferro et al ⁷⁵ or Marcotte et al ⁷⁶ for a more detailed discussion. Essentially, this technique has traditionally been criticized to be time-consuming and not very precise ⁷⁷. It is limited to dental crown observations. Other studies reported inaccuracies of a few millimeters purely due to abrasion or distortion of plaster stone models ^{74,78,79}. However, attention should be drawn to the landmarks used for drawing the mid-sagittal line in this technique. One landmark is the distal aspect of the incisive papilla, and the other at the fovea centralis of the posterior palate ⁸⁰. Similar landmarks within the same region of the anterior and posterior palate were identified and evaluated in this study.

One such landmark is the Nasopalatine Foramen (NPF) a.k.a. Incisive Foramen. Anatomy textbooks usually describe the incisive canal as situated at the midline, posterior to the central incisor teeth ^{81,2}. The nasopalatine nerve and artery passes through this canal and into the incisive papilla. Its palatal opening is the NPF, which has been shown to be a relatively stable area ⁸⁰.

Grayson et al ⁸² presented multi-plane cephalometry by combining two 2-D x-ray radiographs (postero-anterior cephalogram and lateral cephalogram) to construct one of the earliest forms of 3-D representation of the skull for multi-dimensional assessment. However, this is not a true 3-D reconstruction and was subjected to inherent analysis bias ⁸³. Conceptual construction of a mid-sagittal line was attempted by combining midlines of both 2-D films,

although the “mid-sagittal plane” showed warping, particularly in patients with facial asymmetry ⁸².

The skeletal midline was drawn using Crista Galli (CG), mid-point between left and right lateral orbital rims (LOrb), Anterior Nasal Spine (ANS), and Menton landmarks ^{19,80,84}. Jugale (J) and Antegonion (AG) are used to measure skeletal maxilla-mandible width. Perpendicular distances from the midline to the J and AG landmarks are then used to measure the extent of asymmetry ^{19,30,85}. The ratio of the maxilla width (left J to right J) to mandibular width (left AG to right AG) is also used to measure the severity of the posterior crossbite.

Projection errors still existed on the respective films, and the 2-D landmarks identification still demonstrated challenges. The projection error on the postero-anterior cephalogram was reflected by magnification of distance between left and right Jugale by 2% compared to actual dimensions, and two-fold magnification (4%) between left and right Antegonion ²⁷.

In general, great difficulty has been reported in using these 2-D headfilms to evaluate 3-D skeletal and dental changes ^{18,26,27} due to problems of patient head positioning ²⁹, anatomical overlap ^{26,27,30}, and magnification errors ^{19,31,32}. Many 2-D cephalometric measurements are distorted in the presence of facial asymmetry ²⁸.

2.5 3-D Measurement Techniques

Cone-beam computed tomography (CBCT) has become the recommended imaging technique for 3-D expansion treatment changes, and symmetry assessment ¹⁵⁻¹⁸. As mentioned previously, traditional 2-D landmarks may not always be applicable in the 3-D domain ⁸⁶. For example, menton and condylion landmarks are located on a wide radius of the mandible, making it very difficult to locate precisely in 3-D. Transition to the use of 3-D landmarks demands extension of landmark definitions into the new dimension ⁸⁷. As these anatomical landmarks will form the basis of all orthodontic radiographic measurements, this 3-D extension demands greater understanding of the accuracy, stability and reliability of each individual reference landmark.

Regarding the equipment accuracy of CBCT, negligible amounts of projection error and a 1:1 ratio have been reported in all three dimensions ^{20,88}. CBCT also has the ability to

generate sub-millimeter voxel-sized high-resolution images; down to the range of 0.4 mm to 0.125 mm in the three axes ^{21,22}.

Since the Cartesian coordinate system used in each CBCT scan is determined at the time of acquisition ⁸⁹, changes in dimensions cannot be observed through by merely taking values of any one axis alone; instead, the formula for Euclidean distances is required in order to determine transverse, vertical, and sagittal measurements. However, in the past decade, several studies ^{15,83,89,90,91} have expressed the need to establish 3-D reference planes.

To illustrate limits to Euclidean distance measurements, Figure 2.1 shows how the measured distance can overestimate actual changes in the dimension of interest. Consider the scenario where the initial transverse distance between the left and right molars (represented AB) is of interest. Now, assume one of the molars moved vertically without transverse movement (the molar depicted on the right). Using the same dental landmarks, the new measured distance would be the greater AC instead. As such, this study investigated into acquiring a reference plane, similar to mid-sagittal lines constructed in 2-D, and then used orthogonal distances instead. By using orthogonal distances, the measured changes in Figure 2.1 will now be the difference between DB and EC, which matches closer to the actual transverse displacements. This argument can be extended to other dimensions. This method also provides the added benefits of symmetry analysis and helps overcome patient head positioning problems.

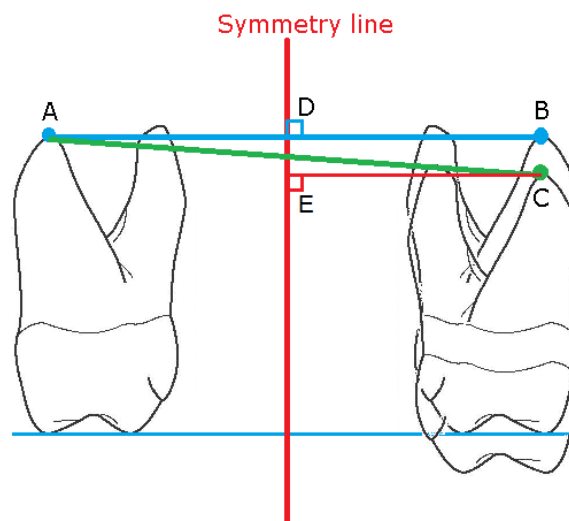


Figure 2.1: Illustrates how Euclidean distance measurement can overestimate actual changes (Image of maxillary first molar teeth adapted from Nelson et al ⁹²).

3-D Planes

Many studies had to manually orient the reference planes, which created another source of error ¹⁵. Reference landmarks can instead be used to construct the planes. In general, higher reproducibility is found when the landmarks used to determine the reference planes were spaced further apart ⁹¹. 2-D landmarks have been used to construct 3-D reference landmarks, including: Sella, Nasion, Orbitale, Porion, Anterior Nasal Spine, and Fronto-nasal suture ^{15,83,90,91,93,94}. However, the disadvantage of these landmarks is that they are influenced by growth and treatment changes, and reported to be considerably difficult to visualize in 3-D as “fuzzy landmarks”.

3-D Landmarks

Lagravere et al ²⁴ advocated use of the mid-point between left and right Foramen Spinosum (Mid.SPIN) and Mesial Dorsum Foramen Magnum (MDFM) as key reference cranial base landmarks. Along with the left and right External Auditory Meatus (EAM) landmarks, they advocated that this 4-point plane orientation technique would be an adequate way to standardize the head orientation of CBCT images ⁹⁵.

SPIN and MDFM landmarks showed excellent intra-examiner reliability and accuracy as indicated by < 1 mm mean variation, and Intra-class correlation coefficients (ICC) of >0.99 in all 3 dimensions ^{24,96,97}. Marmary et al also found that a perpendicular bisector drawn between the two foramina spinosum gave a fairly accurate mid-sagittal line ⁹⁸.

EAM also showed good intra-examiner reliability with ICC > 0.89 in all 3 dimensions. However, Lagravere et al pointed out the difficulty in pinpointing the exact location along the length of the EAM canal, and higher measurement errors were found for EAM in the x-axis, with mean errors of between 2 to 3 mm ²⁴. Landmarks with mean differences over 2 mm should be used with caution as variability above 1.5 mm is considered clinically significant for orthodontic diagnosis and treatment purposes ^{24,96}. This motivated a search for another landmark to aid in the construction of a mid-sagittal plane.

Several 3-D landmarks in the maxillary and mandibular treatment region were found to have < 1.4 mm variability in two other studies ^{24,96}, including: infra-orbital foramen, nasopalatine (incisive) foramen, mental foramen, pulp, apex, and alveolar bone landmarks of

the upper and lower first molar and first premolar teeth. These will serve as a benchmark for new 3-D landmarks.

2.6 Summary

This chapter provides a literature review on the impact of maxillary transverse constriction to better justify the research motivation. This extended into reviewing traditional and current expansion treatments. It revealed that although 3-D technology can provide greater equipment accuracy, the current measurement techniques were still inadequate. It has been stated repeatedly to be a challenging task due to a series of inherent difficulties derived from the extra dimension. Recognizing this, many of the findings from these literatures will be used as a foundation, and as a benchmark for the methods proposed in the remainder of this study.

2.7 References

1. McNamara JA. Maxillary transverse deficiency. *American Journal of Orthodontics and Dentofacial Orthopedics* 2000;117:567-570.
2. Kutin G, Hawes RR. Posterior cross-bites in the deciduous and mixed dentitions. *American journal of orthodontics* 1969;56:491-504.
3. Thilander B, Myrberg N. The prevalence of malocclusion in Swedish schoolchildren. *European Journal of Oral Sciences* 1973;81:12-20.
4. Heikinheimo K, Salmi K, Myllärniemi S. Long term evaluation of orthodontic diagnoses made at the ages of 7 and 10 years. *The European Journal of Orthodontics* 1987;9:151-159.
5. Thilander B, Pena L, Infante C, Parada SS, de Mayorga C. Prevalence of malocclusion and orthodontic treatment need in children and adolescents in Bogota, Colombia. An epidemiological study related to different stages of dental development. *The European Journal of Orthodontics* 2001;23:153-168.
6. Keski-Nisula K, Lehto R, Lusa V, Keski-Nisula L, Varrela J. Occurrence of malocclusion and need of orthodontic treatment in early mixed dentition. *American Journal of Orthodontics and Dentofacial Orthopedics* 2003;124:631-638.
7. da Silva Filho OG, Santamaria Jr M, Filho LC. Epidemiology of posterior crossbite in the primary dentition. *Journal of Clinical Pediatric Dentistry* 2007;32:73-78.
8. Bishara SE, Staley RN. Maxillary expansion: clinical implications. *American Journal of Orthodontics and Dentofacial Orthopedics* 1987;91:3-14.
10. Bell RA. A review of maxillary expansion in relation to rate of expansion and patient's age. *American journal of orthodontics* 1982;81:32-37.
11. Kennedy DB, Osepchook M. Unilateral posterior crossbite with mandibular shift: a review. *Journal-Canadian Dental Association* 2005;71:569.
15. Sievers MM, Larson BE, Gaillard PR, Wey A. Asymmetry assessment using cone beam CT: A Class I and Class II patient comparison. *The Angle Orthodontist* 2011;82:410-417.
16. Sanders DA, Rigali PH, Neace WP, Uribe F, Nanda R. Skeletal and dental asymmetries in Class II subdivision malocclusions using cone-beam computed tomography. *American Journal of Orthodontics and Dentofacial Orthopedics* 2010;138:542. e541-542. e520.
17. Katsumata A, Fujishita M, Maeda M, Ariji Y, Ariji E, Langlais RP. 3D-CT evaluation of facial asymmetry. *Oral Surgery, Oral Medicine, Oral Pathology, Oral Radiology, and Endodontology* 2005;99:212-220.
18. Baek S-H, Cho I-S, Chang Y-I, Kim M-J. Skeletodental factors affecting chin point deviation in female patients with class III malocclusion and facial asymmetry: a three-dimensional analysis using computed tomography. *Oral Surgery, Oral Medicine, Oral Pathology, Oral Radiology, and Endodontology* 2007;104:628-639.
19. Jacobson A, RL J. *Radiographic Cephalometry: From Basics to 3-D Imaging*, (Book/CD-ROM set), Chapter 23. 2007.
20. Lagravère MO, Carey J, Toogood RW, Major PW. Three-dimensional accuracy of measurements made with software on cone-beam computed tomography images. *American Journal of Orthodontics and Dentofacial Orthopedics* 2008;134:112-116.

21. Scarfe WC, Farman AG, Sukovic P. Clinical applications of cone-beam computed tomography in dental practice. *Journal-Canadian Dental Association* 2006;72:75.
22. Yajima A, Otonari-Yamamoto M, Sano T, Hayakawa Y, Otonari T, Tanabe K et al. Cone-beam CT (CB Throne) applied to dentomaxillofacial region. *The Bulletin of Tokyo Dental College* 2006;47:133-141.
24. Lagravère MO, Gordon JM, Guedes IH, Flores-Mir C, Carey JP, Heo G et al. Reliability of traditional cephalometric landmarks as seen in three-dimensional analysis in maxillary expansion treatments. *The Angle orthodontist* 2009;79:1047-1056.
26. Lee K-M, Hwang H-S, Cho J-H. Comparison of transverse analysis between posteroanterior cephalogram and cone-beam computed tomography. *Angle Orthodontist* 2013;84:715-719.
27. Ghafari J, Cater PE, Shofer FS. Effect of film-object distance on posteroanterior cephalometric measurements: suggestions for standardized cephalometric methods. *American Journal of Orthodontics and Dentofacial Orthopedics* 1995;108:30-37.
28. Gateno J, Xia JJ, Teichgraber JF. Effect of facial asymmetry on 2-dimensional and 3-dimensional cephalometric measurements. *Journal of Oral and Maxillofacial Surgery* 2011;69:655-662.
29. Thiesen G, Gribel BF, Freitas MPM. Facial asymmetry: a current review. *Dental press journal of orthodontics* 2015;20:110-125.
30. Betts N, Vanarsdall R, Barber H, Higgins-Barber K, Fonseca R. Diagnosis and treatment of transverse maxillary deficiency. *The International journal of adult orthodontics and orthognathic surgery* 1994;10:75-96.
31. Chien P, Parks E, Eraso F, Hartsfield J, Roberts W, Ofner S. Comparison of reliability in anatomical landmark identification using two-dimensional digital cephalometrics and three-dimensional cone beam computed tomography in vivo. *Dentomaxillofacial Radiology* 2014.
32. Oz U, Orhan K, Abe N. Comparison of linear and angular measurements using two-dimensional conventional methods and three-dimensional cone beam CT images reconstructed from a volumetric rendering program in vivo. *Dentomaxillofac Radiol* 2011;40:492-500.
33. Lin L, Ahn H-W, Kim S-J, Moon S-C, Kim S-H, Nelson G. Tooth-borne vs bone-borne rapid maxillary expanders in late adolescence. *The Angle Orthodontist* 2014;85:253-262.
34. Lagravère MO, Carey J, Heo G, Toogood RW, Major PW. Transverse, vertical, and anteroposterior changes from bone-anchored maxillary expansion vs traditional rapid maxillary expansion: A randomized clinical trial. *American Journal of Orthodontics and Dentofacial Orthopedics* 2010;137:304.e301-304.e312.
35. Krebs A. Expansion of the midpalatal suture, studied by means of metallic implants. *Acta Odontologica Scandinavica* 1959;17:491-501.
36. Wehrbein H, Göllner P. Skeletal Anchorage in Orthodontics - Basics and Clinical Application. *Journal of Orofacial Orthopedics / Fortschritte der Kieferorthopädie* 2007;68:443-461.
37. Hansen L, Tausche E, Hietschold V, Hotan T, Lagravère M, Harzer W. Skeletally-anchored Rapid Maxillary Expansion using the Dresden Distractor. *Journal of Orofacial Orthopedics / Fortschritte der Kieferorthopädie* 2007;68:148-158.

38. Baydas B, Yavuz İ, Uslu H, Dagsuyu İM, Ceylan İ. Nonsurgical rapid maxillary expansion effects on craniofacial structures in young adult females: a bone scintigraphy study. *The Angle orthodontist* 2006;76:759-767.
39. Tausche E, Hansen L, Hietschold V, Lagravère MO, Harzer W. Three-dimensional evaluation of surgically assisted implant bone-borne rapid maxillary expansion: A pilot study. *American Journal of Orthodontics and Dentofacial Orthopedics* 2007;131:S92-S99.
40. Rakosi T, Graber T. *Orthodontic and Dentofacial Orthopedic Treatment*, Chapter 7 2009:155-176.
41. Hassan AH, AlGhamdi AT, Al-Fraidi AA, Al-Hubail A, Hajrassy MK. Unilateral cross bite treated by corticotomy-assisted expansion: two case reports. *Head & face medicine* 2010;6:1.
42. Hesse KL, Årtun J, Joondeph DR, Kennedy DB. Changes in condylar position and occlusion associated with maxillary expansion for correction of functional unilateral posterior crossbite. *American Journal of Orthodontics and Dentofacial Orthopedics* 1997;111:410-418.
43. Harrison JE, Ashby D. *Orthodontic treatment for posterior crossbites*. The Cochrane Library 2001.
44. Thilander B, Wahlund S, Lennartsson B. The effect of early interceptive treatment in children with posterior cross-bite. *The European Journal of Orthodontics* 1984;6:25-34.
45. Schröder U, Schröder I. Early treatment of unilateral posterior crossbite in children with bilaterally contracted maxillae. *The European Journal of Orthodontics* 1984;6:65-69.
46. O'Byrn BL, Sadowsky C, Schneider B, BeGole EA. An evaluation of mandibular asymmetry in adults with unilateral posterior crossbite. *American Journal of Orthodontics and Dentofacial Orthopedics* 1995;107:394-400.
47. Pirttiniemi P, Kantomaa T, Lahtela P. Relationship between craniofacial and condyle path asymmetry in unilateral cross-bite patients. *The European Journal of Orthodontics* 1990;12:408-413.
48. De Felipe NLO, Da Silveira AC, Viana G, Kusnoto B, Smith B, Evans CA. Relationship between rapid maxillary expansion and nasal cavity size and airway resistance: short-and long-term effects. *American Journal of Orthodontics and Dentofacial Orthopedics* 2008;134:370-382.
49. Rodrigues Ado P, Monini Ada C, Gandini LG, Jr., Santos-Pinto A. Rapid palatal expansion: a comparison of two appliances. *Braz Oral Res* 2012;26:242-248.
50. Myers DR, Barenie JT, Bell RA, Williamson EH. Condylar position in children with functional posterior crossbites: before and after crossbite correction. *Pediatr Dent* 1980;2:190-194.
51. Piancino MG, Talpone F, Dalmaso P, Debernardi C, Lewin A, Bracco P. Reverse-sequencing chewing patterns before and after treatment of children with a unilateral posterior crossbite. *The European Journal of Orthodontics* 2006;28:480-484.
52. Iodice G, Danzi G, Cimino R, Paduano S, Michelotti A. Association between posterior crossbite, skeletal, and muscle asymmetry: a systematic review. *The European Journal of Orthodontics* 2016:cjw003.

53. Ileri Z, Basciftci FA. Asymmetric rapid maxillary expansion in true unilateral crossbite malocclusion: A prospective controlled clinical study. *The Angle Orthodontist* 2015;85:245-252.
54. Baka ZM, Akin M, Ucar FI, Ileri Z. Cone-beam computed tomography evaluation of dentoskeletal changes after asymmetric rapid maxillary expansion. *American Journal of Orthodontics and Dentofacial Orthopedics* 2015;147:61-71.
55. Proffit W FH, Sarver D.,. *Contemporary orthodontics*. Mosby; 2013.
56. Davidovitch M, Efstathiou S, Sarne O, Vardimon AD. Skeletal and dental response to rapid maxillary expansion with 2-versus 4-band appliances. *American Journal of Orthodontics and Dentofacial Orthopedics* 2005;127:483-492.
57. Isaacson RJ, Wood JL, Ingram AH. Forces produced by rapid maxillary expansion: I. Design of the force measuring system. *The Angle Orthodontist* 1964;34:256-260.
58. Zimring JF, Isaacson RJ. Forces Produced By Rapid Maxillary Expansion. 3. Forces Present During Retention. *Angle Orthod* 1965;35:178-186.
59. Chaconas SJ, Caputo AA. Observation of orthopedic force distribution produced by maxillary orthodontic appliances. *Am J Orthod* 1982;82:492-501.
60. Garib DG, Henriques JFC, Janson G, de Freitas MR, Fernandes AY. Periodontal effects of rapid maxillary expansion with tooth-tissue-borne and tooth-borne expanders: a computed tomography evaluation. *American journal of orthodontics and dentofacial orthopedics* 2006;129:749-758.
61. Weissheimer A, de Menezes LM, Mezomo M, Dias DM, de Lima EMS, Rizzato SMD. Immediate effects of rapid maxillary expansion with Haas-type and hyrax-type expanders: a randomized clinical trial. *American Journal of Orthodontics and Dentofacial Orthopedics* 2011;140:366-376.
62. Garrett BJ, Caruso JM, Rungcharassaeng K, Farrage JR, Kim JS, Taylor GD. Skeletal effects to the maxilla after rapid maxillary expansion assessed with cone-beam computed tomography. *American Journal of Orthodontics and Dentofacial Orthopedics* 2008;134:8.e1-8.e11.
63. Garib DG, Henriques JFC, Janson G, Freitas MR, Coelho RA. Rapid maxillary expansion-tooth tissue-borne versus tooth-borne expanders: a computed tomography evaluation of dentoskeletal effects. *The Angle orthodontist* 2005;75:548-557.
64. Bazargani F, Feldmann I, Bondemark L. Three-dimensional analysis of effects of rapid maxillary expansion on facial sutures and bones: a systematic review. *The Angle Orthodontist* 2013;83:1074-1082.
65. Langford S, Sims M. Root surface resorption, repair, and periodontal attachment following rapid maxillary expansion in man. *American journal of orthodontics* 1982;81:108-115.
66. Barber AF, Sims M. Rapid maxillary expansion and external root resorption in man: a scanning electron microscope study. *American journal of orthodontics* 1981;79:630-652.
67. Garib DG, Henriques JF, Janson G, de Freitas MR, Fernandes AY. Periodontal effects of rapid maxillary expansion with tooth-tissue-borne and tooth-borne expanders: a computed tomography evaluation. *Am J Orthod Dentofacial Orthop* 2006;129:749-758.

68. Ramieri GA, Spada MC, Austa M, Bianchi SD, Berrone S. Transverse maxillary distraction with a bone-anchored appliance: dento-periodontal effects and clinical and radiological results. *International Journal of Oral and Maxillofacial Surgery* 2005;34:357-363.
69. Parr JA, Garetto LP, Wohlford ME, Arbuckle GR, Roberts WE. Sutural expansion using rigidly integrated endosseous implants: an experimental study in rabbits. *The Angle orthodontist* 1997;67:283-290.
70. Shapiro P, Kokich V. Uses of implants in orthodontics. *Dental Clinics of North America* 1988;32:539-550.
71. Baccetti T, Franchi L, Cameron CG, McNamara Jr JA. Treatment timing for rapid maxillary expansion. *The Angle orthodontist* 2001;71:343-350.
72. Lee HK, Bayome M, Ahn CS, Kim S-H, Kim KB, Mo S-S et al. Stress distribution and displacement by different bone-borne palatal expanders with micro-implants: a three-dimensional finite-element analysis. *The European Journal of Orthodontics* 2012;cjs063.
73. MacGinnis M, Chu H, Youssef G, Wu KW, Machado AW, Moon W. The effects of micro-implant assisted rapid palatal expansion (MARPE) on the nasomaxillary complex—a finite element method (FEM) analysis. *Progress in orthodontics* 2014;15:1.
74. Zhou Y, Long H, Ye N, Xue J, Yang X, Liao L et al. The effectiveness of non-surgical maxillary expansion: a meta-analysis. *The European Journal of Orthodontics* 2013:cjt044.
75. Ferro F, Spinella P, Lama N. Transverse maxillary arch form and mandibular asymmetry in patients with posterior unilateral crossbite. *American Journal of Orthodontics and Dentofacial Orthopedics* 2011;140:828-838.
76. Marcotte MR. The use of the occlusogram in planning orthodontic treatment. *American journal of orthodontics* 1976;69:655-667.
77. Fiorelli G, Melsen B. The "3-D occlusogram" software. *Am J Orthod Dentofacial Orthop* 1999;116:363-368.
78. Canuto LFG, de Freitas MR, Janson G, de Freitas KMS, Martins PP. Influence of rapid palatal expansion on maxillary incisor alignment stability. *American Journal of Orthodontics and Dentofacial Orthopedics* 2010;137:164. e161-164. e166.
79. Moussa R, O'Reilly MT, Close JM. Long-term stability of rapid palatal expander treatment and edgewise mechanotherapy. *American Journal of Orthodontics and Dentofacial Orthopedics* 1995;108:478-488.
80. Alavi DG, BeGole EA, Schneider BJ. Facial and dental arch asymmetries in Class II subdivision malocclusion. *American Journal of Orthodontics and Dentofacial Orthopedics* 1988;93:38-46.
81. Mraiwa N, Jacobs R, Van Cleynenbreugel J, Sanderink G, Schutyser F, Suetens P et al. The nasopalatine canal revisited using 2D and 3D CT imaging. *Dentomaxillofac Radiol* 2004;33:396-402.
82. Grayson B, Cutting C, Bookstein FL, Kim H, McCarthy JG. The three-dimensional cephalogram: theory, techniques, and clinical application. *American Journal of Orthodontics and Dentofacial Orthopedics* 1988;94:327-337.

83. Swennen GR, Schutyser F, Barth E-L, De Groeve P, De Mey A. A new method of 3-D cephalometry Part I: the anatomic Cartesian 3-D reference system. *Journal of craniofacial surgery* 2006;17:314-325.
84. Kusayama M, Motohashi N, Kuroda T. Relationship between transverse dental anomalies and skeletal asymmetry. *American Journal of Orthodontics and Dentofacial Orthopedics* 2003;123:329-337.
85. Ricketts RM. Perspectives in the clinical application of cephalometrics: the first fifty years. *The Angle orthodontist* 1981;51:115-150.
86. Ludlow JB, Gubler M, Cevidanes L, Mol A. Precision of cephalometric landmark identification: cone-beam computed tomography vs conventional cephalometric views. *American Journal of Orthodontics and Dentofacial Orthopedics* 2009;136:312. e311-312. e310.
87. de Oliveira AEF, Cevidanes LHS, Phillips C, Motta A, Burke B, Tyndall D. Observer reliability of three-dimensional cephalometric landmark identification on cone-beam computerized tomography. *Oral Surgery, Oral Medicine, Oral Pathology, Oral Radiology, and Endodontology* 2009;107:256-265.
88. Mah J HD. Three-dimensional craniofacial imaging. *Am J Orthod Dentofacial Orthop* 2004;126:308-309.
89. Lagravere MO, Hansen L, Harzer W, Major PW. Plane orientation for standardization in 3-dimensional cephalometric analysis with computerized tomography imaging. *Am J Orthod Dentofacial Orthop* 2006;129:601-604.
90. Park S-H, Yu H-S, Kim K-D, Lee K-J, Baik H-S. A proposal for a new analysis of craniofacial morphology by 3-dimensional computed tomography. *American Journal of Orthodontics and Dentofacial Orthopedics* 2006;129:600.e623-600.e634.
91. Shibata M, Nawa H, Kise Y, Fuyamada M, Yoshida K, Katsumata A et al. Reproducibility of three-dimensional coordinate systems based on craniofacial landmarks. *The Angle Orthodontist* 2012;82:776-784.
92. Nelson SJ. *Wheeler's dental anatomy, physiology and occlusion*. Elsevier Health Sciences; 2014.
93. Hayashi K, Uechi J, Mizoguchi I. Three-Dimensional Analysis of Dental Casts Based on a Newly Defined Palatal Reference Plane. *The Angle Orthodontist* 2003;73:539-544.
94. Porto OCL, de Freitas JC, de Alencar A, Estrela C. The use of three-dimensional cephalometric references in dentoskeletal. *Dental Press J Orthod* 2014;19:78-85.
95. Lagravere MO, Major PW, Carey J. Sensitivity analysis for plane orientation in three-dimensional cephalometric analysis based on superimposition of serial cone beam computed tomography images. *Dentomaxillofac Radiol* 2010;39:400-408.
96. Naji P, Alsufyani NA, Lagravère MO. Reliability of anatomic structures as landmarks in three-dimensional cephalometric analysis using CBCT. *The Angle Orthodontist* 2013;84:762-772.
97. Lagravère MO, Gordon JM, Flores-Mir C, Carey J, Heo G, Major PW. Cranial base foramen location accuracy and reliability in cone-beam computerized tomography. *American Journal of Orthodontics and Dentofacial Orthopedics* 2011;139:e203-e210.

98. Arat ZM, Rübendüz M, Arman Akgül A. The displacement of craniofacial reference landmarks during puberty: a comparison of three superimposition methods. *The Angle orthodontist* 2003;73:374-380.

Chapter 3

3. Reliability and Accuracy of three-dimensional reference planes and landmarks related to maxillary expansion

3.1 Introduction

Anatomic landmarks are often identified, selected for specific interests, and used extensively for quantifying treatment changes and diagnosis in orthodontics. Indubitably, one must account for the possible errors to ensure landmarks are sufficiently accurate and reliable for its purposes.

Landmark identification is a major source of measurement error⁹⁹. These are errors that arise in the process of identifying specific landmarks with factors including, but not limited to, sharpness of radiographic image, landmark definitions, examiner's (a.k.a. human) error, and procedural errors^{100,101}. 3-D imaging has been shown to greatly reduce projection errors compared to traditional 2-D techniques³². These are all necessary considerations that guide much of the landmark selection process.

In this document's context, only landmarks that are related to the maxillary expansion were examined. This involved specially selecting landmarks used for transverse, vertical, and antero-posterior measurements. Afterwards, the landmarks' accuracy and reliability were evaluated for its respective purpose.

Traditional methods were reviewed for relevant landmark definitions and findings that are still applicable in the 3-dimensional domain.

3.2 Landmark Selection

3.2.1 Selection Criteria

This study follows four main aspects for landmark selection criteria: accuracy, reliability, relevance, and stability. Stability is the level of invariance exhibited with regards to natural growth and treatment changes. Relevance is the representativeness of the landmark(s) in reflecting the actual displacement of the anatomical structure of interest. In the context of this section, Intra-examiner Reliability is the deviation of repeated measured values obtained on the same image of the same patient by one examiner. Intra-examiner

Accuracy is the deviation of repeated measured values obtained on different images of the same patient by one examiner.

Reliability and accuracy can both be affected by identification error. In this regard, specific indicators were used to evaluate each landmark, as detailed in section 3.7. With 2-D cephalometry, linear measurement errors of between 0.3 mm to 1.4 mm have been reported to be satisfactory¹⁰². This low level of measurement error must be maintained when selecting appropriate 3-D landmarks. Baumrind and Frantz have also pointed out that any anatomic landmark there can be a non-uniform envelope of measurement error in all axes (x-, y- and z-axes)^{103,104}. Therefore, errors in all axes were independently analyzed.

In general, the choice of relevant landmarks depends on the objective of the study¹⁰¹. Reference landmarks should be located on invariant structures that will not be influenced by growth or treatment changes. Cranial base landmarks are considered to remain stable with growth, since >85% of growth has been completed in this region by the age of 7¹⁰⁵. The neurovascular bundles through the foramina of the cranial base remain largely as a non-violated biological function during growth and development^{98,106}. Suitable landmarks with small identification errors are generally located in areas of high density-contrast and located on sharply curved or pointed bony structures. The center-point within small and consistently rounded foramen serve as promising candidates during landmark selection²⁴.

3.2.2 Mid-Sagittal Plane

This section presents the candidate landmarks identified from the literature review in section 2.4 and 2.5, along with their relevance in the construction of the mid-sagittal plane. This reference plane is used for measuring transverse changes.

The postero-anterior and lateral cephalometric analyses involved a collection of landmarks for transverse skeleto-dental assessment. However, landmarks such as Menton and Antegonion (AG) lie on a wide radius of the bone; while Jugale (J) lie on the intersection between two overlapping bone structures²⁶ making it difficult to pinpoint reliably. The Anterior Nasal Spine (ANS) landmark can be partially or completely destroyed after RME treatment²⁴, and it can be off-centered for patients who have maxillary asymmetry^{15,99}.

The Nasopalatine Foramen (NPF) landmark was selected to replace ANS, as it was shown to be a relevant and stable landmark for midline definition⁸¹. NPF is an important

landmark to represent how the mid-sagittal plane dissects the anterior palate. The nasopalatine nerve and artery passes through this canal and into the incisive papilla. Its palatal opening is the NPF, which has been shown a relatively stable area⁸⁰. One recent study attempted to evaluate NPF as a stable landmark, but found difficulties in pinpointing the exact geometric center of this foramen due to its broad obliquity⁹⁶. In recognition of this, the left and right NPF was used to calculate the NPF mid-point (Mid.NPF), instead of locating the center of NPF directly in this study.

The superior tip of the CG landmark was also chosen from the postero-anterior cephalogram technique. It is consistently located on the mid-sagittal plane and has a sharply pointed bony structure which can minimize identification error²⁴.

From two previous CBCT studies^{24,96} (discussed in section 2.5), both SPIN and MDFM landmarks were shown to be suitable as mid-sagittal 3-D landmarks. Furthermore, Marmary et al also found that a perpendicular bisector drawn between the two foramina spinosum gave a fairly accurate mid-sagittal line^{98,107}. MDFM also corresponded to the widely used 2-D cephalometric landmark, the Basion⁹¹. Basion is the most anterior-inferior point of the foramen magnum where the spinal cord exits the posterior cranial base¹⁰⁰.

Posterior Vidian canal opening (PVID) was another candidate landmark in the cranial base which satisfies the criteria of having a small diameter. It has a consistently round cross-section of about 1.4 mm ± 0.6 mm diameter¹⁰⁸. The Vidian canal gives passage to the Vidian artery and the Vidian nerve, and runs in a relatively straight antero-posterior direction at the base of each medial pterygoid plate of the sphenoid bone¹⁰⁸. The vidian canal was found to be bilaterally equidistant to mid-sagittal plane in 77% based on a sample of 167 subjects according to Chen 2015 et al¹⁰⁹.

Collectively, SPIN, Mid.NPF, MDFM, CG, and PVID were all candidate landmarks analyzed for mid-sagittal plane construction in 3-D.

3.2.3 Palatal Plane

The palatal plane used by lateral cephalogram was constructed using two landmarks: ANS and Posterior Nasal Spine (PNS). However, ANS is not reliable and PNS is not a 3-D point (see section 3.2.2). To replace PNS, the greater palatine foramen (GPF) landmark was selected. Langenegger et al found in 96% of cases, GPF were located distal to the mid-palatal

aspect of the maxillary third molar. It was also found to be situated 15 mm bilaterally equidistant from the mid-palatal suture. To replace ANS, the NPF candidate landmark presented in section 3.2.2 was selected as it is located posterior to the maxillary central incisors.

Collectively, the Mid.NPF, left GPF, and right GPF together were the candidate 3-D landmarks used for posterior palatal plane construction.

3.2.4 Frontal Plane

To determine antero-posterior changes of the anterior maxilla in 2-D cephalometry, a perpendicular line is drawn from Nasion (N-perp) down to A-point (most concave point on the anterior maxilla)¹¹⁰. Although widely used for its strategic location, the landmarks Point A and Nasion has been reported as a non-ideal 3-D reference point since they are located on relatively flat bony surfaces and both are subjected to changes with growth¹¹¹.

In 3-D, sharply pointed bony structure or small foramen would provide a more reliable landmark. This led us to analyze bilateral Infra-orbital foramina (IORB) in replacement of N-perp for sagittal dimension assessment. To replace the A-point, the NPF candidate landmark presented in section 3.2.2 was selected as it is located posterior to the maxillary central incisors. IORB has been used to analyse skeletal maxillary changes in a previous maxillary expansion study³⁴. It is situated several millimeters apical to the roots of upper premolars bilaterally and unlikely to be influenced by orthodontic tooth movement¹¹². An anatomical study found the IORB to be located at a mean distance of 26 mm away from the mid-sagittal plane of the skull¹¹³. One previous study has also reported high intra-examiner reliability and low measurement errors (< 0.8 mm mean variability) for the infra-orbital foramen (IORB)⁹⁶.

Collectively, the left IORB, right IORB, and Mid.NPF, together were the candidate 3-D landmarks used for frontal plane construction.

3.2.5 Treatment Landmarks

Based on two previous studies^{34,96}, a collection of relevant 3-D landmarks have been reported with low identification errors (< 1.4 mm mean variability), and high intra-examiner reliability (ICC > 0.90). These existing landmarks will serve as treatment landmarks, namely, mental foramen, root apex, and alveolar bone of the upper first molar, lower first molar, and upper first premolar teeth as reported by Lagravere et al³⁴.

3.3 Purpose of study

The purpose of this study is to re-define several existing landmarks and also introduce new 3-D landmarks. The goal of re-defining landmarks is to improve the accuracy and reliability for 3-D measurements. This will be assessed by comparing CBCT measurements of dry skulls, with and without radio-opaque markers in the maxilla and cranial base. Reassessing existing landmarks allows this study to determine whether its finding agrees with previous studies. Precise operational definitions of new landmarks will be tabulated in all three axes to help maintain accuracy and reliability during repeated measurements.

3.4 Materials & Methods

Ten well-preserved dry skulls with stable occlusion were used for this study. Institutional Research Ethical Review Board approval was obtained for this study (Pro #00044781). The skulls were enclosed by a double-layered Plexiglass box (26 cm X 24.6 cm X 22 cm). The outer compartment of the Plexiglass box was filled with water before each scan, in order to simulate soft tissue attenuation without altering the CBCT machine settings (Figure 3.1 to Figure 3.2) ⁹⁷. The specimens were mounted onto a pedestal inside the CBCT scanner (I-CAT, Imaging Science International, Hatfield, PA, USA) using a standardized protocol (large field of view (FOV) 9 in x 12 in, voxel size 0.3 mm, 120 kVp, 23.87 mAS, 8.9 seconds). The I-CAT laser light system was used to orient each skull specimen. Putty and foam were used for stabilization of specimens before each scan.

Accurate representation of information from individual 3D landmarks can be difficult to obtain. To be prudent, all landmarks measurements were repeated three times.

CBCT volumes represent true anatomic linear measurements (1:1 ratio) of 3-D anatomical structures ^{20,88}. In addition, it has been shown that linear measurements made on 3-D surface models were accurate when compared to direct caliper anatomical measurements ¹¹⁴. In 3-D surface models with a voxel size of 0.25 mm, a mean absolute error of 0.07 ± 0.05 mm was found, while with 3-D surface models of 0.4 mm voxel size, a mean absolute error of 0.05 ± 0.04 mm was found, both with an excellent level of agreement as indicated by intra-class correlation coefficient (ICC) of > 0.99 ¹¹⁴.

Each dry skull was imaged twice using CBCT. No radiopaque markers were inserted at this initial round of imaging. Then prior to the second round of imaging, multiple radiopaque markers (Gutta Percha, Dentsply-Maillefer, Tulsa, OK) were carefully placed inside the skull, to pinpoint the true exact location of each anatomical structure for subsequent analysis (Figure 3.3 to Figure 3.4).



Figure 3.1: Dry Skull Specimen enclosed by Plexiglass mounted on CBCT machine

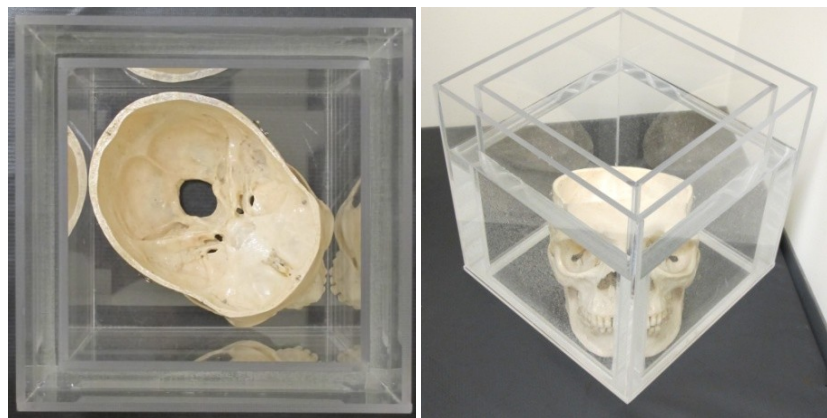


Figure 3.2: Double-layered Plexiglass box (Left), filled with water in the external layer (Right).

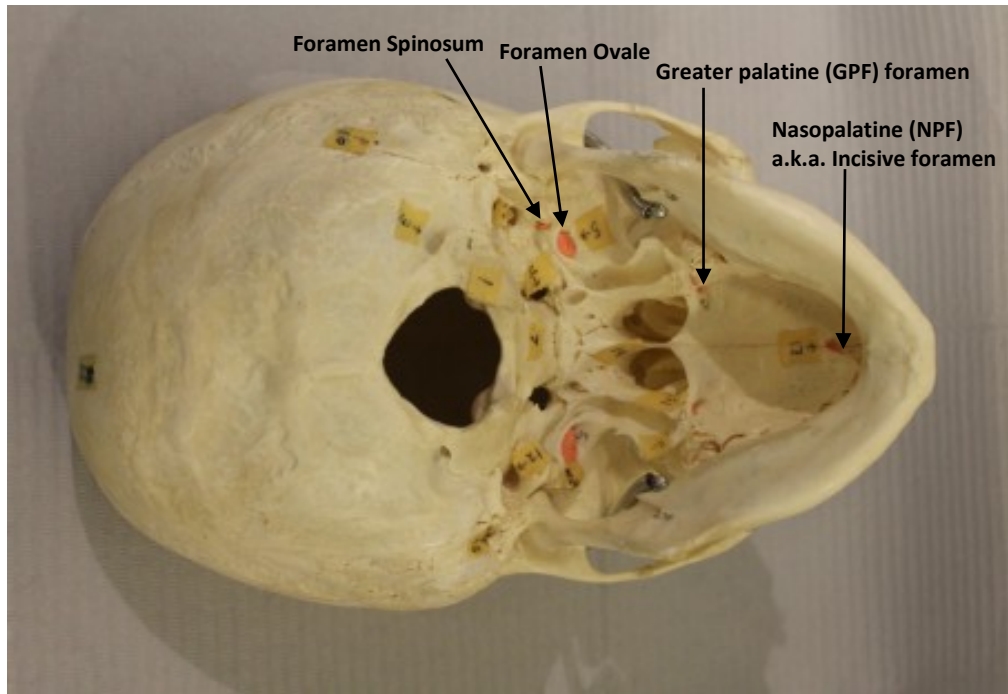


Figure 3.3: Example of a Dry skull with Gutta Percha markers

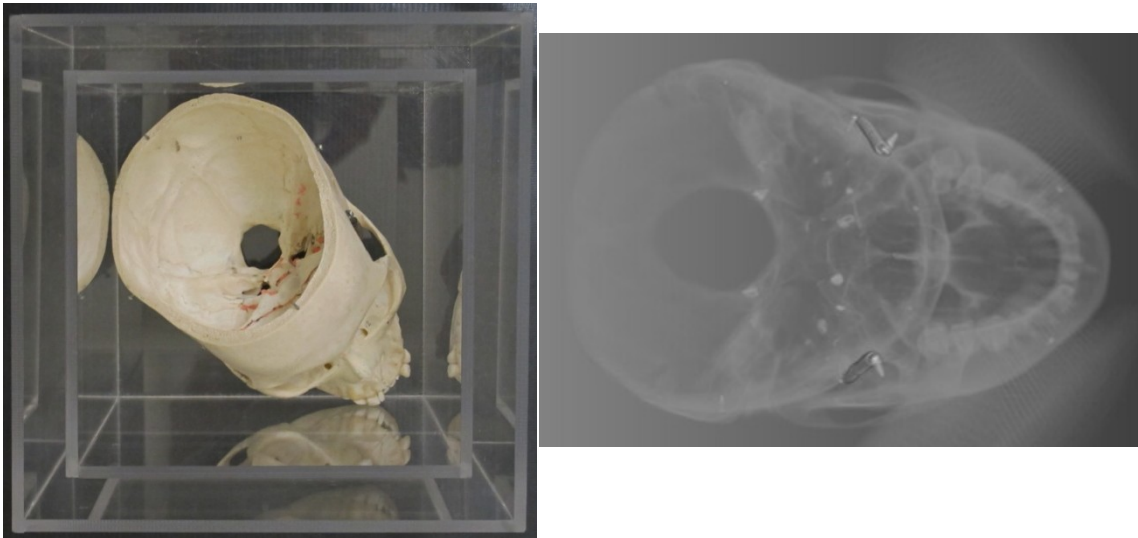


Figure 3.4: Dry skull with Gutta Percha markers inside Plexiglass box (Left), CBCT scan (Right).

A total of twenty six sets of anatomic landmarks were investigated, including: 2 singular and 5 paired landmarks in the Cranial base, 4 pairs in the maxillary and mandibular jaws, 5 pairs of dental crown, 5 pairs of root apex, and 5 pairs of alveolar bone landmarks.

All CBCT scans were exported as DICOM files (Digital Imaging and Communications in Medicine), and subsequently loaded into the AVIZO version 8.0 software for analysis (Visualization Sciences Group, Burlington, MA, USA). A Cartesian coordinate system was used for each CBCT volume, with the origin of the x,y,z axis determined at the time of scan.

The CBCT volumes were viewed in three planes: the x-y axial (right-left), x-z coronal (superior-inferior), and y-z sagittal (anterior-posterior). The principal investigator marked each landmark in the AVIZO software using virtual sphere markers of 0.20 mm diameter. The center of the virtual marker was used to determine the position of the landmark in this software; hence the marker size did not affect the position of the landmark. Each CBCT was first viewed in the most appropriate planar view (in the "Special note" column in Table 3-1 to Table 3-3), then adjusted in each of the remaining planar views.

To assess intra-examiner reliability, three independent repeated measurements were performed on CBCT images without Gutta percha markers, and each measurement were taken at least 5 days apart. Each volume were identified by code and randomized in order to reduce examiner bias.

To assess the identification accuracy of the 3-D anatomic landmarks, the dry skull CBCT volumes with Gutta percha markers, were read by the principal investigator once. Then readings from one randomly selected reading of the CBCT images without Gutta percha markers were compared to the readings of CBCT images with Gutta percha. Since the skulls cannot be oriented in the exact position in the CBCT machine (while imaged without Gutta percha and with Gutta percha), the x,y,z landmark coordinates of CBCT volumes taken at the two time-points could not be directly compared. Therefore, linear distances between the 3-D coordinates were measured using the following Euclidean distance formula:

$$d = \sqrt{(X_1 - X_2)^2 + (Y_1 - Y_2)^2 + (Z_1 - Z_2)^2}$$

With this formula, d represented the distance (mm) between two anatomic landmarks, while (X_1, Y_1, Z_1) and (X_2, Y_2, Z_2) are the respective coordinates of any two given landmarks of

interest. Each landmark was included in at least 3 linear distances in different dimensions in order to provide an assessment in all dimensions.

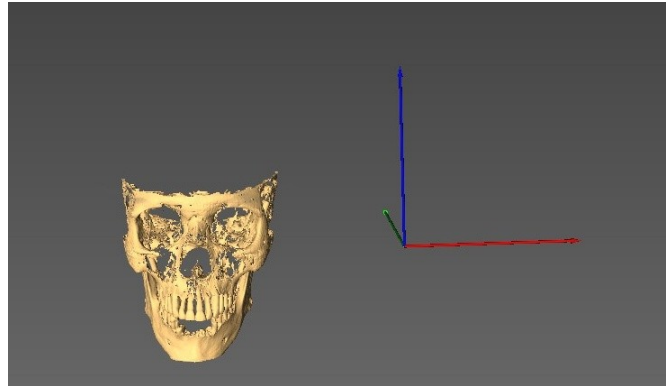


Figure 3.5: Orientation of the 3 axes: X-axis (Red, Transverse), Y-axis (Green, Anterior-posterior), Z-axis (Dark Blue, Vertical).

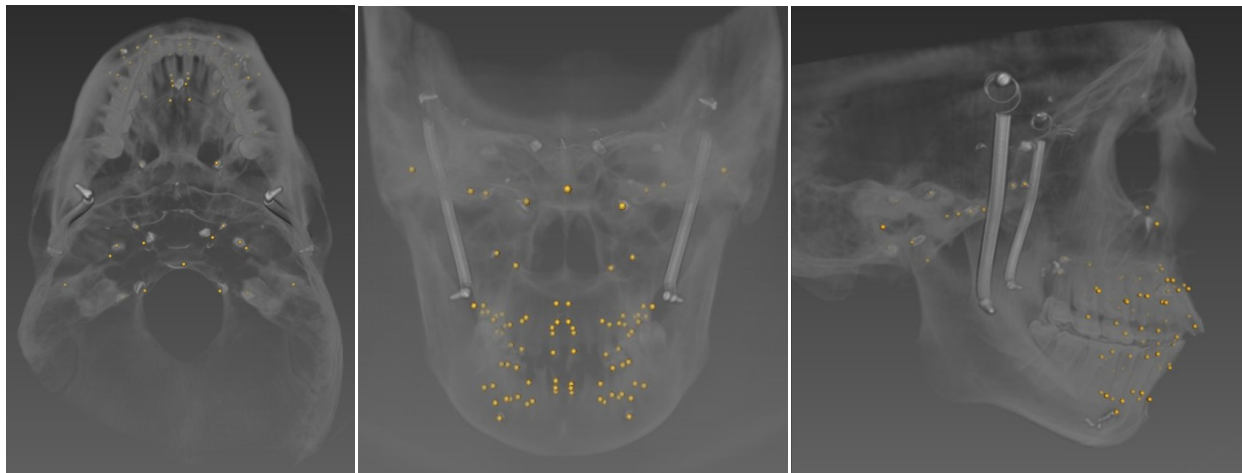


Figure 3.6: 3-D Landmarks viewed from axial, coronal, and sagittal planes (Left to Right) using the 3-D visualization software (AVIZO)

Table 3-1: 3-D Maxilla-mandibular skeletal landmark definitions

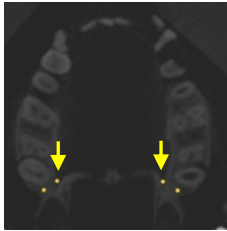
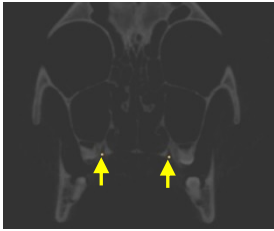
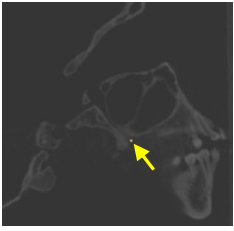
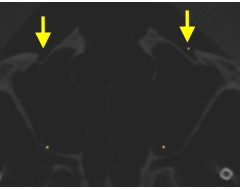
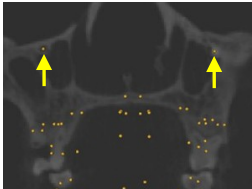
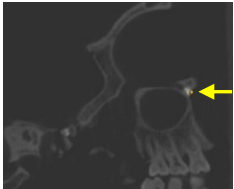
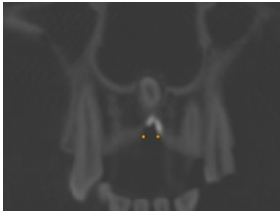
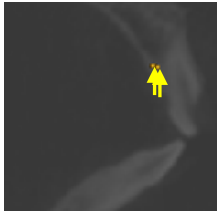
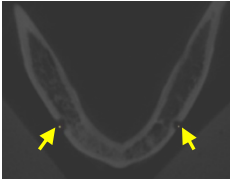
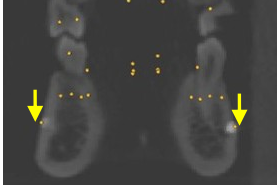
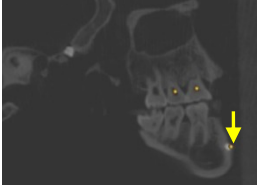
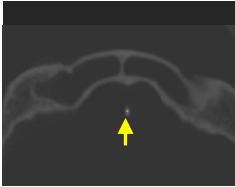
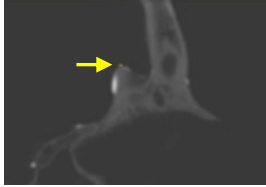
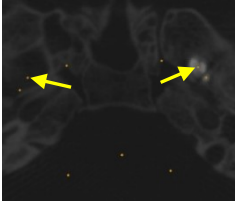
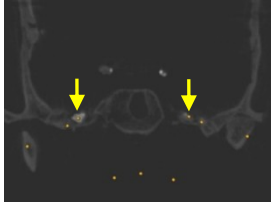
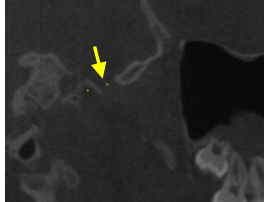
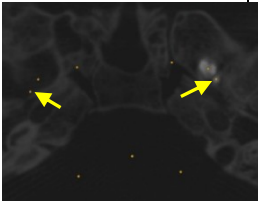
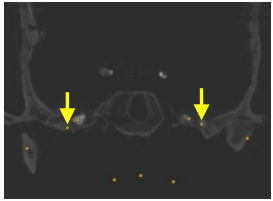
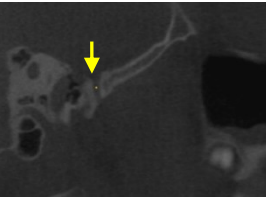
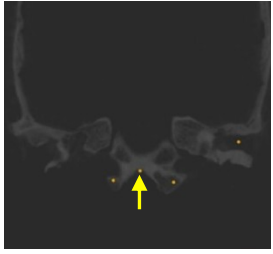
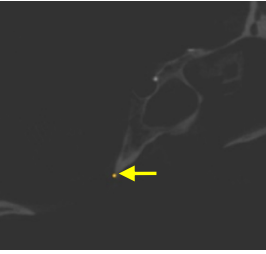
Maxilla-Mandibular Skeletal Landmarks				
Landmarks	Special Note	Axial view (XY)	Coronal view (XZ)	Sagittal view (YZ)
Greater Palatine Foramina (GPF.L&R)	First use Coronal view. Find orifice at level of the nasal floor.	Center-most 	Inferior-Center-most 	Center-most 
Anterior-most Orifice of the Infraorbital Foramina (IORB.L&R)	First use Axial & Coronal view. Find orifice along the canal.	Center-most 	Center-most 	Anterior-Center-most 
Nasopalatine (Incisive) Foramina (NPF.L&R)	First use Axial view. Mark most concave bony cortical rims for both L&R halves.	Concave, Internal & Center-Most 	Concave, Internal & Center-Most 	Lateral-most Internal Cortical Border 
Mental Foramina (MENT.L&R)	First use Coronal view to find middle slice. Then use Axial.	Center-most 	Central-Lateral-most 	Central-Lateral-most 

Table 3-2: 3-D Cranial base skeletal landmark definitions

Cranial Base Skeletal Landmarks				
Landmarks	Special Note	Axial view (XY)	Coronal view (XZ)	Sagittal view (YZ)
Crista Galli (CG)	First use Axial view, then Coronal.	Superior-most Tip 	Center-most Tip 	Center-most Tip 
Foramina Ovale (OVAL.L&R)	First use Axial view then Coronal.	Center-most 	Center-most 	Center-most 
Foramina Spinosum (SPIN.L&R)	First use Axial view. Guide using Mandibular condyles.	Center-most 	Center-most 	Center-most 
Mesial-most point of Dorsum Foramen Magnum (MDFM a.k.a. Basion) when left + right bony cortices first join	First use Sagittal, then Axial. Find Mesial-Inferior most sharp point (Basion).	Mesial-Inferior-Posterior-most Bony Cortex 	Inferior-Center-most 	Inferior-Posterior-most 

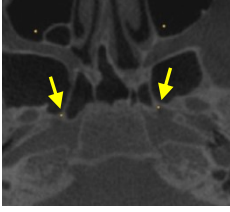
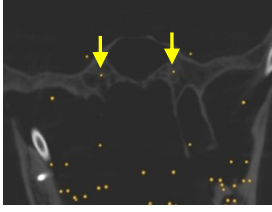
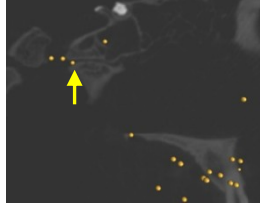
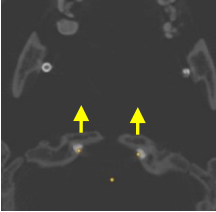
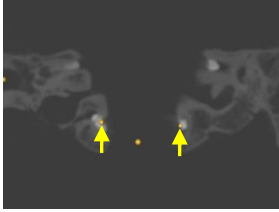
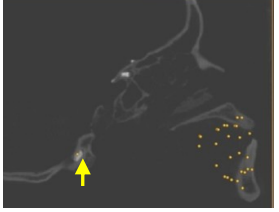
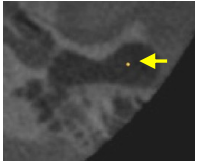
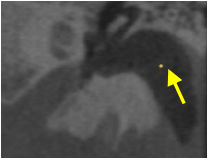
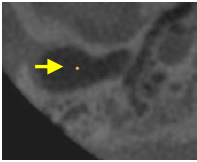
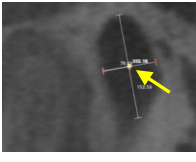
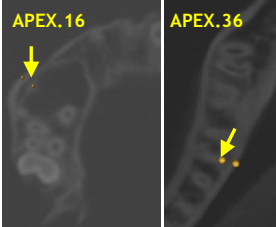
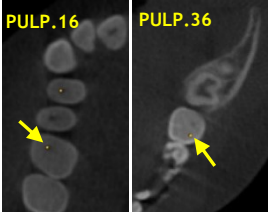
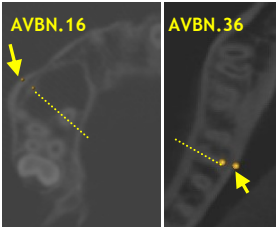
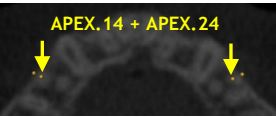
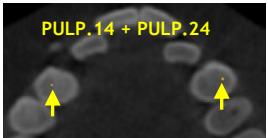
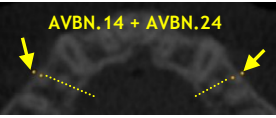
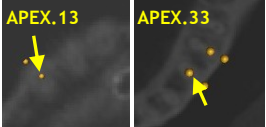
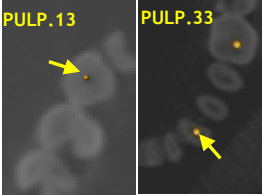
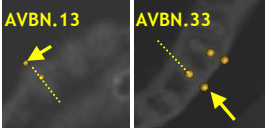
Posterior Vidian Canals (PVID.L&R)	First use Axial then Coronal. Use OVAL and SPIN as guides.	Posterior-most 	Center-most 	Posterior-most 
Hypoglossal Canals (HYPO.L&R)	First use Coronal view. Find the Medial-most Orifice openings.	Medial-Center-most 	Center-most 	Medial-Center-most 
External Auditory Meatus (EAM.L) (Bony portion)	First use Coronal view.	Center-most 	Center-most 	Center-most 
External Auditory Meatus (EAM.R)	First use Coronal view.	Center-most 	Center-most 	Center-most 

Table 3-3: 3-D Dental Root (PULP, APEX, AVBN) landmark definitions

Landmarks	Axial (XY) Definition	Landmarks	Axial (XY) Definition
Mesio-Buccal Molar APEX Tip Upper & Lower	 <p>Center-most-Tip</p>	Molar PULP (Buccal-Mesial Tip of Pulp Horn) Upper & Lower	 <p>Center-most-Tip</p>
Buccal Alveolar Cortical Bone of Molar (AVBN) Upper & Lower	 <p>Exact level with APEX, along imaginary line parallel to root canal and center of root apex</p>		
Buccal Root Premolar APEX Tip Upper only	 <p>Center-most-Tip</p>	Premolar PULP (Buccal Tip of Pulp Horn) Upper only	 <p>Center-most-Tip</p>
Buccal Alveolar Cortical Bone of Premolar (AVBN) Upper only	 <p>Exact level with APEX, along imaginary line parallel to root canal and center of root apex</p>		

<p>Canine APEX Tip Upper & Lower</p>	 <p>Center-most-Tip</p>	<p>Canine PULP (Buccal Tip of Pulp Horn) Upper & Lower Canine/Premolar</p>	 <p>Center-most-Tip</p>
<p>Buccal Alveolar Cortical Bone of Canine (AVBN) (Upper & Lower)</p>	 <p>Exact level with APEX, along imaginary line parallel to root canal and center of root apex</p>		

3.5 Plane construction

Given the coordinates of three reference landmarks for a plane, 3-D visualization software can compute the plane. But entering the three-point coordinates usually is a time-consuming repetitive manual process. Similar argument applies to determining the perpendicular distance. As a remedy, this study reproduced the mathematic procedure in Microsoft Excel. This allows the reference planes and perpendicular distances to be automatically calculated whenever the landmark coordinates were updated. Therefore, for sake of completeness, the 3-D geometry used for plane construction is presented in this section.

In 3-D geometry, three non-collinear points can be used to construct a reference plane. This involved selection of three reference landmarks (P_0 , P_1 , P_2) located as far apart as possible within the head, along a plane with respect to the region of interest.

The general formula representing a plane is given by $ax+by+cz+d=0$. The values for a , b , c , and d can be derived from coordinates of three points that lies on the plane¹¹⁵.

Let the coordinates of the three landmarks (points) on the plane be denoted as:

$$P_0 = (x_0, y_0, z_0), P_1 = (x_1, y_1, z_1), P_2 = (x_2, y_2, z_2).$$

Then:

$$a = (y_1 - y_0) \times (z_0 - z_2) - (z_1 - z_0) \times (y_0 - y_2)$$

$$b = (z_1 - z_0) \times (x_0 - x_2) - (x_1 - x_0) \times (z_0 - z_2)$$

$$c = (x_1 - x_0) \times (y_0 - y_2) - (y_1 - y_0) \times (x_0 - x_2)$$

$$\text{Thus, } d = - (ax_0 + by_0 + cz_0)$$

3.5.1 Mid-Sagittal plane

The following figures illustrates the mid-sagittal plane constructed by the landmarks: Mid.NPF (mid-point calculated from NPF.L and NPF.R), Mid.SPIN (mid-point calculated from SPIN.L and SPIN.R), and MDFM. This allows assessment of transverse changes and symmetry after maxillary expansion (Figure 3.7).

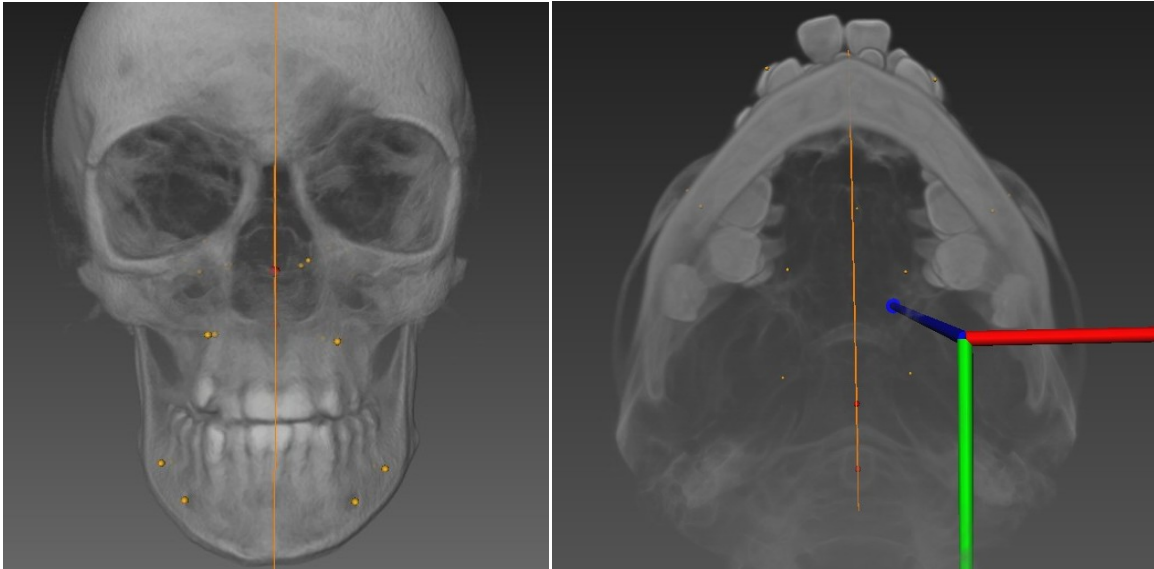


Figure 3.7: 3-D Mid-sagittal Reference Plane

3.5.2 Posterior Palatal plane

The following figure illustrates the posterior palatal plane constructed by the landmarks: Mid.NPF, GPF.L, and GPF.R. This plane extended from anterior palate to posterior palate, intersecting maxillary roots mid-way (Figure 3.8), and to allow assessment of bite opening after maxillary expansion.

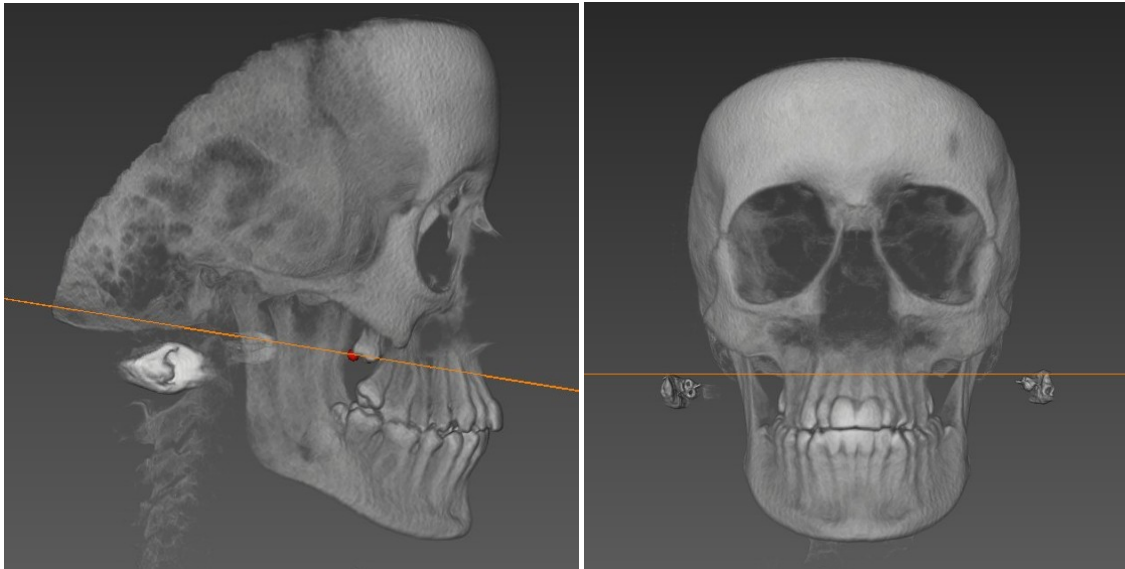


Figure 3.8: 3-D Posterior Palatal Reference Plane

3.5.3 Frontal plane

The following figure illustrates the frontal plane constructed by the landmarks: Mid.NPF (mid-point calculated from NPF.L and NPF.R), IORB.R and IORB.L (Figure 3.9) to allow assessment of antero-posterior dental changes after maxillary expansion.

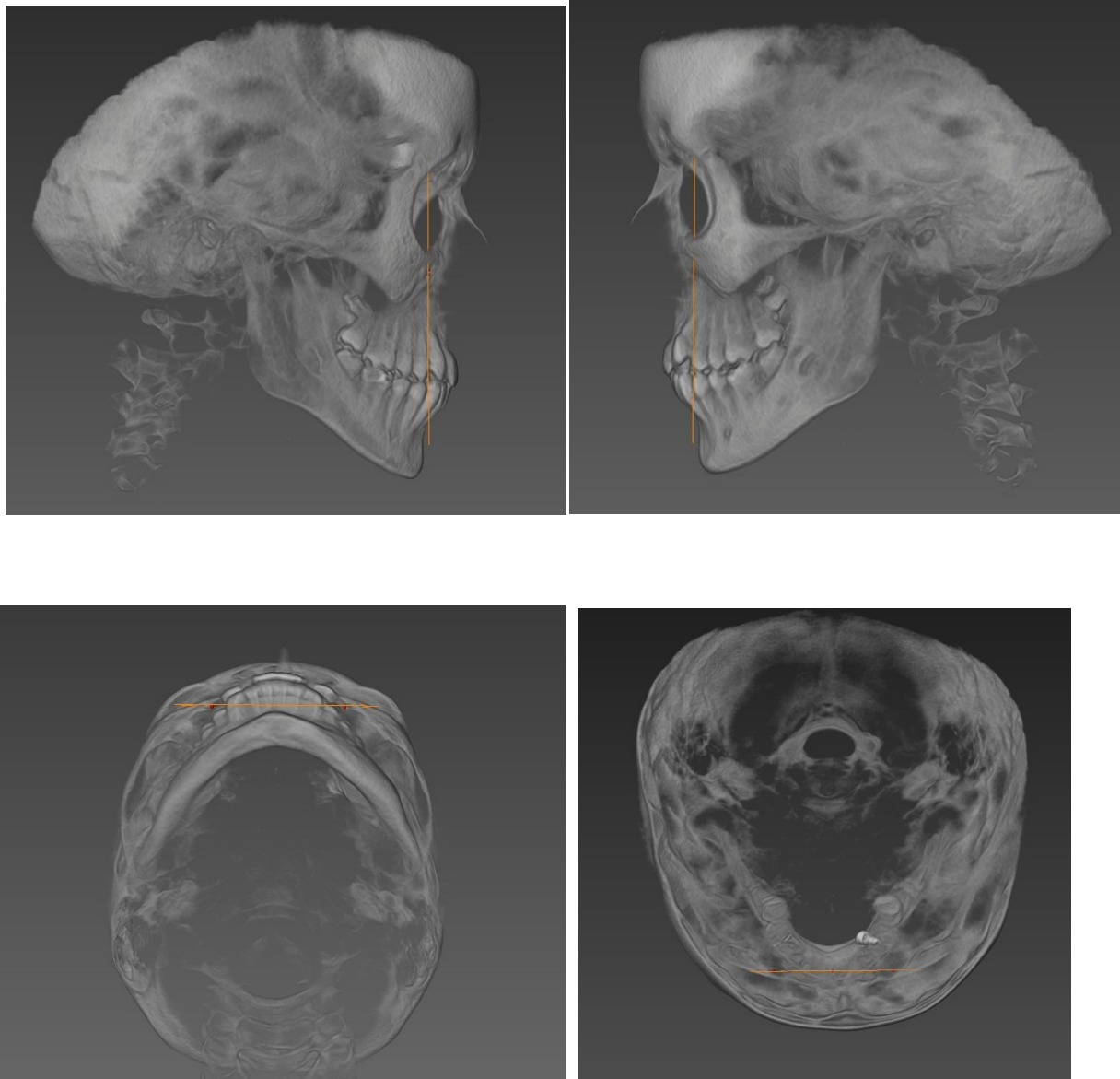


Figure 3.9: 3-D Frontal Reference Plane

3.6 Finding orthogonal distances from landmark of interest to the reference plane

Once all final coordinates were obtained in AVIZO software, the dataset was exported into a spreadsheet database (Excel 2007, Microsoft, Redmond, Wash). Using Excel, orthogonal distances (shortest perpendicular, or normal distance) were calculated for each landmark from its corresponding reference plane using this formula:

$$D = \frac{ax_0 + by_0 + cz_0 + d}{\sqrt{a^2 + b^2 + c^2}}$$

With this formula, D represented the signed perpendicular distance (mm) between the 3-D landmark of interest to the reference plane ¹¹⁵.

Note that orthogonal distances in each of the 3 dimensions, were assessed relative to their individual reference planes, to isolate changes in the particular dimension of interest. For example, transverse orthogonal changes were all measured with respect to the Mid-sagittal plane, and vertical orthogonal changes were all measured with respect to the Palatal plane.

3.7 Statistical analysis

The IBM SPSS statistical software was used for statistical data analysis (SPSS Statistics for Windows, Version 22.0. Armonk, NY).

3.7.1 Accuracy for 3-D landmarks

Agreement for accuracy was assessed using Intra-class Correlation Coefficient (ICC), in order to measure the level of agreement of CBCT measurements between the skull without gutta percha compared to the skull with gutta percha. The two-way mixed model, single measures with consistency was used, to ensure consistency in one rater's individual measurements while the subjects were chosen randomly. The ICC values were interpreted as per Portney and Watkins' recommendations, for all three axes. The absolute mean measurement error differences (in mm) were also calculated for all landmarks in all three axes in order to assess landmark accuracy.

Table 3-4: Portney and Watkins' ICC recommendation

ICC > 0.90	Excellent agreement
0.75 < ICC < 0.89	Good agreement
0.51 < ICC < 0.74	Moderate agreement
ICC < 0.50	Poor agreement

3.7.2 Intra-examiner reliability for 3-D landmarks

Intra-examiner reliability was also assessed in the X, Y, Z axes, using Intra-class Correlation Coefficient (ICC), to measure the agreement between the three repeated measurements of skull without gutta percha by the principal investigator. ICC interpreted based on the general recommendations of Portney and Watkins ¹¹⁶ in Table 3-4. The chosen statistical model was a two-way mixed model, single measures with consistency, to ensure consistency in one rater's individual measurements while the subjects were chosen randomly.

The absolute mean differences of each landmark (in millimeters) were also reported in all three axes (x, y, and z) for each measurement to assess landmark dispersion between measurements trials.

3.7.3 Intra-examiner reliability for reference plane construction

This was assessed by repeating the nine 3-D reference landmarks used for reference plane construction, and measuring the mean differences for twenty treatment landmarks in the X, Y, and Z axes (in millimeters).

3.8 Results

A summary of ease/difficulties encountered during landmark identification in each of the 3 axes are presented in Table 3-5.

3.8.1 Intra-examiner reliability of 3-D landmarks

Using the determined 3-D landmark definitions, excellent agreement for intra-examiner reliability was found for all skeletal landmarks in the 3 axes as indicated by an ICC ≥ 0.98 . Excellent agreement was also found for all dental landmarks with ICC ≥ 0.98 in both transverse and vertical (x- and z-axes), and ICC ≥ 0.99 in the sagittal (y-axis). The only exception was AVBN.36 which showed ICC of 0.96 in the transverse (x-axis), still excellent intra-examiner reliability.

Mean variability of ≤ 0.4 mm and ≤ 0.5 mm were found for all skeletal and dental landmarks respectively (Appendix 1 & 2). Profile plots in all three axes are presented in Appendix 5-7.

3.8.2 Accuracy of 3-D landmarks

Majority of investigated landmarks (22 of the 26 sets) showed excellent agreement (ICC ≥ 0.92) for accuracy between true anatomical landmarks (with gutta-percha markers) and those on skulls imaged without gutta percha markers (Table 3-6 to Table 3-8). IORB showed good agreement (ICC 0.88 and 0.80) in the antero-posterior dimension, and excellent agreement in the other two dimensions. NPF showed good agreement (ICC 0.87) in the transverse dimension, and excellent agreement in the other two dimensions. HYPO and AVBN.33 which showed moderate agreement in the antero-posterior dimension (ICC 0.65 and 0.60 respectively), and excellent agreement in the other two dimensions.

With the exception of two landmarks, almost all landmarks (24 of the 26 sets) showed low mean identification errors ≤ 0.85 mm in all 3 axes. Hypoglossal (HYPO) canal landmark was the main exception, with mean error of 1.28 mm in the antero-posterior and vertical axes; hence it was no longer preferred or considered as a reference landmark. MENT showed mean errors of ≤ 1.3 mm only in the antero-posterior direction, but only ≤ 0.55 mm and ≤ 0.20 mm in the vertical and transverse respectively. MENT landmark was kept in the pool of final landmarks, for its small amount of error in the vertical and transverse dimensions, although it was not as accurate in the antero-posterior dimension.

Table 3-5: Ease of Identification of the investigated 3-D landmarks

Landmarks	Definition	Transverse	Vertical	Sagittal	Reason	
Cranial Base						
1	SPIN.L&R	Center of Foramen Spinosum	Simple	Simple	Difficult	Small diameter, short canal simplified the identification
2	OVALE.L&R	Center of Foramen Ovale	Simple	Difficult	Difficult	Large diameter, oval elongated foramen, made it difficult
3	PVID.L&R	Center point of the Posterior-most aspect of the Vidian Canal Foramen Orifice	Simple	Simple	Difficult	Small diameter, fairly straight canal with a horizontal canal orientation, but posterior-most 10 mm of the canal ended on a taper which made it difficult
4	MDFM	Mesial-most point on the Anterior-Inferior portion of Dorsum Foramen Magnum (corresponds to Basion)	Simple	Simple	Simple	Like 2-D Basion landmark, this point was easy to identify accurately and reliably.
5	CG	Most Superior point of the Crista Galli	Simple	Difficult	Simple	Sharp point, allows easy identification
6	EAM.L&R	Center of the Bony portion of the External Auditory Canal	Difficult	Difficult	Difficult	Extremely large diameter, tortuous canal, bone blended with cartilage portion
7	HYPO.L&R	Center point of the Medial-most Endocranial Orifice Opening of the Hypoglossal Canal	Difficult	Difficult	Difficult	Tapered densely radiopaque Canal opening which made it difficult to identify
Maxilla						
8	GPF.L&R	Center point of the Inferior-most level of the Greater Palatine Canal Foramen Orifice	Simple	Simple	Difficult	Thin palatal bone, tougher to determine antero-posterior limit
9	NPF.L&R	Center point of the Mesial and Distal Halves of the Inferior-most level of the Nasopalatine/ Incisive Canal Orifice (Oral aspect)	Simple	Simple	Difficult	Large diameter, with tapered exit into oral cavity, mild difficulty in delineating cortical bony limits
10	IORB.L&R	Center point of the Anterior-most level of the Infraorbital Canal Foramen Orifice	Difficult	Difficult	Simple	Most Anterior 15-20 mm of the Canal Orifice Tapers Obliquely in a Medial-Inferior direction.
11	PULP.(tooth)	Tip of the Buccal-Mesial-most Pulp horn of the specified tooth	Simple	Difficult	Simple	Tip was simple to identify
12	APEX.(tooth)	Tip of the Buccal-Mesial-most Root Apex of the specified tooth	Simple	Simple	Simple	Tip was simple to identify

13	AVBN.(tooth)	Point on the Buccal Cortical Plate that aligns parallel to and at the same level as the specified root apex of the involved tooth	Simple	Difficult	Difficult	In the absence of reference based on the root apex tip, there is no vertical or antero-posterior stop to localize this point
Mandible						
14	MENT.L&R	Center point of the Lateral-most Foramen Orifice of the Mental Canal	Simple	Difficult	Difficult	Large diameter, broadly radiopaque tapered opening, made it difficult
15	PULP.(tooth)	Tip of the Mesial- Buccal-most Pulp horn of the specified tooth	Simple	Simple	Simple	Tip was simple to identify
16	APEX.(tooth)	Tip of the Mesial-Buccal-most Root Apex of the specified tooth	Simple	Simple	Simple	Tip was simple to identify
17	AVBN.(tooth)	Point on the Buccal Cortical Plate that aligns parallel and at the same level as the specified root apex of the involved tooth	Simple	Difficult	Difficult	In the absence of reference based on the root apex tip, there is no vertical or antero-posterior stop to localize this point

Table 3-6: Accuracy of Cranial Base Landmarks, based on ICC and Mean Identification Errors

Cranial Base Landmarks	Transverse	Vertical	Antero-posterior	Transverse	Vertical	Antero-posterior
	ICC (Intra-class Correlation Coefficient)			Mean measurement errors \pm SD (mm)		
Mid.SPIN	n/a [†]	≥ 0.99	≥ 1.00	n/a [†]	$\leq 0.51 \pm 0.3$	$\leq 0.50 \pm 0.3$
SPIN	≥ 0.99	≥ 0.99	≥ 0.97	$\leq 0.55 \pm 0.3$	$\leq 0.65 \pm 0.3$	$\leq 0.85 \pm 0.8$
Mid.PVID	n/a [†]	≥ 0.99	≥ 1.00	n/a [†]	$\leq 0.40 \pm 0.5$	$\leq 0.51 \pm 0.3$
PVID	≥ 1.00	≥ 0.99	≥ 1.00	$\leq 0.30 \pm 0.3$	$\leq 0.50 \pm 0.5$	$\leq 0.65 \pm 0.5$
Mid.OVAL	n/a [†]	≥ 1.00	≥ 0.98	n/a [†]	$\leq 0.40 \pm 0.2$	$\leq 0.85 \pm 0.8$
OVAL	≥ 0.99	≥ 0.99	≥ 0.98	$\leq 0.50 \pm 0.4$	$\leq 0.55 \pm 0.4$	$\leq 0.81 \pm 0.8$
CG	n/a [†]	≥ 0.99	≥ 0.99	n/a [†]	$\leq 0.75 \pm 0.5$	$\leq 0.55 \pm 0.5$
MDFM	n/a [†]	≥ 1.00	≥ 1.00	n/a [†]	$\leq 0.49 \pm 0.3$	$\leq 0.85 \pm 0.5$
EAM	≥ 0.98	≥ 0.99	≥ 0.99	$\leq 0.70 \pm 0.4$	$\leq 0.55 \pm 0.4$	$\leq 0.75 \pm 0.9$
HYPO	≥ 0.95	≥ 0.98	≥ 0.65	$\leq 0.51 \pm 0.4$	$\leq 1.10 \pm 1.0$	$\leq 1.28 \pm 1.5$

[†] n/a: not applicable in the transverse dimension, since this is a singular or midline landmark.

Table 3-7: Accuracy of Maxillo-mandibular Landmarks, based on ICC and Mean Identification Errors

Skeletal Max/Mand Landmarks	Transverse	Vertical	Antero- posterior	Transverse	Vertical	Antero- posterior
	ICC (Intra-class Correlation Coefficient)			Mean measurement errors \pm SD (mm)		
NPF	≥ 0.87	≥ 0.99	≥ 0.92	$\leq 0.52 \pm 0.3$	$\leq 0.55 \pm 0.4$	$\leq 0.85 \pm 0.5$
GPF	≥ 0.98	≥ 0.99	≥ 0.99	$\leq 0.52 \pm 0.3$	$\leq 0.51 \pm 0.4$	$\leq 0.65 \pm 0.5$
IORB	≥ 0.96	≥ 0.99	≥ 0.88	$\leq 0.69 \pm 0.5$	$\leq 0.55 \pm 0.3$	$\leq 0.85 \pm 0.5$
MENT	≥ 1.00	≥ 0.99	≥ 0.94	$\leq 0.20 \pm 0.2$	$\leq 0.55 \pm 0.3$	$\leq 1.30 \pm 1.3$

Table 3-8. Accuracy of Dental Landmarks, based on ICC and Mean Identification Errors.

Dental Max/Mand Landmarks	Transverse	Vertical	Antero- posterior	Transverse	Vertical	Antero- posterior
	ICC (Intra-class Correlation Coefficient)			Mean measurement errors \pm SD (mm)		
PULP	≥ 0.97	≥ 0.99	≥ 0.90	$\leq 0.30 \pm 0.3$	$\leq 0.75 \pm 0.4$	$\leq 0.50 \pm 0.5$
APEX	≥ 0.95	≥ 0.99	≥ 0.80	$\leq 0.50 \pm 0.4$	$\leq 0.70 \pm 0.4$	$\leq 0.60 \pm 0.5$
AVBN	≥ 0.92	≥ 0.70	≥ 0.60	$\leq 0.70 \pm 0.5$	$\leq 0.90 \pm 0.7$	$\leq 0.90 \pm 0.8$

3.8.3 Intra-examiner reliability of 3-D reference plane construction

Based on twenty selected landmarks, low mean errors were found for the orthogonal distances to the averaged reference planes constructed by repeatedly locating the reference landmarks three times (Table 3-9). The mean errors were ≤ 0.55 mm, ≤ 0.35 mm, and ≤ 0.45 mm, in the Mid-sagittal plane (Transverse orthogonal distances), Palatal plane (Vertical orthogonal distances), and Frontal plane (Antero-posterior orthogonal distances) respectively. This meant that the reference planes were suitable for clinical use. Note that each of the planes were used individually based on the dimension of interest. For example, Transverse

The following diagrams illustrate the directions and magnitude of plane deviation induced by imposing an artificial 0.2 mm of error into the reference landmarks responsible for each plane (Figure 3.10 - Figure 3.12).

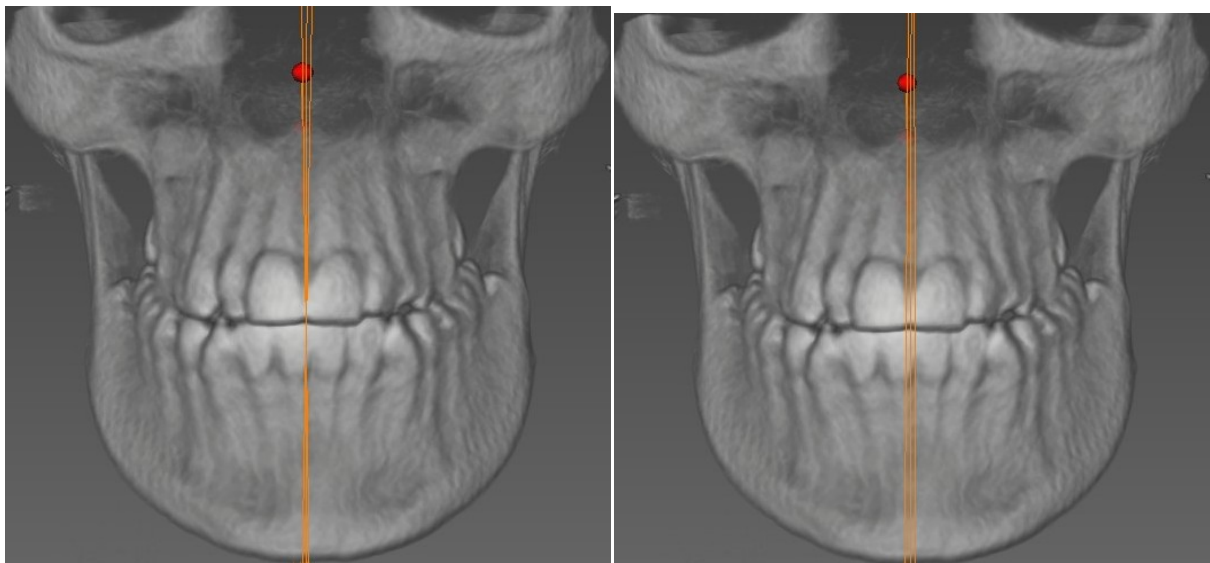


Figure 3.10: Mid-sagittal planes with 0.2 mm imposed errors in X-axis of
A) MDFM and Mid.SPIN (Left Picture), B) MDFM and Mid.NPF (Right picture).

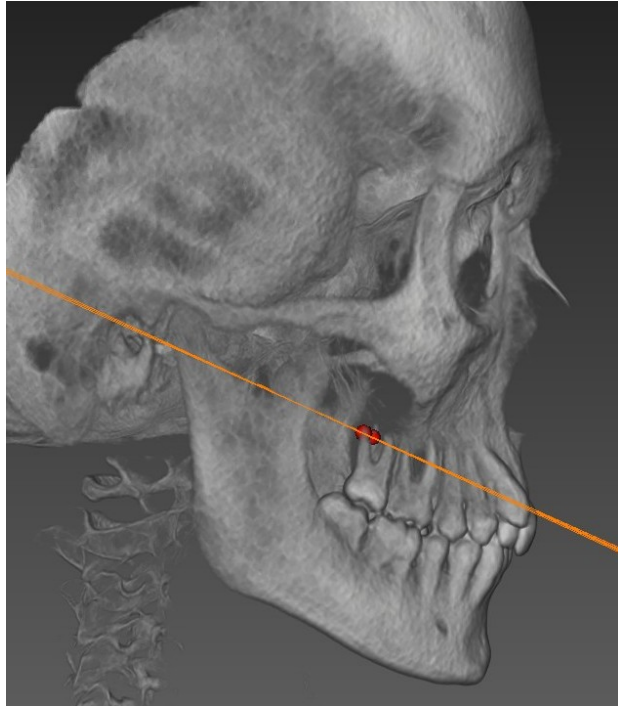


Figure 3.11: Posterior Palatal planes with 0.2 mm imposed error in Z-axis of GPF.L&R and Mid.NPF

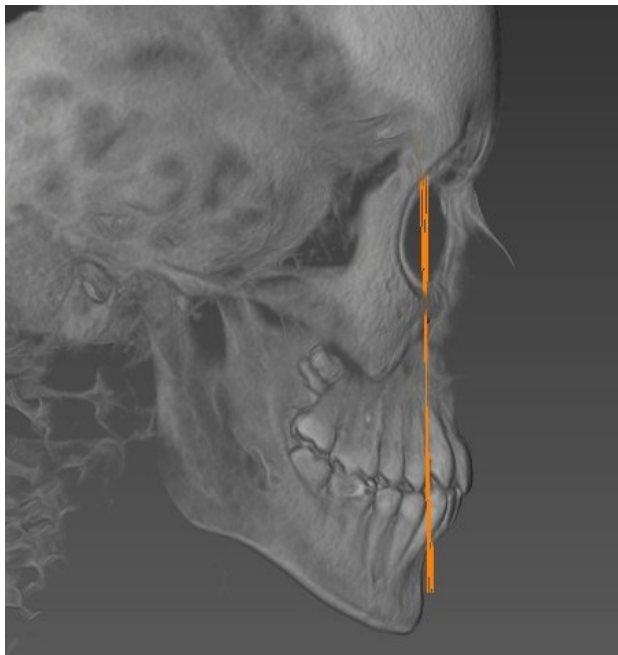


Figure 3.12: Frontal planes with 0.2 mm imposed error in Y-axis of IORB.L&R and Mid.NPF

Table 3-9: Mean errors (in mm) of orthogonal distances, from 3 repeated reference plane constructions for 20 landmarks.

Landmark	Transverse			Vertical			Antero-posterior		
	Mean \pm SD (mm)	Max (mm)	Min (mm)	Mean \pm SD (mm)	Max (mm)	Min (mm)	Mean \pm SD (mm)	Max (mm)	Min (mm)
PULP.16	0.19 \pm 0.15	0.38	0.01	0.12 \pm 0.20	0.65	0.01	0.20 \pm 0.12	0.38	0.05
PULP.26	0.20 \pm 0.17	0.51	0.04	0.12 \pm 0.20	0.63	0.01	0.20 \pm 0.12	0.37	0.05
PULP.46	0.35 \pm 0.27	0.69	0.02	0.13 \pm 0.21	0.67	0.01	0.29 \pm 0.17	0.51	0.07
PULP.36	0.34 \pm 0.28	0.82	0.03	0.12 \pm 0.21	0.65	0.01	0.29 \pm 0.17	0.48	0.06
APEX.16	0.10 \pm 0.08	0.23	0.01	0.14 \pm 0.23	0.73	0.02	0.14 \pm 0.10	0.30	0.04
APEX.26	0.14 \pm 0.11	0.37	0.01	0.13 \pm 0.21	0.67	0.01	0.14 \pm 0.10	0.29	0.04
APEX.46	0.44 \pm 0.36	0.91	0.02	0.14 \pm 0.22	0.70	0.02	0.35 \pm 0.21	0.64	0.08
APEX.36	0.45 \pm 0.37	0.99	0.02	0.13 \pm 0.21	0.64	0.01	0.36 \pm 0.21	0.62	0.08
OVAL.R	0.12 \pm 0.09	0.26	0.01	0.16 \pm 0.24	0.77	0.03	0.15 \pm 0.07	0.25	0.04
OVAL.L	0.12 \pm 0.10	0.33	0.01	0.17 \pm 0.26	0.84	0.03	0.15 \pm 0.08	0.27	0.04
PVID.R	0.11 \pm 0.09	0.28	0.01	0.26 \pm 0.47	1.50	0.01	0.14 \pm 0.07	0.25	0.04
PVID.L	0.12 \pm 0.10	0.33	0.03	0.27 \pm 0.49	1.57	0.01	0.15 \pm 0.08	0.29	0.04
MENT.R	0.53 \pm 0.44	1.19	0.01	0.18 \pm 0.29	0.91	0.01	0.44 \pm 0.25	0.76	0.10
MENT.L	0.54 \pm 0.46	1.32	0.02	0.18 \pm 0.29	0.90	0.01	0.44 \pm 0.25	0.75	0.10
IORB.R	0.25 \pm 0.18	0.50	0.04	0.17 \pm 0.29	0.94	0.04	n/a [†]		
IORB.L	0.23 \pm 0.18	0.48	0.02	0.17 \pm 0.27	0.88	0.03	n/a [†]		
GPF.R	0.08 \pm 0.06	0.22	0.01	n/a [†]			0.05 \pm 0.03	0.10	0.01
GPF.L	0.09 \pm 0.07	0.22	0.01	n/a [†]			0.05 \pm 0.04	0.10	0.01
MID.SPIN	n/a [†]			0.33 \pm 0.27	0.84	0.02	0.30 \pm 0.39	1.32	0.03
MDFM	n/a [†]			n/a [†]			0.24 \pm 0.14	0.51	0.08
Mid.NPF	n/a [†]			n/a [†]			n/a [†]		

[†] n/a: not applicable, since this landmark was used for plane construction.

3.9 Discussion

3.9.1 Overview

The purpose of this study was to select suitable landmarks for assessment of transverse, vertical, and antero-posterior changes after rapid maxillary expansion therapy. Based on ten dry human skulls, almost all investigated landmarks (24 out of 26 sets) proved to be suitable for clinical use based on an ICC of > 0.92 for accuracy. HYPO and AVBN.33 were the two exceptions in the antero-posterior dimension, showing moderate agreement in the y-axis (ICC 0.65 and 0.60 respectively), and excellent agreement in the other two dimensions.

Based on previous studies, landmarks with mean identification errors < 1 mm are considered precise and not clinically significant, those between 1.5 mm - 2.0 mm are considered clinically significant and should be used with caution; errors over 2.5 mm are considered inappropriate^{97,101}. In general, deviations in measurements under 1.5 mm is not considered to have a significant impact on clinical decisions⁹⁶.

With the exception of two landmarks, almost all landmarks (24 of the 26 sets) showed low mean identification errors of ≤ 0.85 mm in all 3 axes. Hypoglossal (HYPO) canal landmark was the main exception, with mean error of 1.28 mm in the antero-posterior and vertical axes; hence it was no longer preferred or considered in the pool of reference landmarks.

MENT showed mean errors of ≤ 1.3 mm only in the antero-posterior direction, but only ≤ 0.55 mm and ≤ 0.20 mm in the vertical and transverse respectively. MENT landmark was kept in the pool of final landmarks, for its small amount of error in the vertical and transverse dimensions, although it was not as accurate in the antero-posterior dimension. Furthermore, MENT has been used in previous studies, and has been found to more reliable and accurate than the Lingula (triangular projection immediately in front of the mandibular foramen) for evaluation of mandibular changes⁹⁶.

3.9.2 Reference landmarks used for Plane construction

From this study's observations, the preferred landmarks for mid-sagittal plane were: Mid.Nasopalatine Foramen (Mid.NPF), Mesial Dorsal Foramen Magnum (MDFM), and Foramen Spinosum (SPIN). The preferred landmarks for frontal plane were: IORB left & right, and

Mid.NPF. The preferred landmarks for palatal plane were: GPF left & right, and Mid.NPF. These landmarks and combinations, proved to be comparatively superior to other options.

All the remaining candidates including CG, Posterior Vidian canal (PVID), External Auditory Meatus (EAM), and Foramen Ovale (OVAL) showed promising accuracy and reliability, but they were not chosen due to their relative weaknesses.

Nasopalatine Foramen (NPF) & Mid.NPF

The Nasopalatine foramen (NPF or incisive foramen) has already been shown to be a relatively stable area ⁸⁰. In the transverse, NPF.L&R showed excellent intra-examiner reliability (ICC >0.99), good agreement for accuracy (ICC of 0.87), with low mean identification errors ≤ 0.55 mm. Its mid-point (Mid.NPF), i.e. mid-point of the left and right NPF, was used to pinpoint the center of the wide NPF opening, which can be up to 6 mm ⁸¹. The Mid.NPF (average of the left and right NPF) replaces the 2-D landmark Anterior Nasal Spine (ANS), which has been used for midline definition ⁸¹.

NPF is an important landmark to represent how the mid-sagittal plane dissects the anterior palate. Extension of the reference plane from posterior to anterior region of interest (i.e. maxillary molar, premolar and canine teeth) will help reduce extrapolation errors. This agrees with the established principle, discussed by Nagasaka et al ¹¹⁷ and Lagravere et al ⁹⁵, of choosing landmarks further spaced apart to reduce measurement errors during plane construction.

In the vertical dimension, NPF proved to have comparable accuracy and reliability as SPIN. Mean identification errors were ≤ 0.55 mm for NPF, but ≤ 0.65 for SPIN. Both NPF and SPIN showed excellent intra-examiner reliability (ICC > 0.99). These results justified the choice of Mid.NPF for the palatal plane construction in combination with GPF.L&R, instead of using Mid.SPIN.

In the antero-posterior dimension, NPF also showed excellent intra-examiner reliability and agreement for accuracy (ICC > 0.92) and low mean identification errors ≤ 0.85 mm. Its stable and distinct location in the anterior palate justified the choice of Mid.NPF for frontal plane construction in combination with IORB.L&R.

Foramen Spinosum (SPIN) & Mid.SPIN

Foramen Spinosum (SPIN) and Mid.SPIN (a.k.a. ELSA ⁹⁵) was chosen based on several factors. It is a blunt-ended and short canal of only 2-3 mm. It has consistent position along the mid-sagittal plane, and its cross-section is consistently rounded and small (2.4x2.0 mm) ¹¹⁸. According to Berge and Bergman, SPIN was never absent bilaterally (0%, or 0/92) and found to be equal-sized bilaterally (within 0.5 mm) in large majority of case (84%, 77/92) ¹¹⁸. Marmary et al also advocated using Mid.SPIN as a perpendicular bisector to produce an accurate midline which was relatively unaffected by environmental factors ^{98,119}. In agreement with a past 2-D cephalometric study by Williamson et al, SPIN was found to have the smallest identification errors in the vertical and horizontal dimensions as explained by its narrow diameter ¹²⁰. In this study, SPIN had ≤ 0.55 mm mean error in the transverse, and Mid.SPIN had ≤ 0.51 mm mean errors in the vertical and antero-posterior dimensions.

Overall, this makes SPIN and Mid.SPIN a valuable 3-D reference landmark for future clinical analyses. This observation aligns with several other previous 3-D studies, including Lagravere et al, Tausche et al, and Hansen et al ^{34,37,39}.

Mesial Dorsal Foramen Magnum (MDFM)

Mesial Dorsal Foramen Magnum (MDFM) showed excellent agreement for accuracy and intra-examiner reliability (ICC >0.99) in this study. MDFM was chosen based on its ease of identification and consistent position along the mid-sagittal plane. MDFM is analogous to the widely used 2-D cephalometry landmark, Basion ¹²¹. Additionally, analogous to NPF being the most anterior landmark within the set, MDFM is the most posterior. As mentioned previously, this allows maximum posterior-anterior distance for reducing extrapolation errors ⁹⁵.

IORB (Infra-orbital foramen) left & right

The left and right Infra-orbital landmarks (IORB.L&R) proved superior to other candidates and were chosen for frontal plane construction, in combination with Mid.NPF. Based on these ten dry skulls, the orientation of this plane tended to parallel mid-arch maxillary teeth such as the first and second premolars and first molars. This was a best attempt for measurement of antero-posterior movement of premolar and molar teeth after

maxillary expansion, although no attempts were made to account for the anterior-most or posterior-most teeth (such as central incisors or second molars) owing to the natural Curve of Spee found along the occlusal plane ¹²².

To construct an effective frontal plane, there needs to be 3+ reference landmarks vertically aligned along a plane that would ideally parallel the long axis of the teeth to be measured in order to reflect isolated antero-posterior changes. For the purpose of orthodontics, the choice of MENT was not considered due to the likelihood of mandibular deviation in posterior crossbite patients, and also because MENT proved to have mean identification errors of between 0.75 mm to 1.3 mm. The use of CG in combination with IORB or Mid.NPF could also be evaluated and compared with these results in a future study. However CG was not used in this study because the superior aspect of its tip was marginally just captured on this dry skull sample, and would likely be collimated off in CBCT scans on young growing children seeking orthodontic treatment. The limitation of IORB is its densely radiopaque tapering opening, making it difficult to mark its exact geometric center in the three dimensions. However by using the specified 3-D definition of the landmark (Table 4.1-4.4) and verifying the landmark from all planar views, good to excellent reliability and low errors were found based on this study. Given the mentioned limitations, IORB.L&R and Mid.NPF proved to serve as an effective frontal plane for assessment of anterior-posterior changes limited to the premolar and first molar teeth.

Greater Palatine foramen (GPF) left & right

Greater palatine foramen (GPF) was another important landmark particularly for constructing the palatal plane in this study. It is located on the horizontal plate of the palatal bone. The greater palatine foramina (GPF) has been reported to maintain a set distance from to the posterior margin of the osseous palate by Serjen et al and Damgaard et al ¹²³, and to not change significantly with age. Antero-posterior growth of the palate is believed to take place at the Transverse palatine suture (TPS), which is positioned anterior to the GPF. Greater differential osseous growth occurs on the maxillary edge of the suture compared to the palatine edge, and the GPF is reported to be located palatal and posterior to the posterior-most erupted molar teeth ^{123,124}. Studies generally report GPF to be located posterior and palatal to the mid-palatal aspect of the upper third molar although locations

palatal to the region between the third and second molar have also been reported ¹²⁵. Since maxillary expansion appliances are attached to the region between first molars and first premolars, the position of GPF is highly favorable in that it is unlikely to be influenced by orthodontic movements of the posterior teeth, and be able to reflect the skeletal changes experienced by this region ¹²³.

There is an important point to note when using the GPF landmark. One is that the foramen tapers into thin area of bone in the antero-posterior dimension when viewed from the occlusal direction ¹²⁵. This foramen is two-fold longer in the antero-posterior dimension than the medial-lateral/transverse dimension, approximately 2x4 mm on average ¹¹⁸. Therefore, it is critical to give priority to the Coronal view of the GPF, where its diameter is only 2 mm wide, and where the bony nasal floor is present as a guide during the identification process. Excellent agreement for intra-examiner reliability and accuracy (ICC > 0.98) was found using this technique, and mean identification errors were all kept $\leq 0.65 \pm 0.5$ mm in this research. Particularly in the vertical dimension, its low mean identification errors were comparable to that of SPIN and Mid.SPIN; as well as showing excellent agreement for accuracy and reliability as indicated by an ICC ≥ 0.99 in all dimensions.

Remaining candidate reference landmarks

The remaining sets of landmarks proved to be promising for plane construction, but nonetheless were not selected due to their respective identification difficulty. These remaining landmarks were: Posterior Vidian canal opening (PVID), External Auditory Meatus (EAM), Foramen Ovale (OVAL), and Crista galli (CG).

The Posterior Vidian canal opening (PVID) landmark proved to be a satisfactory choice in all dimensions and particularly in the transverse where mean errors were as low as ≤ 0.30 mm. However, two limitations were encountered from using PVID. One is the tapered posterior opening instead of a blunt orifice ¹⁰⁹, making the antero-posterior limit difficult to delineate. Second is PVID's close proximity to similar sized foramen such as the Palatosphenoidal canal ¹²⁶ from the coronal view, making it difficult to distinguish the two. Consequently, Mid.SPIN, with the more distinctive anatomical features, was chosen instead.

Pinpointing the exact geometric center was difficult and time-consuming for the EAM since it had a long tortuous canal with an oval cylindrical cross-section of approximately 5 to

9 mm¹²⁷. Difficulties in identifying Porion, the 2-D analogous landmark to EAM, has also been widely reported in past literature^{128,129}.

Foramen ovale (OVAL) was another landmark with relatively large cross-section area, around 7 mm x 3.5 mm on average¹¹⁸. Its elongated antero-posterior dimension may have contributed to its mean error of -0.85 mm, while errors were only 0.4 mm - 0.55 mm in the other two dimensions. Calculation of Mid.OVAL by taking the average of bilateral OVAL did not reduce the mean errors recorded in the antero-posterior dimension. Furthermore, bilateral OVAL landmarks were reported to be varied in size (>0.5 mm difference), in 56/96 (58%) of subjects according to Berge and Bergeman¹¹⁸.

Crista galli (CG) was a promising landmark, and one used widely in 2-D Postero-anterior cephalometry. However, it was less preferred in this study due to its likelihood of being collimated out of view during CBCT scan. This was due to a medical decision to reduce radiation exposure to young growing children.

3.9.3 Reference plane construction

Based on three repeatedly constructed reference planes for 10 dry skulls as assessed using twenty selected landmarks, low mean errors were found in all 3 dimensions (Table 4.8). The mean errors were ≤ 0.55 mm, ≤ 0.35 mm, and ≤ 0.45 mm, in the Mid-sagittal plane (transverse orthogonal distances), Palatal plane (vertical orthogonal distances), and Frontal plane (antero-posterior orthogonal distances) respectively.

The small mean errors combined with visual verification of the planes, demonstrated that these reference landmarks can be used for plane construction in future clinical studies involving maxillary expansion. It should be noted that upon imposing an artificial 0.2 mm of error into the reference landmarks responsible for each plane, the errors did increase but not directly proportional. Errors were observed to cancel each other out when one landmark was marked closer to origin while the second landmark was marked further from origin. This finding is in agreement with Lagravere et al who commented on the same observation⁹⁵.

Further analysis was performed in attempt to observe the mean errors of orthogonal distances from 3 repeated treatment landmark measurements against an averaged reference

plane. In this test case, the reference planes were constructed based on the average values of three repeated reference landmark measurements.

Almost all measurements (22 out of 26 sets of landmarks) showed ≤ 0.35 mm, ≤ 0.85 mm, and ≤ 0.85 mm of mean errors (not clinically significant) for the Transverse, Vertical, and Antero-posterior orthogonal distances, respectively.

The four exceptions included the antero-posterior orthogonal distances for Posterior Vidian Canal (PVID) and Foramen Ovale (OVAL) which showed mean errors ≤ 1.25 mm; and vertical orthogonal distances for IORB.L and APEX.16 with mean error ≤ 1.24 mm and ≤ 1.10 mm, respectively. These 4 landmarks still showed ≤ 0.35 mm error in the Transverse dimension, and ≤ 0.85 mm in the other dimension (not clinically significant). Nonetheless, these investigated landmarks all showed mean identification errors under 1.5 mm and are not likely to have clinical implications. Hence, these were still kept in the pool of candidate landmarks.

Defining 3D planes can be difficult by itself due to the high degree of freedom in all 3 axes. This study's premise is to have an easily repeatable process for measuring skeletal and dental changes over time. Using this mathematical procedure, given the same reference landmark coordinate input, the computed plane will always be the same. This is a great improvement to earlier methods that requires the examiner to manually draw the mid-sagittal plane, as it will eliminate any human error that process may introduce. It should be noted that this mathematically constructed plane is still susceptible to the measurement errors from the individual reference landmarks itself.

3.9.4 Dental Landmarks for Treatment Evaluation

Root Apices

Root Apices (APEX) showed good-to-excellent agreement for accuracy and intra-examiner reliability in all dimensions (ICC > 0.75). Mean identification errors were kept under ≤ 0.7 mm in all dimensions, which was still highly acceptable. The larger observed identification errors at the APEX compared to the pulp horn may result from the fact that the root apex was less sharply pointed in comparison. More pointed root apices, such as the

mesial-buccal root of the maxillary molar, did show slightly less identification errors compared to the broader singular roots of the canines in this study.

Buccal Alveolar Bone at the level of Root Apex (AVBN)

Buccal alveolar bone landmarks (AVBN) showed good-to-excellent agreement for accuracy and intra-examiner reliability in the transverse and vertical dimensions ($ICC > 0.75$) in this study. It was helpful to use the guiding line to match the root apex level and ensure that it's parallel to the root canal. Without this guiding line, there would be multiple possible landmark placements, particularly depending on the curvature or contours of the buccal bony plate.

It should be noted that the AVBN landmark shall not be used for any antero-posterior measurements since only moderate agreement for accuracy ($ICC \geq 0.60$) was found, and there is no anatomically distinct antero-posterior feature for repeatable identification. Use of this guiding line is possibly the best guide available at this point in time.

Pulp Horn

Tip of Pulp horn (PULP) showed excellent agreement for accuracy and intra-examiner reliability in all three dimensions ($ICC > 0.90$). Identification error in the vertical direction was slightly larger, being ≤ 0.75 mm. Nonetheless, accuracy in this dimension was still ≤ 0.85 mm as with the other landmarks in this study. Mean identification errors was one of the lowest in the transverse dimension (≤ 0.30 mm) and antero-posterior (≤ 0.5 mm) for the maxillary and mandibular molars, maxillary premolar and canine teeth evaluated in this study.

3.9.5 Limitations

Numerous factors need to be considered when interpreting these results. Firstly, the assessment of reference landmark accuracy and intra-examiner reliability was performed on dry skulls. As pointed out by Periago et al ¹³⁰, the presence of nerves or other soft tissue structures inside the foramina may affect the accuracy of landmark identification. In attempt

to mimic the soft tissues around the skull, the principal investigator incorporated a Plexiglass box filled with water around every skull prior to the CBCT scan, in efforts to reduce possible error.

Secondly, the number of dry skull specimens used in this study was 10. As recommended by Springate¹³¹, increasing the number of specimens to 25 to 30 would reduce sampling errors for the statistical analyses in such types of study.

Third, the bone quality and scan quality were factors not fully within our control. The voxel size was 0.3 mm in this study, and this placed a limit to the accuracy level possible. During dry skull selection, efforts were made to check for a full healthy posterior dentition and intact bony structures. Furthermore, the dry skulls were not all collected from adolescent age group which could be commonly seen in subjects requesting for orthodontic treatment. The size and location of the foramina may show slight variation in dry skulls of the mid-ages.

Three-dimension visualization software such as the one used by this study (AVIZO) requires substantial training and patience to operate in general. Locating a 3-D landmark accurately requires constantly switching between the 3 axial planes on the monitor and iterating through hundreds of orthogonal slices. This may change in the near future when 3-D monitors become more commonly available.

3.9.6 Summary & Conclusion

Reference landmarks

- Accuracy: Nearly all investigated landmarks (24 out of 26 sets) showed low mean errors (≤ 0.85 mm) and excellent agreement ($ICC > 0.92$), in all 3 axes, allowing them to be used in future clinical studies.
- Intra-examiner reliability: All 26 sets of landmarks showed excellent intra-examiner reliability ($ICC > 0.96$), with low mean errors of ≤ 0.5 mm, in all 3 axes.

Landmarks used for reference plane construction

- The preferred landmarks for mid-sagittal plane were: Mid.Nasopalatine Foramen (Mid.NPF), Mesial Dorsal Foramen Magnum (MDFM), and Foramen Spinosum (SPIN).

- The preferred landmarks for frontal plane were: Infra-orbital foramina (IORB) left & right, and Mid.NPF.
- The preferred landmarks for palatal plane were: Greater palatine foramina (GPF) left & right, and Mid.NPF.
- These combinations and landmarks, proved to be comparatively superior to other options.
- Based on three repeatedly constructed reference planes for 10 dry skulls as assessed using twenty selected landmarks, low mean errors (≤ 0.55 mm) were found in all 3 dimensions.
- Further analysis to observe the mean errors of orthogonal distances from 3 repeated treatment landmark measurements against an averaged reference plane, also showed low mean errors (≤ 0.85 mm) in all 3 dimensions.
- Measurement errors ≤ 1.5 mm are not likely to have clinical implications from past literature.

Treatment Landmarks

- All teeth root apices (tip), pulp horn (tip), and alveolar bone landmarks (AVBN) showed good to excellent reliability and accuracy particularly in the transverse and vertical dimension; and will be used in the future maxillary expansion assessment study.

3.10 References

15. Sievers MM, Larson BE, Gaillard PR, Wey A. Asymmetry assessment using cone beam CT: A Class I and Class II patient comparison. *The Angle Orthodontist* 2011;82:410-417.
20. Lagravère MO, Carey J, Toogood RW, Major PW. Three-dimensional accuracy of measurements made with software on cone-beam computed tomography images. *American Journal of Orthodontics and Dentofacial Orthopedics* 2008;134:112-116.
24. Lagravère MO, Gordon JM, Guedes IH, Flores-Mir C, Carey JP, Heo G et al. Reliability of traditional cephalometric landmarks as seen in three-dimensional analysis in maxillary expansion treatments. *The Angle orthodontist* 2009;79:1047-1056.
26. Lee K-M, Hwang H-S, Cho J-H. Comparison of transverse analysis between posteroanterior cephalogram and cone-beam computed tomography. *Angle Orthodontist* 2013;84:715-719.
32. Oz U, Orhan K, Abe N. Comparison of linear and angular measurements using two-dimensional conventional methods and three-dimensional cone beam CT images reconstructed from a volumetric rendering program in vivo. *Dentomaxillofac Radiol* 2011;40:492-500.
34. Lagravère MO, Carey J, Heo G, Toogood RW, Major PW. Transverse, vertical, and anteroposterior changes from bone-anchored maxillary expansion vs traditional rapid maxillary expansion: A randomized clinical trial. *American Journal of Orthodontics and Dentofacial Orthopedics* 2010;137:304.e301-304.e312.
37. Hansen L, Tausche E, Hietschold V, Hotan T, Lagravère M, Harzer W. Skeletally-anchored Rapid Maxillary Expansion using the Dresden Distractor. *Journal of Orofacial Orthopedics / Fortschritte der Kieferorthopädie* 2007;68:148-158.
39. Tausche E, Hansen L, Hietschold V, Lagravère MO, Harzer W. Three-dimensional evaluation of surgically assisted implant bone-borne rapid maxillary expansion: A pilot study. *American Journal of Orthodontics and Dentofacial Orthopedics* 2007;131:S92-S99.
80. Alavi DG, BeGole EA, Schneider BJ. Facial and dental arch asymmetries in Class II subdivision malocclusion. *American Journal of Orthodontics and Dentofacial Orthopedics* 1988;93:38-46.
81. Mraiwa N, Jacobs R, Van Cleynenbreugel J, Sanderink G, Schutyser F, Suetens P et al. The nasopalatine canal revisited using 2D and 3D CT imaging. *Dentomaxillofac Radiol* 2004;33:396-402.
88. Mah J HD. Three-dimensional craniofacial imaging. *Am J Orthod Dentofacial Orthop* 2004;126:308-309.
91. Shibata M, Nawa H, Kise Y, Fuyamada M, Yoshida K, Katsumata A et al. Reproducibility of three-dimensional coordinate systems based on craniofacial landmarks. *The Angle Orthodontist* 2012;82:776-784.
95. Lagravere MO, Major PW, Carey J. Sensitivity analysis for plane orientation in three-dimensional cephalometric analysis based on superimposition of serial cone beam computed tomography images. *Dentomaxillofac Radiol* 2010;39:400-408.
96. Naji P, Alsufyani NA, Lagravère MO. Reliability of anatomic structures as landmarks in three-dimensional cephalometric analysis using CBCT. *The Angle Orthodontist* 2013;84:762-772.

97. Lagravère MO, Gordon JM, Flores-Mir C, Carey J, Heo G, Major PW. Cranial base foramen location accuracy and reliability in cone-beam computerized tomography. *American Journal of Orthodontics and Dentofacial Orthopedics* 2011;139:e203-e210.
98. Arat ZM, Rübendüz M, Arman Akgül A. The displacement of craniofacial reference landmarks during puberty: a comparison of three superimposition methods. *The Angle orthodontist* 2003;73:374-380.
99. Trpkova B, Prasad NG, Lam EW, Raboud D, Glover KE, Major PW. Assessment of facial asymmetries from posteroanterior cephalograms: validity of reference lines. *American journal of orthodontics and dentofacial orthopedics* 2003;123:512-520.
100. Athanasiou AE. *Orthodontic cephalometry*. London ; Baltimore: : Mosby-Wolfe; 1995.
101. Major PW, Johnson DE, Hesse KL, Glover KE. Landmark identification error in posterior anterior cephalometrics. *The Angle orthodontist* 1994;64:447-454.
102. MIDTGÅRD J, BJÖRK G, Linder-Aronson S. Reproducibility of cephalometric landmarks and errors of measurements of cephalometric cranial distances. *The Angle orthodontist* 1974;44:56-61.
103. Jacobson A, RL J. *Radiographic Cephalometry: From Basics to 3-D Imaging, (Book/CD-ROM set), Chapter 24; 2007: p. 293-299.*
104. Baumrind S, Frantz RC. The reliability of head film measurements: 1. Landmark identification. *American journal of orthodontics* 1971;60:111-127.
105. Afrand M, Ling CP, Khosrotehrani S, Flores-Mir C, Lagravère-Vich MO. Anterior cranial-base time-related changes: A systematic review. *American Journal of Orthodontics and Dentofacial Orthopedics* 2014;146:21-32.e26.
106. Moss ML, Salentijn L. Differences between the functional matrices in anterior open-bite and in deep overbite. *American journal of orthodontics* 1971;60:264-280.
107. Keith A, Champion GG. A Contribution to the Mechanism of Growth of the Human Face. *International Journal of Orthodontia, Oral Surgery and Radiography* 1922;8:607-633.
108. Bidarkotimath S, Viveka S, Udyavar A. Vidian canal: radiological anatomy and functional correlations. *J Morpholl Sci* 2012;29:27-31.
109. Chen J, Xiao J. Morphological study of the pterygoid canal with high-resolution CT. *Int J Clin Exp Med* 2015;8:9484-9490.
110. Sayinsu K, Isik F, Trakyali G, Arun T. An evaluation of the errors in cephalometric measurements on scanned cephalometric images and conventional tracings. *Eur J Orthod* 2007;29:105-108.
111. Jacobson A, Jacobson RL. *Radiographic Cephalometry: From Basics to 3-D Imaging, (Book/CD-ROM set) ,Chapter 7. 2007.*
112. Gupta T. Localization of important facial foramina encountered in maxillo-facial surgery. *Clinical Anatomy* 2008;21:633-640.
113. Aggarwal A, Kaur H, Gupta T, Tubbs RS, Sahni D, Batra YK et al. Anatomical study of the infraorbital foramen: A basis for successful infraorbital nerve block. *Clin Anat* 2015;28:753-760.

114. Damstra J, Fourie Z, Slater JJH, Ren Y. Reliability and the smallest detectable difference of measurements on 3-dimensional cone-beam computed tomography images. *American journal of orthodontics and dentofacial orthopedics* 2011;140:e107-e114.
115. Weisstein EW. "Point-Plane Distance.". *MathWorld--A Wolfram Web Resource*. <http://mathworld.wolfram.com/Point-PlaneDistance.html>; 2016.
116. Portney L WM. *Foundations of clinical research: applications to practice.*: Prentice Hall, Upper Saddle River 2008.
117. Nagasaka S, Fujimura T, Segoshi K. Development of a non-radiographic cephalometric system. *Eur J Orthod* 2003;25:77-85.
118. Berge JK, Bergman RA. Variations in size and in symmetry of foramina of the human skull. *Clinical anatomy* 2001;14:406-413.
119. Marmary Y, Zilberman Y, Mirsky Y. Use of foramina spinosa to determine skull midlines. *The Angle Orthodontist* 1979;49:263-268.
120. Williamson PC, Major PW, Nebbe B, Glover KE, West K. Landmark identification error in submentoververtex cephalometrics: a computerized method for determining the condylar long axis. *Oral Surgery, Oral Medicine, Oral Pathology, Oral Radiology, and Endodontology* 1998;86:360-369.
121. Madsen DP, Sampson WJ, Townsend GC. Craniofacial reference plane variation and natural head position. *The European Journal of Orthodontics* 2008;30:532-540.
122. Braun S, Hnat WP, Johnson BE. The curve of Spee revisited. *American journal of orthodontics and dentofacial orthopedics* 1996;110:206-210.
123. Damgaard C, Caspersen LM, Kjaer I. Maxillary sagittal growth evaluated on dry skulls from children and adolescents. *Acta Odontol Scand* 2011;69:274-278.
124. Sejrsen B, Jakobsen J, Kjær I. Human palatal growth evaluated on medieval crania using nerve canal openings as references. *American journal of physical anthropology* 1996;99:603-611.
125. Ikuta CRS, Cardoso CL, Ferreira-Júnior O, Lauris JRP, Souza PHC, Rubira-Bullen IRF. Position of the greater palatine foramen: an anatomical study through cone beam computed tomography images. *Surgical and Radiologic Anatomy* 2013;35:837-842.
126. Pinheiro-Neto CD, Fernandez-Miranda JC, Rivera-Serrano CM, Vaezi AE, Snyderman CH, Gardner PA. Endoscopic Anatomy of the Palatovaginal Canal (Palatosphenoidal Canal): A Landmark for Dissection of the Vidian Nerve during Endonasal Transpterygoid Approaches. *Skull Base* 2011;21:A045.
127. Mahboubi H, Wu EC, Jahanbakhshi R, Coale K, Rothholtz VS, Zardouz S et al. A novel method to determine standardized anatomic dimensions of the osseous external auditory canal. *Otol Neurotol* 2012;33:715-720.
128. Pancherz H, Gökbüget K. The reliability of the Frankfort horizontal in roentgenographic cephalometry. *The European Journal of Orthodontics* 1996;18:367-372.
129. Choi JW, Jung SY, Kim H-J, Lee S-H. Positional symmetry of porion and external auditory meatus in facial asymmetry. *Maxillofacial plastic and reconstructive surgery* 2015;37:1.

-
130. Periago DR, Scarfe WC, Moshiri M, Scheetz JP, Silveira AM, Farman AG. Linear accuracy and reliability of cone beam CT derived 3-dimensional images constructed using an orthodontic volumetric rendering program. *The Angle orthodontist* 2008;78:387-395.
131. Springate S. The effect of sample size and bias on the reliability of estimates of error: a comparative study of Dahlberg's formula. *The European Journal of Orthodontics* 2012;34:158-163.

Chapter 4

4. Three-dimensional changes between tooth-borne versus bone-borne (Dresden-type) rapid maxillary expansion in adolescents: A randomized clinical trial.

4.1 Introduction

Posterior crossbite (PXB) is one of the most easily recognized clinical signs that result from a transverse constricted maxilla¹. This narrow maxillary width relative to the mandible, causes a mismatch between opposing posterior teeth when biting into maximum intercuspation^{1,8,9}. This can bring a negative cosmetic and functional impact on patients, including, but not limited to excess buccal corridor spaces when smiling, crowded anterior teeth, and uneven dental attrition^{1,10}.

This study is interested specifically in the true maxillary constriction cases where the primary treatment is through rapid maxillary expansion. As discussed in chapter 2, conventional correction of maxillary constriction was often done using a Tooth-borne Rapid Maxillary Expander (T-RME). Due to its dental attachment, T-RME has long been reported to induce greater dental than skeletal expansion (70% dental vs. 30% skeletal)³⁵. Mild levels of undesirable maxillary molar crown tipping, and bite opening have been reported in previous studies evaluating short-term effects of T-RME, although this has not been consistent throughout the literature^{13,34,132,133}. Consequently, B-RME was designed to hopefully reduce the various dental side-effects^{36,37}. B-RME attempts to minimize dental structures disturbance and maximize skeletal expansion by directly inserting either shortened palatal implants or temporary anchorage devices (TADs)^{36,37} into the two halves of the bony maxillary palate.

The Dresden B-RME design was chosen to be used in adolescents for the first time in this study. This appliance had been used in two previous studies on ten mature adult patients who underwent surgically-assisted rapid maxillary expansion in the study by Tausche et al³⁹ and Hansen et al³⁷. The Dresden B-RME has a unique design feature where it is anchored by an osteointegrated implant on one side and a mini-implant-anchor (a.k.a. Temporary Anchorage Devices, or TAD) on the other.

Efforts from the previous chapter (see chapter 3) provided a set of 3-D reference planes that have been experimentally proven to be accurate and reliable. Using these planes

along with selected treatment landmarks allows a quantitative measure of transverse, vertical, and antero-posterior changes after T-RME/B-RME/no treatment after 6 months' observation.

This study focuses on the maxillary changes, since spontaneous mandibular correction is not very predictable beyond the early mixed dentition phase^{11,44}. Furthermore, correction of the maxillary base allows more normal growth from an “unlocked” mandible^{75,134}.

The primary objective of this study is to understand the 3-dimensional skeletal and dental maxillary effects of the Dresden Bone-Borne Rapid Maxillary Expander (B-RME) and the 4-Band Tooth-Borne Rapid Maxillary Expander (T-RME). Both of these treatments will be used in patients with maxillary transverse constriction.

4.2 Materials & Methods

4.2.1 Subjects

This study was granted ethics approval by the Health Research Ethics Board at the University of Alberta (Pro#00013379). Fifty healthy adolescent patients (27 females and 23 males) with transverse maxillary constriction and unilateral or bilateral posterior crossbite who presented to the University of Alberta Orthodontic Clinic from Sept 2007 to Sept 2010 were included. All eligible patients were aged between 11-18 years, non-syndromic, and diagnosed by an orthodontist to require at least 5 mm of maxillary transverse constriction correction as directly measured using calipers. Maxillo-mandibular width difference was determined by calculating the difference between maxillary and mandibular inter-molar widths. Maxillary inter-molar width was measured from the palatal cusp tips of the left and right upper first molars. Mandibular inter-molar width was measured between central fossae of the left and right lower first molars. A 20% overcorrection was then added to the total expansion requirements in order to account for potential maxillary relapse. Patients were only eligible when no surgical or other orthodontic treatments were assigned during the expansion period.

A minimum sample size of 45 patients (15 patients per treatment group) was calculated using a statistical power of 0.9 considering a significance level of 0.05¹¹⁶, based on

a previous study by Lagravère et al ²⁴. Subjects were randomly allocated into one of three groups (Table 4-1). Mean ages of the 3 groups were approximately 13 - 14 years.

4.2.2 RME Design and Activation Protocol

The chosen Bone-borne expander (B-RME) was the Dresden-type hyrax expander. Its design consisted of a temporary anchorage device (TAD-side) on one side and a shortened-implant (Implant-side) on the other. This Dresden-B-RME had the same design as the type used by Tausche et al ³⁹ and Hansen et al ³⁷. The only difference is that their studies involved surgically-assisted RME (SARME) in ten adults with skeletal maxillary constriction (Figure 4.1B, Figure 4.2).

The TAD anchor of this B-RME appliance had a length of 8 mm, diameter of 1.5 mm and made of titanium (Straumann, Andover, Mass). The self-tapping shortened palatal implant (Implant-side), had a reduced length of 4 mm, diameter of 3.5 mm, made of Titanium (Straumann, Andover, Mass). Both bone anchors were inserted paramedian to the midpalatal suture, between the maxillary second premolars and first molars on an individualized basis. Prior to TAD and palatal implant insertion, all patients received a 2-minute chlorhexidine (0.12%) pre-rinse. All bone-borne expanders were placed by one orthodontist under topical and local anesthesia. A total of 17 subjects were treated using the Dresden-B-RME. There was 1 week of healing period before activation of the B-RME expander screw. The expansion screw (Palex II Extra-Mini Expander, Summit Orthodontic Services, OH, USA) was only activated by 0.25-mm daily. This was to take precautions and prevent potential palatal shelf fractures ^{33,34}.

A traditional 4-band Tooth-borne expander (T-RME) design was used in 17 subjects. The appliance was cemented to maxillary first molar and first premolar (Figure 4.1A). The expansion screw was activated by 0.50-mm daily.

Both treatment groups received a minimum of 5 mm expander screw activation, until the PXB was fully corrected and the palatal cusps of the maxillary molars met with the buccal cusp of the lower molars according to the McNamara protocol. The expanders in both treatment groups were left in passive state and sealed with light-cured composite, to prevent screw unwinding in the additional 4 to 6 months of bony consolidation after active expansion.

The control group were age-matched and gender-matched adolescents with PXB who had treatment delayed for 6 months, where there were no negative consequences regarding the patient's treatment outcome. The purpose of the untreated control group was to control for natural growth differences that may have occurred over the six month period without treatment.



Figure 4.1. Clinical Photo of the A) Tooth-borne (Left), and B) Bone-borne Expander (Right)



Figure 4.2. Bone-borne RME (B-RME) with Mini-Hyrax jackscrew supported by TAD on one side (TAD-anchor side), and palatal implant (Implant-anchor side) on the other.

Table 4-1. Subject Demographics

Appliance	n	Gender (F/M)		Mean Age ± S.D. at T1 (y)	Age Range at T1 (y)	Mean Age ± S.D. at T2 (y)	Age Range at T2 (y)	Time Interval T2 - T1 (y)
B-RME	17	10	7	14.1 ± 1.6	12.0 - 17.6	14.7 ± 1.6	12.7 - 18.2	0.6 ± 0.1
T-RME	17	9	8	13.7 ± 1.1	11.9 - 16.4	14.3 ± 1.1	12.5 - 16.9	0.6 ± 0.1
Ctrl	16	8	8	13.3 ± 1.7	10.5 - 15.8	14.1 ± 1.9	11.1 - 16.6	0.8 ± 0.6

Table 4-2. Subject Demographics within B-RME group

B-RME Analysis	n	Gender (F/M)		Mean Age ± S.D. at T1 (y)	Age Range at T1 (y)	Mean Age ± S.D. at T2 (y)	Age Range at T2 (y)	Time Interval T2 - T1 (y)
TAD- L (IMP-R)	10	7	4	13.8 ± 1.3	12.0 - 15.9	14.5 ± 1.3	12.7 - 17.0	0.7 ± 0.1
TAD- R (IMP-L)	7	3	3	14.6 ± 1.9	12.5 - 17.6	15.2 ± 2.0	13.1 - 18.2	0.6 ± 0.1

4.3 Identification of CBCT Landmarks

The CBCT scans of 0.3-mm voxel size were taken with the I-CAT 1st generation machine (9 sec exposure time, 13 cm x 16 cm FOV, 0.3 mm voxel size, Imaging Sciences International, Hatsfield, PA) at 120 kV, 5 mAs with 8 mm aluminum filtration according to manufacturer's settings. The head position of all subjects were aligned and standardized using the vertical laser beam (aimed at Mid-sagittal plane) and horizontal laser beam (aimed at Frankfort horizontal) during radiographic acquisition. CBCT imaging was done before treatment (T1) and 6 months after full PXB correction with overexpansion (T2) in all three groups. The CBCT data were exported as DICOM files (Digital Imaging and Communications in Medicine) and then loaded into AVIZO 8.1 software (FEI Visualization Sciences Group, Burlington, Mass) for further analysis. A Cartesian coordinate system was used for each CBCT volume, with the origin of the x,y,z axis determined at the time of scan.

The CBCT volumes were viewed in three planes: x-y axial (right-left), x-z coronal (superior-inferior), and y-z sagittal (anterior-posterior). The principal investigator marked all

3-D landmarks using virtual sphere markers of 0.20 mm diameter. The center position of the virtual marker was used to determine the landmark's precise location in this software; hence the marker size did not affect the landmark position. The pre-determined 3-D definitions detailed in chapter 3 (Table 3-1 - Table 3-3) were used to identify the landmarks. The examiner was blinded to the subjects' age, treatment group and time of acquisition to reduce bias.

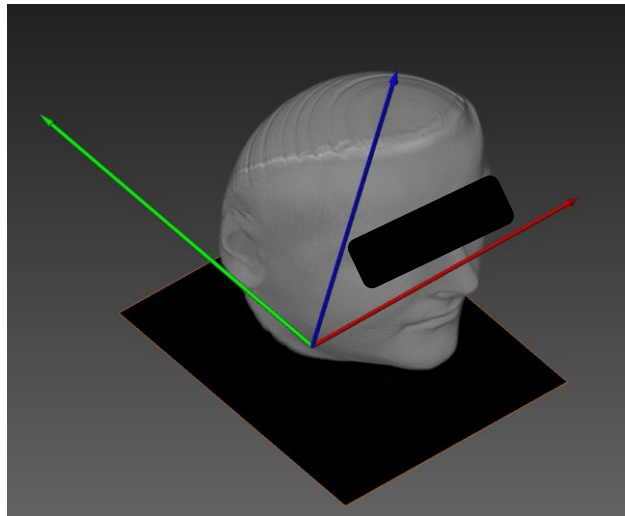


Figure 4.3: Orientation of the 3 axes:

X-axis (Red, Transverse), Y-axis (Green, Anterior-posterior), Z-axis (Blue, Vertical).

4.3.1 Orthogonal distances between landmarks to planes

Using the experimentally proven technique in chapter 3, a set of accurate and reliable 3-D landmarks were identified and used to calculate orthogonal distances relative to respective reference planes, in order to quantitatively compare the transverse, vertical and antero-posterior differences between and within the three treatment groups, across both T1 (baseline) and T2 (6 months after). The reference and treatment landmarks all showed excellent accuracy and intra-examiner reliability agreement, along with low identification errors (ICC > 0.92; mean errors ≤ 0.85 mm) (see chapter 3).

4.4 Results

4.4.1 Measurement error

To assess measurement error of orthogonal distances relative to the reference planes, 24 randomly selected CBCT volumes were selected, and the reference landmarks used to construct the three reference planes were repeated three times. Small mean measurement errors of ≤ 0.55 mm, ≤ 0.55 mm, and ≤ 0.30 mm, were found in the Mid-sagittal plane (Transverse orthogonal distances), Palatal plane (Vertical orthogonal distances), and Frontal plane (Antero-posterior orthogonal distances) respectively (Table 4-3).

Table 4-3: Mean errors (in mm) from 3 repeated reference plane constructions for the skeletal and dental landmarks.

Landmarks	Transverse			Vertical			Antero-posterior		
	Mean +/- SD (mm)	Max (mm)	Min (mm)	Mean +/- SD (in mm)	Max (mm)	Min (mm)	Mean +/- SD (in mm)	Max (mm)	Min (mm)
PULP.16	0.31 ± 0.24	0.67	0.05	0.23 ± 0.21	0.58	0.03	0.21 ± 0.16	0.42	0.08
PULP.26	0.35 ± 0.26	0.68	0.05	0.26 ± 0.32	0.83	0.05	0.20 ± 0.04	0.27	0.09
PULP.14	0.25 ± 0.28	0.77	0.06	0.37 ± 0.32	0.91	0.04	0.19 ± 0.16	0.42	0.07
PULP.24	0.26 ± 0.29	0.78	0.05	0.38 ± 0.41	1.09	0.07	0.20 ± 0.08	0.29	0.09
PULP.13	0.30 ± 0.32	0.81	0.04	0.47 ± 0.37	1.05	0.04	0.22 ± 0.17	0.48	0.03
PULP.23	0.33 ± 0.35	0.82	0.07	0.48 ± 0.45	1.22	0.05	0.20 ± 0.13	0.34	0.09
PULP.46	0.46 ± 0.40	1.07	0.06	0.24 ± 0.17	0.50	0.03	0.21 ± 0.17	0.49	0.06
PULP.36	0.49 ± 0.46	1.26	0.06	0.24 ± 0.27	0.71	0.12	0.23 ± 0.13	0.40	0.08
APEX.16	0.17 ± 0.22	0.59	0.04	0.19 ± 0.13	0.39	0.04	0.22 ± 0.10	0.38	0.15
APEX.26	0.17 ± 0.22	0.60	0.02	0.23 ± 0.26	0.69	0.08	0.25 ± 0.10	0.37	0.18
APEX.14	0.24 ± 0.24	0.66	0.05	0.30 ± 0.22	0.65	0.04	0.20 ± 0.13	0.36	0.04
APEX.24	0.22 ± 0.23	0.67	0.04	0.33 ± 0.31	0.85	0.06	0.20 ± 0.06	0.28	0.11
APEX.13	0.27 ± 0.22	0.67	0.05	0.35 ± 0.25	0.73	0.03	0.18 ± 0.10	0.31	0.07
APEX.23	0.27 ± 0.22	0.67	0.05	0.35 ± 0.30	0.85	0.05	0.18 ± 0.04	0.22	0.12

APEX.46	0.55 ± 0.49	1.49	0.07	0.27 ± 0.20	0.59	0.03	0.26 ± 0.19	0.57	0.11
APEX.36	0.55 ± 0.46	1.46	0.07	0.28 ± 0.31	0.82	0.02	0.25 ± 0.17	0.47	0.07
AVBN.16	0.17 ± 0.21	0.58	0.04	0.18 ± 0.12	0.37	0.05	0.23 ± 0.10	0.39	0.16
AVBN.26	0.18 ± 0.22	0.60	0.01	0.24 ± 0.26	0.71	0.10	0.23 ± 0.14	0.46	0.10
AVBN.14	0.24 ± 0.24	0.66	0.05	0.30 ± 0.22	0.65	0.04	0.18 ± 0.12	0.37	0.03
AVBN.24	0.22 ± 0.23	0.67	0.04	0.31 ± 0.32	0.86	0.07	0.21 ± 0.07	0.31	0.11
OVAL.R	0.26 ± 0.48	1.22	0.03	0.55 ± 0.31	0.91	0.04	0.27 ± 0.27	0.75	0.09
OVAL.L	0.25 ± 0.43	1.12	0.04	0.54 ± 0.27	0.80	0.19	0.24 ± 0.08	0.35	0.15
PVID.R	0.24 ± 0.44	1.14	0.02	0.55 ± 0.30	0.94	0.23	0.28 ± 0.24	0.65	0.04
PVID.L	0.22 ± 0.40	1.04	0.02	0.46 ± 0.27	0.78	0.16	0.22 ± 0.13	0.34	0.03
MENT.R	0.55 ± 0.69	2.08	0.05	0.39 ± 0.26	0.87	0.03	0.29 ± 0.20	0.60	0.10
MENT.L	0.55 ± 0.69	2.09	0.06	0.39 ± 0.40	1.09	0.10	0.26 ± 0.24	0.60	0.06
IORB.R	0.53 ± 0.42	1.61	0.08	0.42 ± 0.25	0.78	0.17	n/a †		
IORB.L	0.52 ± 0.42	1.56	0.07	0.39 ± 0.42	1.06	0.11	n/a †		
GPF.R	0.19 ± 0.16	0.43	0.06	n/a †			0.17 ± 0.09	0.32	0.07
GPF.L	0.26 ± 0.24	0.61	0.06	n/a †			0.23 ± 0.16	0.50	0.10
ELSA	n/a †			0.41 ± 0.29	0.53	0.10	0.23 ± 0.13	0.39	0.03
MDFM	n/a †			0.49 ± 0.27	0.59	0.13	0.18 ± 0.09	0.27	0.05
Mid.NPF	n/a †			n/a †			n/a †		

† n/a: not applicable, since this landmark was used for plane construction.

4.4.2 Statistical analysis

The IBM SPSS statistical software was used for statistical data analysis (SPSS Statistics for Windows, Version 22.0. Armonk, NY). A total of 24 sets of landmarks were analyzed. A *p*-value of less than 0.05 was considered significant.

Repeated measures multiple analysis of covariance (rm-MANCOVA) was used (followed by post-hoc analysis) to test for any differences between the three treatment groups (T-RME, B-RME, Ctrl). The baseline values of all dento-skeletal variables (orthogonal distances for each landmark) at T1 of all three groups were compared using rm-MANCOVA. Then, a second

rm-MANCOVA was carried out for the T2-T1 data to assess treatment effects. A follow-up univariate analysis (Bonferroni tests) was then used for between-group and within-group pairwise comparisons. The null hypothesis was that neither between-group nor within-group differences exist for any of the parameters. Both rm-MANCOVA T1 and T2-T1 analysis were performed to compare the starting age at T1, gender, along with dental and skeletal measurements of the side of landmark measures (e.g. left, or right sided molar measurements, named as the LRSide).

Before performing the rm-MANCOVA, model assumptions were evaluated. Assumptions were met for independence (independent samples), sphericity (assumption did not apply, since there were only 2 time points) and multivariate normality. All data were checked for multivariate normality by visual examination of the P-P and Q-Q-plot (Appendix 15A), and by box plot of the Mahalanobis distance of the difference between T1 and T2 of each measured distance (dependent variable) (Appendix 15B). Furthermore, multiple analysis of covariance (MANCOVA) is robust to reasonable deviations in normality and equal variances when sample sizes are fairly large such as in this study. Assumption of linearity of repeated measures was met by visual assessment of bivariate scatter plots (Appendix 16-18); no obvious curved relationship was seen, which suggested normal distribution. Correlation was assessed by regression analysis on the covariates (age, gender) for all the dependent variables. The mentioned covariates were not well correlated ($r < 0.5$) with the dependent variables. Overall, the rm-MANCOVA results suggested that age and gender did not have a significant effect as a covariate. Consequently, the covariates were eliminated and the analysis was repeated without the covariate.

With covariates eliminated, the repeated measures multivariate analysis of variance (rm-MANOVA) was run to compare baseline characteristics. There was no interaction between the term Group*LRSide*Age*Gender ($p = .518$). To account for this finding, rm-MANOVA was re-run by dropping the interaction terms one at a time. No significant difference were found for the interaction terms Group*LRSide*Age ($p = 0.575$), Group*LRSide*Gender ($p = 0.673$), Group*LRSide ($p = .117$) and LRSide*Age ($p = .658$), so they were dropped, rm-MANOVA was re-run, and finally tested against the main effects. No significant differences were found for Group ($p = .207$), LRSide ($p = .371$), Gender ($p = .563$) and Age ($p = .542$). Mean baseline measurements (T1) in the transverse, vertical and antero-posterior (AP) dimension are shown in Table 4-4.

Table 4-4. Baseline (T1) orthogonal distances (in mm) for all groups, from variable landmark to respective planes (Transverse (T*), Vertical (V*), and Antero-posterior (AP*) dimensions).

Group	B-RME			Ctrl			T-RME			
	T1	T*	V*	AP*	T*	V*	AP*	T*	V*	AP*
Variables	Mean ± S.D. (mm)	Mean ± S.D. (mm)	Mean ± S.D. (mm)	Mean ± S.D. (mm)	Mean ± S.D. (mm)	Mean ± S.D. (mm)	Mean ± S.D. (mm)	Mean ± S.D. (mm)	Mean ± S.D. (mm)	Mean ± S.D. (mm)
PULP. 16	-21.73 ± 2.20	14.71 ± 3.40	-18.20 ± 3.49	-22.17 ± 2.22	12.04 ± 3.80	-18.95 ± 2.91	-21.65 ± 1.72	13.73 ± 4.71	-18.98 ± 2.28	
PULP. 26	21.15 ± 2.03	16.07 ± 3.90	-18.69 ± 3.15	21.27 ± 2.20	12.43 ± 2.74	-19.70 ± 2.29	21.03 ± 2.12	13.79 ± 4.45	-19.52 ± 2.18	
PULP. 14	-17.20 ± 1.53	16.56 ± 5.70	-6.32 ± 2.71	-17.86 ± 1.73	13.22 ± 3.71	-7.19 ± 3.28	-16.71 ± 1.50	13.97 ± 5.73	-6.85 ± 2.39	
PULP. 24	16.94 ± 1.79	16.94 ± 5.50	-6.42 ± 2.45	17.76 ± 2.23	13.51 ± 3.56	-7.62 ± 3.41	16.38 ± 1.69	13.76 ± 6.12	-7.03 ± 2.33	
PULP. 13	-15.33 ± 1.66	17.38 ± 6.83	0.99 ± 2.67	-15.96 ± 1.84	15.44 ± 6.67	1.22 ± 3.51	-15.65 ± 1.48	16.44 ± 6.50	1.04 ± 2.99	
PULP. 23	14.52 ± 3.78	17.86 ± 6.74	0.03 ± 2.52	15.98 ± 2.17	15.11 ± 5.81	0.41 ± 3.73	15.42 ± 1.86	16.40 ± 5.53	0.52 ± 3.16	
PULP. 46	-22.81 ± 1.83	25.45 ± 3.95	-19.19 ± 4.29	-23.18 ± 1.93	24.24 ± 3.36	-21.19 ± 5.55	-23.42 ± 2.20	25.10 ± 4.02	-21.07 ± 3.95	
PULP. 36	22.32 ± 2.66	25.62 ± 4.41	-20.35 ± 4.53	22.25 ± 2.70	24.70 ± 3.47	-21.84 ± 5.21	22.24 ± 2.28	24.61 ± 3.99	-21.39 ± 3.86	
APEX. 16	-23.21 ± 1.73	1.03 ± 2.55	-14.63 ± 2.77	-23.60 ± 2.31	0.73 ± 2.20	-15.19 ± 2.58	-22.85 ± 2.17	0.72 ± 3.67	-14.63 ± 1.84	
APEX. 26	23.72 ± 1.81	1.85 ± 4.41	-15.62 ± 3.27	23.86 ± 1.58	1.21 ± 3.78	-15.57 ± 1.92	22.70 ± 2.37	0.14 ± 3.02	-14.72 ± 1.92	
APEX. 14	-16.50 ± 1.37	2.65 ± 3.70	-5.60 ± 2.37	-18.09 ± 1.53	2.32 ± 2.59	-6.23 ± 2.25	-16.88 ± 1.84	1.44 ± 4.70	-5.19 ± 2.09	
APEX. 24	17.08 ± 2.00	3.39 ± 3.97	-6.40 ± 1.59	18.55 ± 1.53	2.77 ± 3.00	-6.65 ± 2.42	17.22 ± 1.89	1.00 ± 4.70	-5.37 ± 2.29	
APEX. 13	-12.11 ± 2.16	-1.06 ± 5.26	-1.92 ± 1.33	-12.66 ± 1.74	-3.44 ± 5.40	-2.24 ± 1.66	-12.08 ± 1.71	-1.56 ± 4.38	-2.43 ± 1.85	
APEX. 23	12.15 ± 1.87	-0.87 ± 4.56	-2.76 ± 1.28	13.29 ± 1.55	-3.25 ± 4.62	-3.00 ± 1.98	12.17 ± 1.60	-1.63 ± 3.64	-2.40 ± 1.78	
APEX. 46	-25.42 ± 2.19	36.35 ± 3.59	-21.76 ± 4.81	-25.44 ± 1.64	35.17 ± 4.77	-23.63 ± 5.13	-26.26 ± 2.39	35.78 ± 6.80	-23.81 ± 5.19	
APEX. 36	25.69 ± 3.35	36.93 ± 4.44	-22.70 ± 4.50	24.75 ± 2.03	35.41 ± 3.60	-24.07 ± 5.04	25.20 ± 2.16	35.66 ± 6.13	-23.88 ± 4.90	
AVBN. 16	-27.45 ± 2.15	0.82 ± 2.55	-13.91 ± 3.35	-29.46 ± 3.36	0.55 ± 2.40	-14.34 ± 3.31	-27.03 ± 2.46	1.05 ± 3.95	-13.92 ± 2.01	
AVBN. 26	27.91 ± 1.95	1.13 ± 2.84	-14.93 ± 3.51	29.17 ± 2.44	1.02 ± 3.57	-15.12 ± 2.66	26.99 ± 2.61	0.56 ± 3.01	-14.23 ± 1.80	
AVBN. 14	-18.75 ± 1.29	2.69 ± 3.88	-4.49 ± 2.92	-20.68 ± 1.45	2.22 ± 2.65	-5.88 ± 2.33	-18.99 ± 1.68	1.71 ± 4.68	-4.66 ± 1.85	
AVBN. 24	20.04 ± 2.23	3.51 ± 4.03	-6.00 ± 1.92	20.96 ± 2.06	2.69 ± 2.93	-6.35 ± 2.69	18.98 ± 1.73	0.97 ± 4.55	-5.05 ± 2.22	
AVBN. 13	-14.35 ± 2.12	-1.32 ± 5.42	0.39 ± 1.49	-15.39 ± 1.94	-3.76 ± 5.67	0.70 ± 1.64	-14.42 ± 1.72	-2.52 ± 4.12	0.13 ± 1.44	
AVBN. 23	15.03 ± 1.75	-0.81 ± 4.69	-0.11 ± 1.32	16.02 ± 1.75	-3.52 ± 4.78	0.14 ± 2.08	15.17 ± 1.51	-2.07 ± 3.84	-0.06 ± 1.70	
AVBN. 46	-28.79 ± 2.22	36.47 ± 4.00	-19.45 ± 4.75	-29.10 ± 2.20	35.05 ± 4.83	-20.96 ± 5.24	-29.78 ± 2.53	35.63 ± 7.14	-20.99 ± 5.14	

AVBN. 36	29.43 ± 3.43	36.69 ± 4.28	-20.53 ± 4.39	28.45 ± 2.23	35.27 ± 3.77	-21.08 ± 5.04	28.88 ± 2.42	35.64 ± 6.24	-21.22 ± 4.75
OVAL_ R	-25.44 ± 1.47	-20.62 ± 3.07	-51.87 ± 4.00	-23.70 ± 1.63	-20.00 ± 2.20	-55.46 ± 4.38	-25.09 ± 1.62	-19.56 ± 4.04	-53.64 ± 5.18
OVAL_ L	25.12 ± 1.97	-20.88 ± 2.18	-51.88 ± 3.71	24.51 ± 0.93	-20.42 ± 1.66	-55.51 ± 3.84	24.93 ± 1.53	-19.95 ± 3.45	-52.95 ± 4.65
PVID_ R	-15.29 ± 1.90	-21.31 ± 2.57	-51.49 ± 3.96	-14.63 ± 0.96	-20.22 ± 2.40	-54.40 ± 4.09	-14.67 ± 1.78	-20.19 ± 4.78	-52.03 ± 5.03
PVID_ L	14.66 ± 2.60	-21.64 ± 2.05	-51.30 ± 3.78	14.87 ± 1.35	-20.61 ± 2.06	-55.00 ± 4.29	14.98 ± 1.53	-20.39 ± 4.38	-52.86 ± 5.06
MENT _R	-22.13 ± 1.94	41.92 ± 4.51	-14.56 ± 5.00	-22.84 ± 1.53	40.64 ± 4.54	-14.18 ± 5.48	-22.50 ± 2.87	42.31 ± 6.66	-15.16 ± 5.41
MENT _L	22.06 ± 1.99	42.26 ± 5.16	-14.30 ± 4.99	21.91 ± 2.75	39.90 ± 5.42	-14.05 ± 5.12	21.48 ± 2.87	41.80 ± 5.83	-15.12 ± 5.69
IORB_ R	-23.60 ± 2.09	-19.00 ± 4.31	n/a †	-24.34 ± 2.48	-19.07 ± 2.40	n/a †	-23.43 ± 2.94	-19.00 ± 4.30	n/a †
IORB_ L	23.10 ± 2.69	-18.64 ± 3.99	n/a †	24.27 ± 2.07	-19.78 ± 2.01	n/a †	23.68 ± 1.99	-19.52 ± 4.16	n/a †
GPF_R	-14.14 ± 1.18	n/a †	-29.77 ± 2.32	-13.82 ± 1.25	0.00 ± 0.00	-30.52 ± 2.17	-14.04 ± 1.36	0.00 ± 0.00	-30.61 ± 2.05
GPF_L	13.89 ± 1.23	n/a †	-29.75 ± 2.59	13.76 ± 1.37	0.00 ± 0.00	-31.16 ± 2.43	13.45 ± 1.45	0.00 ± 0.00	-30.73 ± 2.17

† n/a: not applicable, since this landmark was used for plane construction.

Summary of Pre-treatment (T1) Findings

- Subjects of all three groups had similar pre-treatment characteristics with regards to age, gender, sample size, time interval, and pre-treatment dental and skeletal measurements.
- In the Control group, mean total inter-molar width was 43.44 mm in the maxilla, and 45.03 mm in the mandible (mean 1.59 mm transverse discrepancy).
- In the B-RME group, mean total inter-molar width was 42.88 mm in the maxilla, and 45.33 mm in the mandible (mean 2.45 mm transverse discrepancy).
- In the T-RME group, mean total inter-molar width was 42.18 mm in the maxilla, and 45.66 mm in the mandible (mean 1.74 mm transverse discrepancy).

4.4.3 Treatment Changes (T2-T1)

A repeated measures multivariate analysis of variance (rm-MANOVA) was run for the treatment changes (T2-T1). The interaction term Group*LRSide*Age*Gender (p=.579) was not found to be significant and rm-MANOVA was rerun by dropping this interaction term. There was no significant difference for the interaction terms Group*LRSide*Gender (p=.552),

Group*LRSide*Age ($p=.276$), Group*LRSide ($p=.104$) and LRSide*Age ($p=.531$). Therefore, the model was reduced and re-run without the interaction term to assess the main effects. No significant differences were found for LRSide ($p=.112$), gender ($p=.577$), and age ($p=.526$), but a significant difference was reported for Group ($p=.012$).

Then, rm-MANOVA was run for only B-RME subjects, using the interaction term LRSide*TADSide ($p=.267$) but no significant difference was found. This interaction was dropped, and the model was re-run in order to assess the main effects. The main effect LRSide ($p=.089$) was not statistically significant, but a significant difference was reported for TADSide ($p=.035$). A follow-up univariate analysis (Bonferroni tests) was then used for between-group (Table 4-5 to Table 4-7) and within-group pairwise comparisons (Table 4-8 to Table 4-12).

4.4.4 Between-Group Comparisons (T2-T1)

Transverse dento-skeletal changes relative to the mid-sagittal plane

- More buccal displacement was noted by T-RME compared to B-RME group for the variables:
 - PULP.16 (1.10 mm ; $p=.010$),
 - PULP.14 (1.49 mm ; $p<.001$),
 - PULP.24 (1.50 mm ; $p<.001$),
 - APEX.26 (1.03 mm ; $p=.010$).
- Compared to Control group, B-RME group showed statistically significant more buccal displacement (expansion):
 - PULP.16 (1.18 mm ; $p=.010$),
 - PULP.26 (2.52 mm ; $p<.001$),
 - APEX.26 (0.96 mm ; $p=.030$),
 - PULP.24 (1.19 mm ; $p=.030$),
 - GPF.L (0.91 mm ; $p<.001$).
- Compared to Control group, T-RME group showed statistically significant greater buccal displacement (expansion):
 - PULP.16 (2.27 mm ; $p<.001$),
 - PULP.26 (2.92 mm ; $p<.001$),

- APEX.26 (1.98 mm ; $p < .001$),
- PULP.24 (2.68 mm ; $p < .001$),
- GPF.L (0.83 mm ; $p < .001$),
- APEX.13 (1.31 mm ; $p < .001$),
- APEX.23 (1.09 mm ; $p < .001$),
- APEX.14 (1.54 mm ; $p < .001$),
- APEX.24 (1.20 mm ; $p < .001$),
- APEX.16 (1.38 mm ; $p < .001$),
- PULP.23 (1.09 mm ; $p < .001$),
- PULP.14 (2.19 mm ; $p < .001$).

Vertical distance changes relative to the palatal plane

- Compared to Control, B-RME group TAD-side showed 1.31 mm greater superior skeletal displacement of IORB, with statistical significance ($p < .05$).
- Compared to Control, T-RME group showed greater inferior dental displacement of PULP.26 (1.50 mm) and PULP.24 (1.80 mm), with statistical significance ($p < .05$).
- Between B-RME and T-RME, no significant differences were found.

Antero-posterior distance changes relative to the frontal plane

- Compared to Control, T-RME group showed greater forward (anterior) displacement of PULP.14 (0.35 mm), with statistical significance ($p < .05$).
- Compared to B-RME, T-RME group showed greater anterior movement of APEX.16 (1.46 mm) and APEX.26 (1.23 mm), with statistical significance ($p < .05$).
- B-RME group showed no statistically significant differences compared to Control.

4.4.5 Within-Group Comparisons (T2-T1)

Left versus Right-side transverse discrepancy

- In the T-RME and Control groups, no significant differences were found between the left- and right-sides for any transverse changes (mean differences < 0.60 mm).

B-RME group: TAD versus Implant-side transverse discrepancy

- Compared to Implant-side from T2-T1, TAD-side showed greater expansion at the molar crown by 1.84 mm ($p=.014$), with statistical significance.
- Compared to the Implant-side from T2-T1, TAD-side showed statistically significant expansion of the premolar crown and apex, by 1.43 mm ($p=.010$), and 1.44 mm ($p=.008$) respectively (Table 4-9).

B-RME group: TAD- versus Implant-side vertical discrepancy

- From T2-T1, TAD-side showed greater superior skeletal displacement of IORB.L by 1.50 mm, compared to the Implant-side, with statistical significance ($p=.011$).
- Note that there were no statistical significant differences in any other vertical dento-skeletal variables at T1 (all differences were < 0.58 mm).

Pulp- versus Apex- transverse discrepancy

- In the T-RME group, greater crown expansion than root expansion (1.25 mm) was noted on the upper left premolar, with statistical significance ($p=.001$). This indicated significant crown tipping. No statistically significant molar crown tipping was noted (<0.85 mm).
- In the B-RME group, greater crown expansion than root expansion (1.39 mm) was noted only on the TAD-side upper molar, with statistical significance ($p=.003$). No statistically significant difference was noted on the upper molar of the Implant-side (0.58 mm). This indicated molar crown tipping on the TAD-side, but not the Implant-side. No significant crown tipping was noted on premolars either side.
- The Control group, showed no statistically significant difference between crown and root expansion (Table 4-12).

Posterior versus Anterior transverse discrepancy

- T-RME group showed greater expansion between the upper molar than between canines by 1.6 mm per side, with statistical significance ($p<.002$). No statistical significant differences between inter-molar and inter-premolar expansion were found.

- In the B-RME group, both the TAD- and Implant-sides produced greater expansion between upper molars than between canines. This difference was 1.1 mm on the Implant-side, and 1.9 mm on the TAD-side, with statistical significance ($p < .001$).
- In the B-RME group, only the TAD-side produced greater upper inter-molar expansion than the inter-premolar (1.3 mm; $p < .001$). This was not statistically significant on the Implant-side ($p = 1.000$).

Upper- to Lower-molar transverse discrepancy

- In the B-RME group, the gains in buccal overjet between the upper and lower molars, showed greater change on the TAD-side than the Implant-side, 2.4 mm ($p < .001$) and 1.4 mm ($p = .038$) respectively, with statistical significance ($p < .001$).
- In the T-RME group, the gains in buccal overjet between upper and lower molars were similar on the left (2.3 mm) and right sides (2.8 mm), with statistical significance ($p < .001$).
- The Control group, showed no statistically significant change in upper and lower buccal overjet. It indicated no significant change in transverse maxillo-mandibular posterior teeth mismatch condition.

Table 4-5. Between-Group Comparisons: Transverse treatment changes (T2-T1), based on orthogonal distances from landmark to Mid-sagittal Plane for all three groups.

	B-RME	Ctrl	T-RME	B-RME-T-RME	B-RME-Ctrl	T-RME-Ctrl
Variable	Group Mean \pm S.D. (mm)			P-value for Group Differences		
PULP.16	1.79 \pm 1.25	0.61 \pm 0.62	2.78 \pm 1.07	.010 **	.010 **	.000 **
PULP.26	2.38 \pm 1.55	-0.14 \pm 0.81	2.88 \pm 1.07	1.000	.000 **	.000 **
PULP.14	1.04 \pm 1.33	0.34 \pm 0.82	2.53 \pm 1.28	.000 **	.270	.000 **
PULP.24	1.09 \pm 1.16	-0.10 \pm 1.08	2.59 \pm 1.47	.000 **	.030 *	.000 **
PULP.13	0.72 \pm 0.95	0.50 \pm 0.95	1.29 \pm 1.20	.360	1.000	.110
PULP.23	0.47 \pm 1.19	0.06 \pm 1.04	1.15 \pm 1.03	.230	.850	.020 *
PULP.46	0.37 \pm 0.88	0.23 \pm 0.93	0.09 \pm 1.32	1.000	1.000	1.000

PULP.36	-0.01 ± 0.85	-0.31 ± 0.99	0.51 ± 1.15	.410	1.000	.070
APEX.16	1.21 ± 1.19	0.66 ± 0.89	2.03 ± 1.39	.140	.560	.000 **
APEX.26	0.99 ± 1.07	0.03 ± 0.80	2.02 ± 1.11	.010 *	.030 *	.000 **
APEX.14	0.79 ± 1.25	0.11 ± 0.84	1.65 ± 1.26	.100	.270	.000 **
APEX.24	0.87 ± 1.15	0.14 ± 0.83	1.34 ± 1.30	.670	.200	.010 **
APEX.13	0.86 ± 1.34	0.20 ± 0.79	1.51 ± 1.18	.300	.300	.010 **
APEX.23	0.62 ± 1.01	0.03 ± 0.75	1.13 ± 0.81	.280	.180	.000 **
APEX.46	0.55 ± 1.13	0.44 ± 1.37	0.16 ± 1.22	1.000	1.000	1.000
APEX.36	0.06 ± 1.24	-0.66 ± 1.29	0.24 ± 0.91	1.000	.250	.090
AVBN.16	1.09 ± 1.04	0.48 ± 1.25	0.85 ± 1.45	1.000	.490	1.000
AVBN.26	0.57 ± 0.93	-0.33 ± 0.63	0.70 ± 0.89	1.000	.010 **	.000 **
AVBN.14	0.80 ± 1.27	-0.03 ± 0.60	1.01 ± 1.27	1.000	.100	.030 *
AVBN.24	0.24 ± 0.93	0.05 ± 0.82	1.09 ± 1.33	.070	1.000	.020 *
AVBN.13	0.87 ± 1.19	0.05 ± 0.93	1.21 ± 1.13	1.000	.110	.010 *
AVBN.23	0.25 ± 1.01	0.16 ± 1.02	0.59 ± 0.92	.950	1.000	.660
AVBN.46	0.38 ± 1.16	0.25 ± 1.35	-0.02 ± 1.34	1.000	1.000	1.000
AVBN.36	-0.14 ± 1.33	-0.51 ± 1.71	0.28 ± 1.14	1.000	1.000	.340
MENT_R	0.20 ± 1.50	0.31 ± 1.42	0.22 ± 1.34	1.000	1.000	1.000
MENT_L	-0.05 ± 1.10	0.08 ± 1.48	0.45 ± 0.98	.710	1.000	1.000
IORB_R	0.83 ± 1.48	0.26 ± 1.26	0.87 ± 1.29	1.000	.690	.580
IORB_L	0.11 ± 1.18	0.20 ± 1.36	0.38 ± 0.98	1.000	1.000	1.000
GPF_R	0.80 ± 0.71	0.40 ± 0.52	0.84 ± 0.72	1.000	.260	.190
GPF_L	0.99 ± 0.61	0.08 ± 0.58	0.91 ± 0.55	1.000	.000 **	.000 **

*: statistically significant P < 0.05, **: statistically significant P < 0.01.

Table 4-6. Between-Group Comparisons: Vertical treatment changes (T2-T1), based on orthogonal distances from landmark to Palatal Plane for all three groups.

	B-RME	Ctrl	T-RME	B-RME-T-RME	B-RME-Ctrl	T-RME-Ctrl
Variable	Group Mean \pm S.D. (mm)			P-value for Group Differences		
PULP.16	0.60 \pm 1.93	0.58 \pm 1.73	-0.44 \pm 1.65	.290	1.000	.320
PULP.26	-0.05 \pm 1.49	1.05 \pm 1.51	-0.46 \pm 1.69	1.000	.150	.030 *
PULP.14	0.13 \pm 2.20	0.38 \pm 1.41	-0.50 \pm 1.87	1.000	1.000	.550
PULP.24	0.08 \pm 1.73	1.12 \pm 2.38	-0.69 \pm 1.93	.820	.450	.040 *
PULP.13	0.94 \pm 1.56	0.88 \pm 2.06	0.15 \pm 1.82	.630	1.000	.770
PULP.23	0.26 \pm 1.66	1.33 \pm 2.22	0.74 \pm 1.34	1.000	.260	1.000
PULP.46	0.73 \pm 1.29	0.35 \pm 1.16	-0.14 \pm 1.39	.170	1.000	.840
PULP.36	0.62 \pm 1.56	0.84 \pm 1.57	0.41 \pm 1.55	1.000	1.000	1.000
APEX.16	-0.02 \pm 1.48	0.28 \pm 0.94	0.60 \pm 1.63	.590	1.000	1.000
APEX.26	0.26 \pm 1.15	-0.62 \pm 1.48	0.36 \pm 1.39	1.000	.210	.130
APEX.14	0.16 \pm 1.53	0.01 \pm 0.80	0.37 \pm 1.36	1.000	1.000	1.000
APEX.24	-0.47 \pm 1.92	0.45 \pm 1.51	0.17 \pm 1.68	.860	.390	1.000
APEX.13	-0.48 \pm 1.14	-0.38 \pm 1.63	0.15 \pm 1.29	.550	1.000	.810
APEX.23	-0.20 \pm 1.80	-0.48 \pm 1.66	0.20 \pm 1.69	1.000	1.000	.790
APEX.46	0.85 \pm 1.81	0.19 \pm 1.43	0.58 \pm 1.85	1.000	.820	1.000
APEX.36	0.27 \pm 2.16	0.66 \pm 1.79	0.76 \pm 1.79	1.000	1.000	1.000
AVBN.16	-0.04 \pm 1.31	0.27 \pm 1.27	0.29 \pm 1.68	1.000	1.000	1.000
AVBN.26	0.36 \pm 1.25	-0.30 \pm 1.26	0.42 \pm 1.43	1.000	.470	.370
AVBN.14	0.10 \pm 1.75	-0.01 \pm 0.87	0.00 \pm 1.72	1.000	1.000	1.000
AVBN.24	-0.37 \pm 1.96	0.78 \pm 1.70	0.38 \pm 1.63	.670	.200	1.000
AVBN.13	-0.45 \pm 1.33	-0.14 \pm 1.32	0.04 \pm 1.38	.880	1.000	1.000
AVBN.23	-0.25 \pm 1.89	-0.44 \pm 1.57	-0.16 \pm 1.72	1.000	1.000	1.000
AVBN.46	0.84 \pm 2.04	0.15 \pm 1.41	0.72 \pm 2.01	1.000	.890	1.000
AVBN.36	0.55 \pm 1.73	0.78 \pm 1.85	0.79 \pm 1.80	1.000	1.000	1.000

MENT_R	0.71 ± 1.55	0.92 ± 1.25	0.04 ± 1.28	.490	1.000	.220
MENT_L	0.43 ± 1.95	0.68 ± 1.55	0.35 ± 1.57	1.000	1.000	1.000
IORB_R	1.13 ± 1.82	0.48 ± 1.23	0.58 ± 1.55	.930	.730	1.000
IORB_L	0.95 ± 1.28	-0.36 ± 1.45	0.61 ± 1.30	1.000	.020 *	.140

*: statistically significant P < 0.05, **: statistically significant P < 0.01.

Table 4-7. Between-Group Comparisons: Antero-posterior treatment changes (T2-T1), based on orthogonal distances from landmark to Frontal Plane for all three groups.

	B-RME	Ctrl	T-RME	B-RME-T-RME	B-RME-Ctrl	T-RME-Ctrl
Variable	Group Mean ± S.D. (mm)			P-value for Group Differences		
PULP.16	-0.11 ± 1.54	0.40 ± 1.58	-0.35 ± 1.38	1.000	.990	.460
PULP.26	-0.24 ± 1.34	0.31 ± 0.99	-0.41 ± 1.41	1.000	.670	.330
PULP.14	0.35 ± 1.27	0.50 ± 1.38	-0.78 ± 1.62	.080	1.000	.040 *
PULP.24	0.53 ± 1.36	0.42 ± 1.56	-0.44 ± 1.61	.210	1.000	.330
PULP.13	-0.07 ± 1.18	-0.53 ± 1.90	0.20 ± 1.16	1.000	1.000	.470
PULP.23	0.48 ± 0.91	-0.31 ± 1.71	-0.06 ± 1.54	.830	.360	1.000
PULP.46	0.25 ± 1.43	0.23 ± 1.71	0.12 ± 1.94	1.000	1.000	1.000
PULP.36	0.11 ± 1.89	0.36 ± 1.76	0.21 ± 1.96	1.000	1.000	1.000
APEX.16	0.74 ± 1.57	0.44 ± 1.98	-0.72 ± 1.11	.030 *	1.000	.120
APEX.26	0.57 ± 1.54	0.06 ± 0.90	-0.66 ± 1.02	.010 *	.680	.260
APEX.14	0.53 ± 1.17	0.33 ± 1.30	-0.36 ± 1.62	.200	1.000	.480
APEX.24	0.04 ± 1.16	0.37 ± 1.02	-0.33 ± 1.48	1.000	1.000	.340
APEX.13	0.31 ± 1.10	0.25 ± 1.03	-0.80 ± 1.75	.060	1.000	.090
APEX.23	-0.02 ± 0.97	0.12 ± 0.75	-0.32 ± 1.17	1.000	1.000	.600
APEX.46	0.83 ± 1.91	0.91 ± 2.77	0.57 ± 2.09	1.000	1.000	1.000
APEX.36	0.53 ± 2.02	0.78 ± 3.04	1.26 ± 2.23	1.000	1.000	1.000
AVBN.16	0.79 ± 1.81	0.26 ± 1.77	-0.74 ± 1.38	.030 *	1.000	.270

AVBN.26	0.39 ± 1.44	-0.06 ± 1.55	-0.41 ± 0.92	.250	1.000	1.000
AVBN.14	0.38 ± 1.15	0.45 ± 1.28	-0.29 ± 1.44	.420	1.000	.320
AVBN.24	0.06 ± 1.08	0.56 ± 1.11	-0.37 ± 1.47	.960	.760	.110
AVBN.13	-0.14 ± 0.79	-0.15 ± 0.83	-0.22 ± 0.79	1.000	1.000	1.000
AVBN.23	0.21 ± 0.82	-0.11 ± 0.72	-0.07 ± 1.03	1.000	.890	1.000
AVBN.46	0.74 ± 1.80	1.05 ± 2.70	1.02 ± 2.13	1.000	1.000	1.000
AVBN.36	0.61 ± 2.31	1.26 ± 2.88	1.36 ± 2.40	1.000	1.000	1.000
MENT_R	0.82 ± 1.57	1.46 ± 2.68	0.88 ± 2.68	1.000	1.000	1.000
MENT_L	0.94 ± 1.88	1.59 ± 2.53	1.21 ± 2.80	1.000	1.000	1.000
GPF_R	0.14 ± 0.84	0.48 ± 1.32	0.17 ± 1.36	1.000	1.000	1.000
GPF_L	0.37 ± 0.83	-0.09 ± 0.90	0.44 ± 1.17	1.000	.550	.370

*: statistically significant P < 0.05, **: statistically significant P < 0.01.

Table 4-8. Within-Group comparisons: Left- to Right-side discrepancy in treatment changes (T2-T1), based on orthogonal distances to the mid-sagittal 3-D plane, for all three groups.

Point A - Point B		B-RME			Ctrl			T-RME		
A) R-sided Landmarks	B) L-sided Landmarks	Mean (mm)	(95% CI)	P-value	Mean (mm)	(95% CI)	P-value	Mean (mm)	(95% CI)	P-value
PULP.16	PULP.26	-0.60	(-2.4, 1.2)	1.000	0.85	(-1.6, 2.6)	1.000	0.10	(-1.7, 1.9)	1.000
PULP.14	PULP.24	-0.05	(-1.8, 1.7)	1.000	0.44	(-1.4, 2.3)	1.000	-0.06	(-1.8, 1.7)	1.000
PULP.13	PULP.23	0.25	(-1.4, 1.9)	1.000	0.44	(-1.2, 2.1)	1.000	0.14	(-1.5, 1.8)	1.000
PULP.46	PULP.36	0.38	(-1.6, 2.4)	1.000	0.55	(-1.5, 2.6)	1.000	-0.41	(-2.4, 1.6)	1.000
MENT.R	MENT.L	0.24	(-2.3, 2.8)	1.000	0.23	(-2.4, 2.8)	1.000	-0.23	(-2.8, 2.3)	1.000
IORB.R	IORB.L	0.71	(-1.6, 3.0)	1.000	0.05	(-2.3, 2.4)	1.000	0.49	(-1.8, 2.8)	1.000
GPF.R	GPF.L	-0.18	(-1.2, 0.8)	1.000	0.32	(-0.7, 1.4)	1.000	-0.07	(-1.1, 0.9)	1.000

*: statistically significant P < 0.05, **: statistically significant P < 0.01.

Table 4-9. Within-Group B-RME comparisons: transverse discrepancy in treatment changes (T2-T1) between TAD- and Implant-side.

Transverse	TAD-anchor side	Implant-anchor side	TAD - IMP	TAD - IMP
Variables	Mean ± S.D. (mm)	Mean ± S.D. (mm)	Mean ± S.E. (mm)	P-value (approx.)
PULP.16 (R-side)	2.03 ± 1.31	1.33 ± 1.09	0.70 ± 0.63	.285
PULP.26 (L-side)	3.58 ± 1.70	1.74 ± 1.05	1.84 ± 0.74	.014 *
APEX.16 (R-side)	1.29 ± 1.40	1.06 ± 0.74	0.23 ± 0.62	.710
APEX.26 (L-side)	1.53 ± 1.58	0.70 ± 0.54	0.84 ± 0.71	.120
PULP.14 (R-side)	1.24 ± 1.46	0.69 ± 1.08	0.55 ± 0.68	.434
PULP.24 (L-side)	2.02 ± 1.06	0.58 ± 0.90	1.43 ± 0.75	.010 **
APEX.14 (R-side)	0.90 ± 1.41	0.59 ± 0.98	0.31 ± 0.65	.640
APEX.24 (L-side)	1.80 ± 0.79	0.36 ± 0.99	1.44 ± 0.81	.008 **

*: statistically significant P < 0.05, **: statistically significant P < 0.01.

Table 4-10. Within-Group B-RME comparisons: vertical discrepancy in treatment changes (T2-T1) between TAD- and Implant-side.

Vertical	TAD-anchor side	Implant-anchor side	TAD - IMP	TAD - IMP
Variables	Mean ± S.D. (mm)	Mean ± S.D. (mm)	Mean ± S.E. (mm)	P-value (approx.)
IORB.R (R-side)	1.62 ± 1.68	0.22 ± 1.87	1.40 ± 0.88	.134
IORB.L (L-side)	1.50 ± 1.10	-0.06 ± 0.99	1.56 ± 0.74	.011 *

*: statistically significant P < 0.05, **: statistically significant P < 0.01.

Table 4-11. Within-Group comparisons: Posterior- vs. Anterior- transverse discrepancy in treatment changes (T2-T1), based on orthogonal distances to the mid-sagittal 3-D plane, for all three groups.

Point A - Point B		B-RME			Ctrl			T-RME		
A) Molar Landmarks	B) Canine and Premolar Landmarks	Mean (mm)	(95% CI)	P-value	Mean (mm)	(95% CI)	P-value	Mean (mm)	(95% CI)	P-value
PULP.16	PULP.13	1.07	(0.0, 2.1)	.026 *	0.11	(-0.9, 1.2)	1.000	1.60	(0.6, 2.6)	.000 **
PULP.26	PULP.23	1.92	(0.6, 3.2)	.000 **	-0.20	(-1.6, 1.2)	1.000	1.63	(0.3, 2.9)	.002 **
PULP.16	PULP.14	0.74	(-0.2, 1.6)	.511	0.27	(-0.7, 1.2)	1.000	0.35	(-0.5, 1.3)	1.000
PULP.26	PULP.24	1.30	(0.3, 2.3)	.001 **	-0.04	(-1.1, 1.0)	1.000	0.19	(-0.8, 1.2)	1.000

*: statistically significant P < 0.05, **: statistically significant P < 0.01.

Table 4-12. Within-Group comparisons: Crown- vs. Root-transverse discrepancy in treatment changes (T2-T1), based on orthogonal distances to the mid-sagittal 3-D plane, for all three groups.

Point A - Point B		B-RME			Ctrl			T-RME		
A) Crown Landmarks	B) Root Landmarks	Mean (mm)	(95% CI)	P-value	Mean (mm)	(95% CI)	P-value	Mean (mm)	(95% CI)	P-value
PULP.16	APEX.16	0.58	(-0.6, 1.7)	1.000	-0.05	(-1.3, 1.2)	1.000	0.85	(-0.3, 2.0)	1.000
PULP.26	APEX.26	1.39	(0.2, 2.5)	.003 **	-0.17	(-1.4, 1.0)	1.000	0.76	(-0.4, 1.9)	1.000
PULP.14	APEX.14	0.25	(-0.8, 1.3)	1.000	0.23	(-0.9, 1.3)	1.000	0.88	(-0.2, 1.9)	.515
PULP.24	APEX.24	0.22	(-0.8, 1.2)	1.000	-0.24	(-1.3, 0.8)	1.000	1.25	(0.3, 2.2)	.001 **
PULP.13	APEX.13	-0.14	(-1.5, 1.2)	1.000	0.30	(-1.1, 1.7)	1.000	-0.22	(-1.6, 1.1)	1.000
PULP.23	APEX.23	-0.39	(-2.1, 1.3)	1.000	-0.14	(-1.9, 1.6)	1.000	-0.36	(-2.0, 1.3)	1.000

*: statistically significant P < 0.05, **: statistically significant P < 0.01.

Table 4-13: : Within-Group comparisons: Upper- vs. Lower- transverse discrepancy in treatment changes (T2-T1), based on orthogonal distances to the mid-sagittal 3-D plane, for all three groups.

Point A - Point B		B-RME			Ctrl			T-RME		
A) Upper Landmarks	B) Lower Landmarks	Mean (mm)	(95% CI)	P-value	Mean (mm)	(95% CI)	P-value	Mean (mm)	(95% CI)	P-value
PULP.16	PULP.46	1.42	(0.0, 2.8)	.038 *	0.38	(-1.1, 1.8)	1.000	2.79	(1.4, 4.2)	.000 **
PULP.26	PULP.36	2.40	(1.0, 3.8)	.000 **	0.18	(-1.3, 1.6)	1.000	2.27	(0.9, 3.7)	.000 **

*: statistically significant P < 0.05, **: statistically significant P < 0.01.

4.5 Discussion

The purpose of this study was to compare the transverse, vertical and antero-posterior, skeletal and dental post-treatment changes for Dresden B-RME, 4-band T-RME, and an untreated control group in a sample of 50 subjects. A secondary objective was to determine if there were statistically significant differences in maxillary treatment effects between the TAD-anchor side and shortened-implant anchor side of the Dresden B-RME group.

Pre-treatment characteristics of all subjects in the three groups showed no statistically significant difference with regards to age, gender, sample size, time interval, baseline skeletal and dental measurements on the left or right-sides for all landmarks relative to reference planes in the transverse, vertical and antero-posterior dimensions at T1 (Table 4-1 & Table 4-2).

As measured from the buccal pulp horn of the upper molar and lower molars, a mean total transverse discrepancy of 1.59 mm, 1.74 mm, and 2.45 mm were found in the control, T-RME, and B-RME groups respectively. There were no statistically differences found between the 3 groups. Due to the buccal pulp horn landmarks used in CBCT analysis, this measurement would be less than the clinical transverse discrepancy measurement taken from the palatal cusp of the upper molar to the central fossae of the lower molar. Clinically, a minimum transverse maxillary expansion of 5 mm was required in order to receive maxillary expansion therapy. In future studies, upper to lower dental CBCT analyses could be extended to more opposing 3-D landmarks on the molar teeth, including, but not limited to, the palatal pulp

horn, the palatal cusp tip, or the buccal cusp tip. This may provide more information regarding the bucco-lingual relationship between opposing molars.

Crossbite Correction Effectiveness

At T2, the control group did not show significant maxillary width expansion. A total mean expansion of less than 0.50 mm was recorded. Majority of the transverse change was skeletal (0.48 mm, measured from GPF) with a mild amount of alveolar bone expansion (0.15 mm, measured from AVBN). The molar crown in fact displaced further towards the lingual (0.15 mm, measured from PULP). No significant change in upper and lower buccal overjet could be found at T2. It indicated no significant change in transverse maxillo-mandibular posterior teeth mismatch condition.

In contrast, both treatment groups (T-RME and B-RME) demonstrated significant maxillary expansion. For the T-RME group, there were similar maxillary inter-premolar and inter-molar width expansions, with a total mean of 5.12 mm and 5.66 mm, respectively. For the B-RME group, maxillary inter-premolar expansion was less than between molars, with a total mean of 2.13 mm and 4.17 mm, respectively. Based solely on this observation, this implies T-RME may be more effective for patients with similar severity of transverse maxillary constriction at the molar level and premolar levels. Meanwhile, B-RME may be more effective for patients with greater constriction at the bilateral maxillary molar level than the premolar level.

In general, maxillary expansion produces a combination of dental expansion, sutural widening, and alveolar bending³³. From this study's observations, the TAD-side (B-RME) showed greater molar crown displacement (1.84 mm) than the Implant-side, with statistical significance of $p < .015$. This indicated the B-RME appliance configuration produced asymmetrical molar expansion. In other words, placement of the TAD-anchor on the side of more severe maxillary constriction may be considered in patients with more pronounced asymmetry. However, it should be noted that the exact source of this discrepancy and the long-term stability is not known. There are some speculative factors including, but not limited to, the difference in anchor length, anchor diameter, and degree of osteointegration between the TAD and Implant anchors and its implications. Therefore, the precise

effectiveness of asymmetrical maxillary transverse correction with this B-RME setup still requires further investigation.

T-RME group showed symmetrical transverse dental and skeletal expansion. The difference between the left and right was less than 0.10 mm for molar expansion, and less than 0.06 mm for premolar. This is as expected and agrees with previous findings^{53,135}, since T-RME is known to expand in a bilateral manner by design.

Based on a comparison between 4-band vs. 2-band T-RME, Davidovitch et al⁵⁶ found the 4-band force system to produce more anterior directed forces to produce greater premolar expansion. The 2-band system was effective in overpowering the posterior sutural resistance, but had difficulty in overcoming anterior sutural resistances⁵⁶. Further investigations into the number of anchor units and force distribution can be performed in the future. However, factors including, but not limited to, the inherent risks of possible infection, invasiveness, and discomfort may also need to be considered.

Antero-posterior and Vertical changes

Both T-RME and B-RME groups showed only mild amounts vertical displacements with respect to the palatal plane. B-RME group showed less than 1.3 mm skeletal superior displacement with weak statistical significant relative to control group ($p < .05$), even though the magnitude was small and not likely to be clinically significant. The T-RME group showed less than 1.8 mm of vertical extrusion of the premolar and molar dental crowns, again this was based on weak statistical significance when compared to the control group ($p < .05$) and there was no statistical significance between the two treatment groups. Additionally, this observation at 6 months post-treatment is even less than previous findings by Lagravere et al³⁴ of 2-3 mm changes, recorded after the end of expansion (approx. a month). Therefore, there is clinically insignificant bite-opening or vertical effect from these treatments.

In the antero-posterior dimension, only T-RME group exhibited minor changes. The T-RME group showed displacements that were less than 1.50 mm with weak statistical significance ($p < .05$) when compared to the control group. B-RME showed no statistically significant antero-posterior changes when compared to the control group. There was also only weak statistical significance between the two treatment groups ($p < .05$). Again, this finding is similar to the highest average displacement of only 1 mm reported by Lagravere et al³⁴.

Minimal changes in the antero-posterior and vertical changes are welcomed as this allows the clinician to focus on the main concern of transverse correction in patients with maxillary constriction.

Dental to Skeletal Ratio

The B-RME group showed a lower ratio of dental expansion compared to T-RME group. The dental to skeletal ratio of expansion in the T-RME group, was roughly 40:60, with 42% dental expansion, 27% alveolar, 31% sutural. While it was approximately 20:80, with 17% dental expansion, 40% alveolar, and 43% sutural, for the B-RME group. Our findings corroborate with that of Lin et al ³³, who reported 26%-43% dental expansion in their T-RME group. They also reported 25-45% dental expansion in their B-RME group, which was again similar to our results. For molar expansion, B-RME is preferred since it has a lower ratio of dental expansion compared to T-RME, to minimize the risks of dental tipping or relapse.

Remarks

The decision to use B-RME or T-RME in adolescents depend upon operator preferences and specific dental and skeletal considerations for the patient. B-RME may be preferred in patients with missing permanent posterior teeth, or periodontal/endodontically compromised dentition, or when a lower ratio of dental to skeletal expansion is desired. Based solely on this study's sample, T-RME may be more effective for patients with similar severity of transverse maxillary constriction at the molar level and premolar levels. Meanwhile, B-RME may be more effective for patients with greater constriction at the bilateral maxillary molar level than the premolar level.

The Dresden B-RME appliance configuration produced asymmetrical molar expansion. Placement of the TAD-anchor on the side of more severe maxillary transverse constriction may be helpful in cases with more pronounced asymmetry. However, identifying exact source of this discrepancy and the long-term stability requires further investigation.

4.5.1 Limitations

While there was a sufficient pool of subjects (34) in the two treatment groups combined, this number did limit us from further assessing relationships between the TAD-side and Implant-side within the B-RME group. It also limited further investigations based on skeletal maturity which may influence final treatment outcomes. Furthermore, this clinical study also evaluated the skeletal and dental post-expansion changes over a relatively short period of time (6 months), and hence long-term inferences cannot be made.

Since this chapter's work is based on the previous chapter, all the limitations mentioned in section 3.9.5 still applies.

4.6 Summary & Conclusions

Transverse

- Both treatment groups (T-RME and B-RME) showed proper bucco-lingual molar interdigitation at this 6 month observation.
- T-RME group showed symmetrical premolar and molar expansion.
- The Dresden B-RME appliance configuration did produce asymmetrical molar expansion.
- The TAD-anchor side of B-RME, showed greater molar crown displacement (mean 1.84 mm) than the Implant-anchor side, with statistical significance of $p < .015$.

Antero-posterior

- T-RME group showed minimal anterior displacement of molar apex and premolar crown (< 1.5 mm), compared to other groups, with only weak statistical significance ($p < .05$).
- No significant antero-posterior changes were found for B-RME group.

Posterior versus Anterior transverse discrepancy

- T-RME group showed greater expansion between the upper molar than between canines by 1.6 mm per side, with statistical significance ($p < .002$). No statistical significant differences between inter-molar and inter-premolar expansion were found.
- In the B-RME group, both the TAD- and Implant-sides produced greater expansion between upper molars than between canines. This difference was 1.1 mm on the Implant-side, and 1.9 mm on the TAD-side, with statistical significance ($p < .001$).

- In the B-RME group, only the TAD-side produced greater upper inter-molar expansion than the inter-premolar (1.3 mm; $p < .001$). This was not statistically significant on the Implant-side ($p = 1.000$).

Vertical

- T-RME showed some dental vertical extrusion of premolar and molar crowns (< 1.8 mm ; $p < .05$), relative to control group.
- No significant dental vertical changes were found for the B-RME group. Minimal skeletal superior displacement at infra-orbital foramen (IORB) was noted for B-RME group (mean < 1.3 mm ; $p < .05$), relative to control group.
- Vertical changes were minimal and non-significant between the B-RME and T-RME groups.

Dental to Skeletal Ratio

- The dental to skeletal ratio of expansion in the T-RME group, was roughly 40:60, with 42% dental expansion, 27% alveolar, 31% sutural.
- The dental to skeletal ratio of expansion in the B-RME group was approximately 20:80, with 17% dental expansion, 40% alveolar, and 43% sutural.

4.7 Future recommendations:

- 1) A more in-depth analysis can be conducted to evaluate the effects of expansion treatment on arch symmetry. This would involve a new randomized clinical trial that accounts for the level of pre-treatment asymmetry. In the case of Dresden B-RME, for example, patients that were significantly asymmetric at pre-treatment should have the TAD inserted into the side with shorter distance from the maxillary midline (greater maxillary constriction), and test for symmetry correction relative to controls. Thus, a careful selection of side for implant placement is crucial to identify the true asymmetry effects of expansion.
- 2) Final symmetry of both the mandibular and maxillary arches relative to the mid-sagittal plane can also be examined. Spontaneous correction of mandibular symmetry correction could also be investigated.

- 3) Specifically for posterior crossbites, future studies can evaluate how well the mandibular and maxillary molars, premolars, canines are interdigitated. This may involve use of landmarks on other parts of a tooth (eg. multiple pulp horns, cusp tips, or root tips) in addition to the buccal pulp horns used in this study.
- 4) Further investigation may investigate the interaction between arch perimeter availability in any quadrants of the maxilla in relation to anterior or posterior dental midlines changes after expansion treatment. Dental midline deviations can also be compared with any skeletal midline deviations.
- 5) Further investigation is needed to examine the effect of mandibular dental tipping and crowding compensations which may contribute to the maxillo-mandibular transverse discrepancy and dental interdigitation. This may involve the use of more 3-D landmarks in the mandible than could be covered in this study.
- 6) This 3-D measurement technique could be extended to assess other orthodontic treatments and the effects.
- 7) Further investigation can be conducted to more extensively validate the effectiveness of this mathematically calculated plane, versus a manually defined plane. In particular, the researcher should focus on the amount of time required to define such a plane, the variations and accuracies compared to manually defined planes, and therefore, be able to quantitatively demonstrate this new technique's reliability.
- 8) The landmarks PVID.L&R and OVALE.L&R could be useful reference landmarks to consider for reference plane construction in future studies.

4.8 References

1. McNamara JA. Maxillary transverse deficiency. *American Journal of Orthodontics and Dentofacial Orthopedics* 2000;117:567-570.
8. Bishara SE, Staley RN. Maxillary expansion: clinical implications. *American Journal of Orthodontics and Dentofacial Orthopedics* 1987;91:3-14.
9. Lagravère MO, Heo G, Major PW, Flores-Mir C. Meta-analysis of immediate changes with rapid maxillary expansion treatment. *The Journal of the American Dental Association* 2006;137:44-53.
10. Bell RA. A review of maxillary expansion in relation to rate of expansion and patient's age. *American journal of orthodontics* 1982;81:32-37.
11. Kennedy DB, Osepchok M. Unilateral posterior crossbite with mandibular shift: a review. *Journal-Canadian Dental Association* 2005;71:569.
13. Lagravere MO, Major PW, Flores-Mir C. Long-term dental arch changes after rapid maxillary expansion treatment: a systematic review. *The Angle orthodontist* 2005;75:155-161.
24. Lagravère MO, Gordon JM, Guedes IH, Flores-Mir C, Carey JP, Heo G et al. Reliability of traditional cephalometric landmarks as seen in three-dimensional analysis in maxillary expansion treatments. *The Angle orthodontist* 2009;79:1047-1056.
33. Lin L, Ahn H-W, Kim S-J, Moon S-C, Kim S-H, Nelson G. Tooth-borne vs bone-borne rapid maxillary expanders in late adolescence. *The Angle Orthodontist* 2014;85:253-262.
34. Lagravère MO, Carey J, Heo G, Toogood RW, Major PW. Transverse, vertical, and anteroposterior changes from bone-anchored maxillary expansion vs traditional rapid maxillary expansion: A randomized clinical trial. *American Journal of Orthodontics and Dentofacial Orthopedics* 2010;137:304.e301-304.e312.
35. Krebs A. Expansion of the midpalatal suture, studied by means of metallic implants. *Acta Odontologica Scandinavica* 1959;17:491-501.
36. Wehrbein H, Göllner P. Skeletal Anchorage in Orthodontics - Basics and Clinical Application. *Journal of Orofacial Orthopedics / Fortschritte der Kieferorthopädie* 2007;68:443-461.
37. Hansen L, Tausche E, Hietschold V, Hotan T, Lagravère M, Harzer W. Skeletally-anchored Rapid Maxillary Expansion using the Dresden Distractor. *Journal of Orofacial Orthopedics / Fortschritte der Kieferorthopädie* 2007;68:148-158.
39. Tausche E, Hansen L, Hietschold V, Lagravère MO, Harzer W. Three-dimensional evaluation of surgically assisted implant bone-borne rapid maxillary expansion: A pilot study. *American Journal of Orthodontics and Dentofacial Orthopedics* 2007;131:S92-S99.
44. Thilander B, Wahlund S, Lennartsson B. The effect of early interceptive treatment in children with posterior cross-bite. *The European Journal of Orthodontics* 1984;6:25-34.
53. Ileri Z, Basciftci FA. Asymmetric rapid maxillary expansion in true unilateral crossbite malocclusion: A prospective controlled clinical study. *The Angle Orthodontist* 2015;85:245-252.

56. Davidovitch M, Efstathiou S, Sarne O, Vardimon AD. Skeletal and dental response to rapid maxillary expansion with 2-versus 4-band appliances. *American Journal of Orthodontics and Dentofacial Orthopedics* 2005;127:483-492.
75. Ferro F, Spinella P, Lama N. Transverse maxillary arch form and mandibular asymmetry in patients with posterior unilateral crossbite. *American Journal of Orthodontics and Dentofacial Orthopedics* 2011;140:828-838.
116. Portney L WM. *Foundations of clinical research: applications to practice.*: Prentice Hall, Upper Saddle River 2008.
132. Garib DG, Henriques JF, Carvalho PE, Gomes SC. Longitudinal effects of rapid maxillary expansion. *Angle Orthod* 2007;77:442-448.
133. Chang JY, McNamara JA, Jr., Herberger TA. A longitudinal study of skeletal side effects induced by rapid maxillary expansion. *Am J Orthod Dentofacial Orthop* 1997;112:330-337.
134. Brin I, Ben-Bassat Y, Blustein Y, Ehrlich J, Hochman N, Marmary Y et al. Skeletal and functional effects of treatment for unilateral posterior crossbite. *Am J Orthod Dentofacial Orthop* 1996;109:173-179.
135. Marshall SD, Southard KA, Southard TE. *Early transverse treatment Seminars in Orthodontics*: Elsevier; 2005: p. 130-139.

Chapter 5

5. Summary of findings

5.1 Introduction

Posterior crossbite is one of the most easily recognized clinical signs that result from a transverse constricted maxilla ¹. This narrow maxillary width relative to the mandible, causes a mismatch between opposing posterior teeth ^{1,8,9}. Conventional correction of maxillary constriction was primarily done through use of a Tooth-borne Rapid Maxillary Expander (RME). Due to its dental attachment, T-RME has been reported to induce greater dental than skeletal expansion (70% dental vs. 30% skeletal)³⁵ Mild levels of undesirable maxillary molar crown tipping, and bite opening have been reported in previous studies evaluating short-term effects of T-RME, although this has not been consistent throughout the literature ^{13,34,132,133}. Consequently, B-RME was designed to hopefully reduce this dental side-effect ^{36,37}. B-RME attempts to minimize dental structures disturbance and maximize skeletal expansion by directly inserting either shortened palatal implants or temporary anchorage devices (TADs) ^{36,37} into the two halves of the bony maxillary palate.

The Dresden B-RME design was chosen to be used in adolescents for the first time in this study. This appliance had been used in two previous studies on ten mature adult patients who underwent surgically-assisted rapid maxillary expansion in the study by Tausche et al and Hansen et al ^{37,39}. The Dresden B-RME has a unique design feature where it is anchored by an osteointegrated implant on one side and a mini-implant-anchor (a.k.a. Temporary Anchorage Devices, or TAD) on the other.

Efforts from chapter 3 provided a set of 3-D reference planes that has been experimentally proven to be accurate and reliable. Using these planes along with selected treatment landmarks allowed a quantitative measure of transverse, vertical, and antero-posterior changes after T-RME/B-RME/no treatment after 6 months' observation.

The main objectives of this thesis were to

- 1) Identify accurate and easily repeatable (intra-examiner reliability) 3-D landmarks in the cranial base, maxilla, and mandible which can be used to quantify treatment changes after rapid maxillary expansion (RME).

- 2) Compare the transverse, vertical and antero-posterior, skeletal and dental post-treatment changes for Dresden B-RME, 4-band T-RME, and an untreated control group.

The research questions of this thesis were

- 1) Which skeletal and dental landmarks are the most accurate and repeatable (intra-examiner reliability) in CBCT images, and can be used to assess transverse, vertical, and antero-posterior treatment changes after maxillary expansion?
- 2) When several dento-skeletal variables are considered simultaneously over time, does age, gender, or treatment group (B-RME/T-RME/No Treatment) affect the final maxillary outcome (transverse, vertical, antero-posterior) in a selected sample of patients with transverse maxillary constriction?
 - i) Are there are significant differences in the amount of maxillary transverse expansion between the TAD-anchor side, and the shortened-implant-anchor side of the Dresden B-RME group?

The major conclusions are summarized below.

5.2 Summary

- 1) Which skeletal and dental landmarks are the most accurate and repeatable (intra-examiner reliability) in CBCT images, and can be used to assess transverse, vertical, and antero-posterior treatment changes after maxillary expansion?

Reference landmarks

- a) Accuracy: Nearly all investigated landmarks (24 out of 26 sets) showed low mean errors (≤ 0.85 mm) and excellent agreement ($ICC > 0.92$), in all 3 axes, allowing them to be used in future clinical studies.
- b) Intra-examiner reliability: All 26 sets of landmarks showed excellent intra-examiner reliability ($ICC > 0.96$), with low mean errors of ≤ 0.5 mm, in all 3 axes.

Landmarks used for reference plane construction

- c) The preferred landmarks for mid-sagittal plane were: Mid.Nasopalatine Foramen (Mid.NPF), Mesial Dorsal Foramen Magnum (MDFM), and Foramen Spinosum (SPIN).
- d) The preferred landmarks for frontal plane were: Infra-orbital foramina (IORB) left & right, and Mid.NPF.
- e) The preferred landmarks for palatal plane were: Greater palatine foramina (GPF) left & right, and Mid.NPF.
- f) These combinations and landmarks, proved to be comparatively superior to other options.
- g) Based on three repeatedly constructed reference planes for 10 dry skulls as assessed using twenty selected landmarks, low mean errors (≤ 0.55 mm) were found in all 3 dimensions.
- h) Further analysis to observe the mean errors of orthogonal distances from 3 repeated treatment landmark measurements against an averaged reference plane, also showed low mean errors (≤ 0.85 mm) in all 3 dimensions.
- i) Measurement errors ≤ 1.5 mm are not likely to have clinical implications from past literature.

Treatment Landmarks

- j) All teeth root apices (tip), pulp horn (tip), and alveolar bone landmarks (AVBN) showed good to excellent reliability and accuracy particularly in the transverse and vertical dimension; and will be used in the future maxillary expansion assessment study.

Remarks

Defining 3D planes can be difficult by itself due to the high degree of freedom in all 3 axes. This study's premise is to have an easily repeatable process for measuring skeletal and dental changes over time. Using this mathematical procedure, given the same reference landmark coordinate input, the computed plane will always be the same. This is a great improvement to earlier methods that requires the examiner to manually draw the mid-sagittal plane, as it will eliminate any human error that process may introduce. It should be noted that this mathematically constructed plane is still susceptible to the measurement errors from the individual reference landmarks itself.

2) When several dento-skeletal variables are considered simultaneously over time, does age, gender, or treatment group (B-RME/T-RME/No Treatment) affect the final maxillary outcome (transverse, vertical, antero-posterior) in a selected sample of patients with maxillary constriction?

- i) Are there are significant differences in the amount of maxillary transverse expansion between the TAD-anchor side, and the shortened-implant-anchor side of the Dresden B-RME group?

Pre-treatment characteristics

- Subjects of all three groups started with similar pre-treatment characteristics with regards to pre-treatment dental and skeletal measurements, age, gender, sample size and observation time interval.

Transverse

- Both treatment groups (T-RME and B-RME) showed proper bucco-lingual molar interdigitation at this 6 month observation.
- T-RME group showed symmetrical premolar and molar expansion.
- The Dresden B-RME appliance configuration did produce asymmetrical molar expansion.
- The TAD-anchor side of B-RME, showed greater molar crown displacement (1.84 mm) than the Implant-anchor side, with statistical significance of $p < .015$.

Antero-posterior

- T-RME group showed minimal anterior displacement of molar apex and premolar crown (< 1.5 mm), compared to other groups, with only weak statistical significance ($p < .05$).
- No significant antero-posterior changes were found for B-RME group.

Posterior versus Anterior transverse discrepancy

- T-RME group showed greater expansion between the upper molar than between canines by 1.6 mm per side, with statistical significance ($p < .002$). No statistical significant differences between inter-molar and inter-premolar expansion were found.

- In the B-RME group, both the TAD- and Implant-sides produced greater expansion between upper molars than between canines. This difference was 1.1 mm on the Implant-side, and 1.9 mm on the TAD-side, with statistical significance ($p < .001$).
- In the B-RME group, only the TAD-side produced greater upper inter-molar expansion than the inter-premolar (1.3 mm; $p < .001$). This was not statistically significant on the Implant-side ($p = 1.000$).

Vertical

- T-RME showed some dental vertical extrusion of premolar and molar crowns (< 1.8 mm ; $p < .05$), relative to control group.
- No significant dental vertical changes were found for the B-RME group. Minimal skeletal superior displacement at infra-orbital foramen (IORB) was noted for B-RME group (mean < 1.3 mm ; $p < .05$), relative to control group.
- Vertical changes were minimal and non-significant between the B-RME and T-RME groups.

Dental to Skeletal Ratio

- The dental to skeletal ratio of expansion in the T-RME group, was roughly 40:60, with 42% dental expansion, 27% alveolar, 31% sutural.
- The dental to skeletal ratio of expansion in the B-RME group was approximately 20:80, with 17% dental expansion, 40% alveolar, and 43% sutural.

Remarks

The decision to use B-RME or T-RME in adolescents depend upon operator preferences and specific dental and skeletal considerations for the patient. B-RME may be preferred in patients with missing permanent posterior teeth, or periodontal/endodontically compromised dentition, or when a lower ratio of dental to skeletal expansion is desired. Based solely on this study's sample, T-RME may be more effective for patients with similar severity of transverse maxillary constriction at the molar level and premolar levels. Meanwhile, B-RME may be more effective for patients with greater constriction at the bilateral maxillary molar level than the premolar level. In addition, the Dresden B-RME appliance configuration produced asymmetrical molar expansion. Placement of the TAD-anchor on the side of more severe maxillary transverse constriction may be helpful in

cases with more pronounced asymmetry. However, identifying exact source of this discrepancy and the long-term stability requires further investigation.

5.3 Limitations:

5.3.1 Reliability & Accuracy chapter:

Numerous factors need to be considered when interpreting these results. Firstly, the assessment of reference landmark accuracy and intra-examiner reliability was performed on dry skulls. As pointed out by Periago et al ¹³⁰, the presence of nerves or other soft tissue structures inside the foramina may affect the accuracy of landmark identification. In attempt to mimic the soft tissues around the skull, the principal investigator incorporated a Plexiglass box filled with water around every skull prior to the CBCT scan, in efforts to reduce possible error.

Secondly, the number of dry skull specimens used in this study was 10. As recommended by Springate ¹³¹, increasing the number of specimens to 25 to 30 would reduce sampling errors for the statistical analyses in such types of study.

Third, the bone quality and scan quality were factors not fully within our control. The voxel size was 0.3 mm in this study, and this placed a limit to the accuracy level possible. During dry skull selection, efforts were made to check for a full healthy posterior dentition and intact bony structures. Furthermore, the dry skulls were not all collected from adolescent age group which could be commonly seen in subjects requesting for orthodontic treatment. The size and location of the foramina may show slight variation in dry skulls of the mid-ages.

Three-dimension visualization software such as the one used by this study (AVIZO) requires substantial training and patience to operate in general. Locating a 3-D landmark accurately requires constantly switching between the 3 axial planes on the monitor and iterating through hundreds of orthogonal slices. At the fastest rate, a minimum of about 2 minutes was required per landmark, including landmark identification, verification in all 3 dimensions, and data input. This may change in the near future with 3-D monitors becoming more commonly available.

5.3.2 Randomized Controlled Clinical trial chapter:

There was an adequate pool of subjects (34) in the two treatment groups combined, however it did limit us from further assessing relationships between the TAD-side and Implant-side within the B-RME group. It also limited further investigations based on skeletal maturity which may influence final treatment outcomes. This clinical study also evaluated the skeletal and dental post-expansion changes over a relatively short period of time (6 months), and hence long-term inferences cannot be made.

Since this chapter's work is based on the previous chapter, all the limitations mentioned in section 3.9.5 still applies.

5.4 Remarks

- a) A more in-depth analysis can be conducted to evaluate the effects of expansion treatment on arch symmetry. This would involve a new randomized clinical trial that accounts for the level of pre-treatment asymmetry. In the case of Dresden B-RME, for example, patients that were significantly asymmetric at pre-treatment should have the TAD inserted into the side with shorter distance from the maxillary midline(greater maxillary constriction), and test for symmetry correction relative to controls. Thus, a careful selection of side for implant placement is crucial to identify the true asymmetry effects of expansion.
- b) Final symmetry of both the mandibular and maxillary arches relative to the mid-sagittal plane can also be examined. Spontaneous correction of mandibular symmetry corection could also be investigated.
- c) Specifically for posterior crossbites, future studies can evaluate how well the mandibular and maxillary molars, premolars, canines are interdigitated. This may involve use of landmarks on other parts of a tooth (eg. multiple pulp horns, cusp tips, or root tips) in addition to the buccal pulp horns used in this study.
- d) Further investigation may investigate the interaction between arch perimeter availability in any quadrants of the maxilla in relation to anterior or posterior dental midlines changes after expansion treatment. Dental midline deviations can also be compared with any skeletal midline deviations.

- e) Further investigation is needed to examine the effect of mandibular dental tipping and crowding compensations which may contribute to the maxillo-mandibular transverse discrepancy and dental interdigitation. This may involve the use of more 3-D landmarks in the mandible than could be covered in this study.
- f) This 3-D measurement technique could be extended to assess other orthodontic treatments and the effects.
- g) Further investigation can be conducted to more extensively validate the effectiveness of this mathematically calculated plane, versus a manually defined plane. In particular, the researcher should focus on the amount of time required to define such a plane, the variations and accuracies compared to manually defined planes, and therefore, be able to quantitatively demonstrate this new technique's reliability.
- h) The landmarks PVID.L&R and OVALE.L&R could be useful reference landmarks to consider for reference plane construction in future studies.
- i) Current common computer monitors and controls are mostly 2-D. Much patience is required in locating 3-D landmarks accurately, including the constant switching between the 3 planes on the monitor and iterating through hundreds of orthogonal slices with a computer mouse. Once 3-D monitors become more commonly available, identification of 3-D landmarks and reference planes may be greatly expedited.

5.5 References

1. McNamara JA. Maxillary transverse deficiency. *American Journal of Orthodontics and Dentofacial Orthopedics* 2000;117:567-570.
8. Bishara SE, Staley RN. Maxillary expansion: clinical implications. *American Journal of Orthodontics and Dentofacial Orthopedics* 1987;91:3-14.
9. Lagravère MO, Heo G, Major PW, Flores-Mir C. Meta-analysis of immediate changes with rapid maxillary expansion treatment. *The Journal of the American Dental Association* 2006;137:44-53.
13. Lagravere MO, Major PW, Flores-Mir C. Long-term dental arch changes after rapid maxillary expansion treatment: a systematic review. *The Angle orthodontist* 2005;75:155-161.
34. Lagravère MO, Carey J, Heo G, Toogood RW, Major PW. Transverse, vertical, and anteroposterior changes from bone-anchored maxillary expansion vs traditional rapid maxillary expansion: A randomized clinical trial. *American Journal of Orthodontics and Dentofacial Orthopedics* 2010;137:304.e301-304.e312.
35. Krebs A. Expansion of the midpalatal suture, studied by means of metallic implants. *Acta Odontologica Scandinavica* 1959;17:491-501.
36. Wehrbein H, Göllner P. Skeletal Anchorage in Orthodontics - Basics and Clinical Application. *Journal of Orofacial Orthopedics / Fortschritte der Kieferorthopädie* 2007;68:443-461.
37. Hansen L, Tausche E, Hietschold V, Hotan T, Lagravère M, Harzer W. Skeletally-anchored Rapid Maxillary Expansion using the Dresden Distractor. *Journal of Orofacial Orthopedics / Fortschritte der Kieferorthopädie* 2007;68:148-158.
39. Tausche E, Hansen L, Hietschold V, Lagravère MO, Harzer W. Three-dimensional evaluation of surgically assisted implant bone-borne rapid maxillary expansion: A pilot study. *American Journal of Orthodontics and Dentofacial Orthopedics* 2007;131:S92-S99.
130. Periago DR, Scarfe WC, Moshiri M, Scheetz JP, Silveira AM, Farman AG. Linear accuracy and reliability of cone beam CT derived 3-dimensional images constructed using an orthodontic volumetric rendering program. *The Angle orthodontist* 2008;78:387-395.
131. Springate S. The effect of sample size and bias on the reliability of estimates of error: a comparative study of Dahlberg's formula. *The European Journal of Orthodontics* 2012;34:158-163.
132. Garib DG, Henriques JF, Carvalho PE, Gomes SC. Longitudinal effects of rapid maxillary expansion. *Angle Orthod* 2007;77:442-448.
133. Chang JY, McNamara JA, Jr., Herberger TA. A longitudinal study of skeletal side effects induced by rapid maxillary expansion. *Am J Orthod Dentofacial Orthop* 1997;112:330-337.

Appendices

Appendix 1: Intra-class correlation coefficients (ICC), for Intra-examiner reliability of Dental landmarks, based on three repeated measurements (in X,Y,Z axes)

Dental Landmarks	X			Y			Z		
	ICC	ICC (Lower Bound)	ICC (Upper Bound)	ICC	ICC (Lower Bound)	ICC (Upper Bound)	ICC	ICC (Lower Bound)	ICC (Upper Bound)
PULP.26	0.99	0.97	1.00	1.00	0.99	1.00	1.00	0.99	1.00
PULP.16	1.00	0.99	1.00	1.00	1.00	1.00	0.99	0.98	1.00
PULP.24	0.99	0.98	1.00	1.00	1.00	1.00	1.00	1.00	1.00
PULP.14	1.00	0.99	1.00	1.00	1.00	1.00	1.00	0.99	1.00
PULP.23	0.99	0.97	1.00	1.00	1.00	1.00	1.00	0.99	1.00
PULP.13	1.00	1.00	1.00	1.00	1.00	1.00	1.00	0.99	1.00
PULP.46	0.99	0.98	1.00	1.00	1.00	1.00	0.99	0.96	1.00
PULP.36	0.99	0.96	1.00	1.00	1.00	1.00	0.99	0.98	1.00
PULP.43	1.00	1.00	1.00	1.00	1.00	1.00	0.99	0.98	1.00
PULP.33	0.99	0.97	1.00	1.00	1.00	1.00	1.00	0.99	1.00
APEX.26	0.99	0.98	1.00	1.00	0.99	1.00	0.99	0.98	1.00
APEX.16	0.99	0.97	1.00	1.00	0.99	1.00	0.99	0.98	1.00
APEX.24	0.99	0.97	1.00	1.00	0.99	1.00	0.99	0.98	1.00
APEX.14	0.99	0.97	1.00	1.00	1.00	1.00	0.99	0.96	1.00
APEX.23	0.99	0.97	1.00	0.99	0.97	1.00	0.98	0.93	0.99
APEX.13	0.99	0.97	1.00	0.99	0.98	1.00	0.98	0.94	0.99
APEX.46	1.00	1.00	1.00	1.00	1.00	1.00	0.99	0.96	1.00
APEX.36	0.99	0.97	1.00	1.00	1.00	1.00	1.00	0.99	1.00
APEX.43	1.00	0.99	1.00	1.00	1.00	1.00	1.00	0.99	1.00
APEX.33	1.00	0.99	1.00	1.00	1.00	1.00	1.00	0.99	1.00
AVBN.26	0.97	0.91	0.99	0.99	0.97	1.00	0.99	0.98	1.00
AVBN.16	0.98	0.95	0.99	0.99	0.98	1.00	0.99	0.96	1.00
AVBN.24	1.00	0.98	1.00	1.00	0.99	1.00	0.99	0.98	1.00
AVBN.14	0.98	0.95	1.00	1.00	0.99	1.00	0.99	0.96	1.00
AVBN.23	0.97	0.93	0.99	0.98	0.95	1.00	0.98	0.94	0.99
AVBN.13	0.98	0.94	0.99	0.99	0.98	1.00	0.98	0.94	0.99
AVBN.46	0.99	0.98	1.00	1.00	1.00	1.00	0.99	0.96	1.00
AVBN.36	0.96	0.88	0.99	1.00	1.00	1.00	1.00	0.99	1.00
AVBN.43	0.99	0.96	1.00	1.00	1.00	1.00	1.00	0.99	1.00
AVBN.33	0.98	0.93	0.99	1.00	1.00	1.00	1.00	0.99	1.00

Appendix 2: Intra-class correlation coefficients (ICC), for Intra-examiner reliability for Skeletal landmarks, based on three repeated measurements (in X,Y,Z axes)

Skeletal Landmarks	X			Y			Z		
	ICC	ICC (Lower Bound)	ICC (Upper Bound)	ICC	ICC (Lower Bound)	ICC (Upper Bound)	ICC	ICC (Lower Bound)	ICC (Upper Bound)
Cranial Base Foramina									
CG	0.99	0.98	1.00	1.00	1.00	1.00	1.00	1.00	1.00
MDFM	0.99	0.96	1.00	1.00	1.00	1.00	1.00	1.00	1.00
EAM.L	1.00	1.00	1.00	1.00	1.00	1.00	1.00	1.00	1.00
EAM.R	1.00	1.00	1.00	1.00	1.00	1.00	1.00	1.00	1.00
MID.SPIN	1.00	0.99	1.00	1.00	0.99	1.00	1.00	1.00	1.00
HYPO.L	0.99	0.97	1.00	1.00	1.00	1.00	1.00	1.00	1.00
HYPO.R	0.98	0.93	0.99	1.00	0.99	1.00	1.00	1.00	1.00
OVAL.L	0.99	0.97	1.00	1.00	0.99	1.00	1.00	1.00	1.00
OVAL.R	0.99	0.98	1.00	1.00	0.99	1.00	1.00	1.00	1.00
ROT.L	1.00	1.00	1.00	1.00	1.00	1.00	1.00	1.00	1.00
ROT.R	1.00	0.99	1.00	1.00	0.99	1.00	1.00	1.00	1.00
SPIN.L	1.00	0.99	1.00	1.00	0.99	1.00	1.00	1.00	1.00
SPIN.R	1.00	0.99	1.00	1.00	0.99	1.00	1.00	0.99	1.00
Maxilla-Mandibular Foramina									
GPF.L	0.99	0.96	1.00	1.00	0.99	1.00	1.00	0.99	1.00
GPF.R	0.98	0.95	1.00	1.00	0.99	1.00	1.00	0.99	1.00
IORB.L	0.98	0.95	1.00	0.99	0.98	1.00	0.99	0.98	1.00
IORB.R	0.98	0.95	1.00	0.99	0.98	1.00	0.99	0.98	1.00
NPF.L	1.00	0.99	1.00	1.00	0.99	1.00	1.00	0.99	1.00
NPF.R	1.00	0.99	1.00	0.99	0.98	1.00	1.00	0.99	1.00
MENT.L	0.99	0.98	1.00	1.00	1.00	1.00	1.00	0.99	1.00
MENT.R	1.00	0.99	1.00	1.00	1.00	1.00	1.00	1.00	1.00
Constructed Midline Landmarks									
Mid.EAM	0.98	0.95	1.00	1.00	1.00	1.00	1.00	1.00	1.00
Mid.GPF	0.99	0.97	1.00	1.00	0.99	1.00	1.00	0.99	1.00
Mid.IORB	0.98	0.95	1.00	1.00	0.99	1.00	1.00	0.98	1.00
Mid.MENT	1.00	0.99	1.00	1.00	1.00	1.00	1.00	1.00	1.00
Mid.NPF	1.00	0.99	1.00	1.00	0.99	1.00	1.00	0.99	1.00
Mid.OVAL	1.00	0.99	1.00	1.00	0.99	1.00	1.00	1.00	1.00

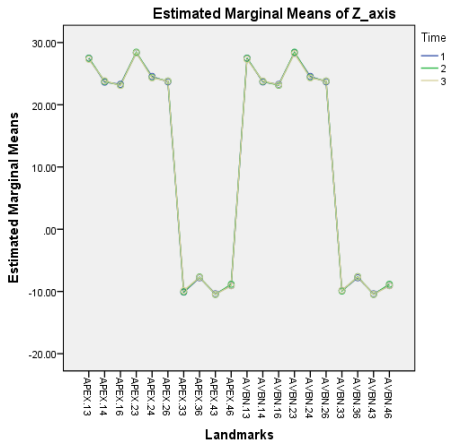
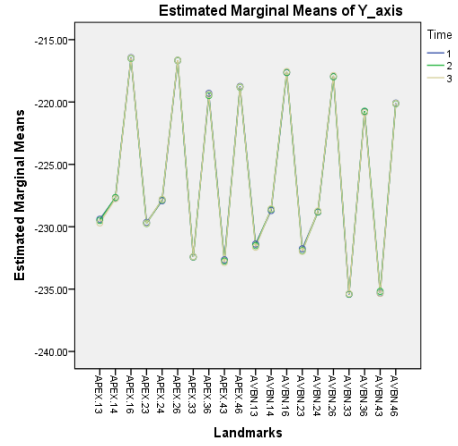
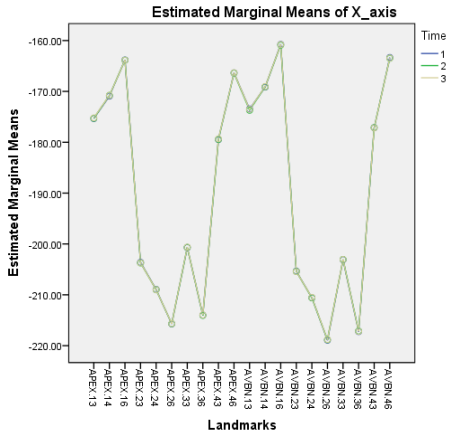
Appendix 3: Intra-examiner reliability mean differences (mm) for Dental landmarks, based on three repeated measurements (in X,Y,Z axes).

Dental Landmarks	N	Mean_X (mm)		Mean_Y (mm)		Mean_Z (mm)		Minimum Error (mm)			Maximum Error (mm)		
		Mean	S.D.	Mean	S.D.	Mean	S.D.	Min_X	Min_Y	Min_Z	Max_X	Max_Y	Max_Z
PULP.26	10	0.17	0.14	0.20	0.13	0.19	0.16	0.06	0.06	0.00	0.54	0.47	0.40
PULP.16	10	0.17	0.08	0.15	0.14	0.23	0.22	0.07	0.03	0.00	0.31	0.53	0.60
PULP.24	10	0.18	0.06	0.11	0.08	0.12	0.19	0.10	0.01	0.00	0.24	0.24	0.60
PULP.14	10	0.22	0.12	0.18	0.18	0.18	0.15	0.09	0.04	0.00	0.44	0.68	0.40
PULP.23	10	0.16	0.06	0.16	0.07	0.28	0.19	0.09	0.08	0.00	0.28	0.30	0.60
PULP.13	10	0.19	0.13	0.15	0.13	0.32	0.23	0.00	0.00	0.00	0.36	0.41	0.60
PULP.46	10	0.20	0.15	0.18	0.10	0.32	0.30	0.03	0.08	0.00	0.56	0.41	0.80
PULP.36	10	0.22	0.18	0.12	0.09	0.27	0.30	0.06	0.04	0.00	0.65	0.36	0.80
PULP.43	10	0.16	0.13	0.19	0.11	0.36	0.30	0.00	0.00	0.00	0.38	0.44	0.80
PULP.33	10	0.16	0.11	0.24	0.16	0.32	0.25	0.05	0.03	0.00	0.36	0.52	0.80
APEX.26	10	0.19	0.13	0.20	0.16	0.34	0.27	0.05	0.02	0.00	0.46	0.48	0.80
APEX.16	10	0.21	0.14	0.25	0.16	0.29	0.21	0.01	0.03	0.00	0.52	0.64	0.60
APEX.24	10	0.22	0.15	0.24	0.16	0.31	0.26	0.10	0.07	0.00	0.52	0.55	0.60
APEX.14	10	0.21	0.10	0.19	0.11	0.44	0.31	0.03	0.02	0.00	0.38	0.31	0.80
APEX.23	10	0.21	0.15	0.32	0.22	0.49	0.26	0.05	0.03	0.00	0.49	0.85	0.80
APEX.13	10	0.26	0.12	0.35	0.26	0.38	0.30	0.09	0.06	0.00	0.44	0.79	0.80
APEX.46	10	0.12	0.07	0.14	0.07	0.43	0.23	0.02	0.04	0.00	0.23	0.25	0.80
APEX.36	10	0.20	0.11	0.25	0.20	0.30	0.18	0.09	0.04	0.07	0.47	0.61	0.60
APEX.43	10	0.16	0.09	0.23	0.19	0.37	0.28	0.05	0.04	0.00	0.32	0.67	0.80
APEX.33	10	0.14	0.12	0.18	0.13	0.34	0.27	0.03	0.05	0.00	0.43	0.48	0.80
AVBN.26	10	0.34	0.17	0.34	0.21	0.34	0.27	0.12	0.07	0.00	0.64	0.75	0.80
AVBN.16	10	0.33	0.17	0.41	0.19	0.31	0.30	0.05	0.05	0.00	0.63	0.74	1.00
AVBN.24	10	0.18	0.07	0.23	0.19	0.31	0.26	0.06	0.02	0.00	0.28	0.62	0.60
AVBN.14	10	0.24	0.18	0.27	0.18	0.44	0.28	0.00	0.00	0.00	0.56	0.58	0.80
AVBN.23	10	0.28	0.21	0.49	0.29	0.46	0.26	0.04	0.17	0.00	0.80	0.86	0.80
AVBN.13	10	0.42	0.25	0.37	0.21	0.38	0.30	0.07	0.07	0.00	0.71	0.64	0.80
AVBN.46	10	0.27	0.13	0.17	0.09	0.43	0.23	0.16	0.04	0.00	0.53	0.32	0.80
AVBN.36	10	0.24	0.18	0.25	0.14	0.29	0.20	0.04	0.06	0.00	0.55	0.43	0.60
AVBN.43	10	0.39	0.25	0.28	0.16	0.37	0.29	0.12	0.06	0.00	0.83	0.54	0.80
AVBN.33	10	0.33	0.21	0.17	0.12	0.31	0.24	0.10	0.04	0.00	0.77	0.40	0.80

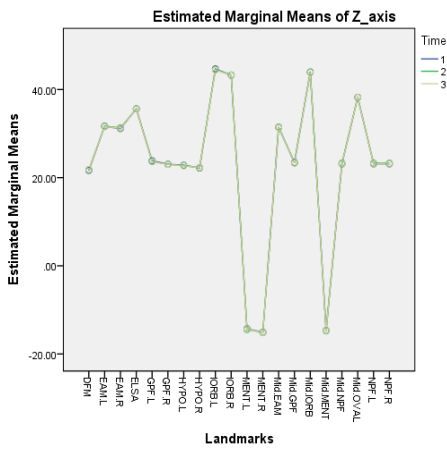
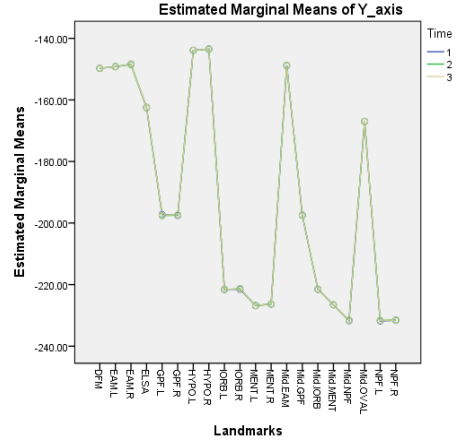
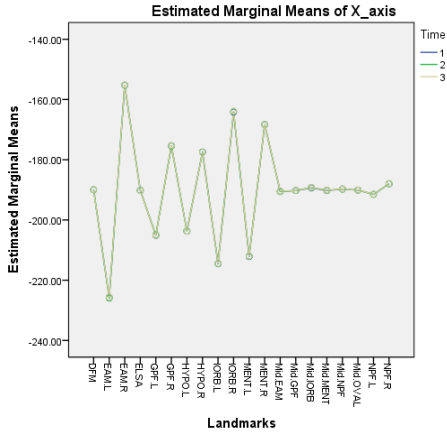
Appendix 4: Intra-examiner reliability mean differences (mm) for Skeletal landmarks, based on three repeated measurements (in X,Y,Z axes).

Skeletal Landmarks	N	Mean_X (mm)		Mean_Y (mm)		Mean_Z (mm)		Minimum Error (mm)			Maximum Error (mm)		
		Mean	S.D.	Mean	S.D.	Mean	S.D.	Min_X	Min_Y	Min_Z	Max_X	Max_Y	Max_Z
Cranial Base Foramina													
CG	10	0.11	0.07	0.12	0.10	0.09	0.10	0.02	0.03	0.00	0.25	0.30	0.20
MDFM	10	0.17	0.12	0.19	0.19	0.36	0.27	0.07	0.05	0.00	0.47	0.70	0.80
EAM.L	10	0.32	0.23	0.16	0.13	0.24	0.12	0.00	0.01	0.06	0.60	0.48	0.39
EAM.R	10	0.29	0.28	0.20	0.08	0.25	0.16	0.00	0.10	0.03	0.80	0.33	0.52
HYPO.L	10	0.22	0.11	0.24	0.11	0.33	0.22	0.09	0.02	0.13	0.40	0.42	0.80
HYPO.R	10	0.31	0.14	0.33	0.18	0.30	0.14	0.09	0.05	0.13	0.55	0.64	0.60
OVAL.L	10	0.21	0.14	0.34	0.18	0.18	0.18	0.06	0.02	0.00	0.46	0.61	0.40
OVAL.R	10	0.16	0.07	0.29	0.15	0.26	0.23	0.02	0.04	0.00	0.27	0.52	0.80
ROT.L	10	0.06	0.06	0.07	0.09	0.12	0.20	0.00	0.00	0.00	0.20	0.20	0.67
ROT.R	10	0.08	0.06	0.14	0.28	0.07	0.07	0.00	0.00	0.00	0.20	0.60	0.21
SPIN.L	10	0.15	0.07	0.25	0.16	0.29	0.17	0.04	0.08	0.00	0.25	0.60	0.60
SPIN.R	10	0.15	0.08	0.19	0.12	0.36	0.30	0.04	0.02	0.00	0.32	0.34	0.80
Maxilla-Mandibular Foramina													
GPF.L	10	0.23	0.17	0.32	0.23	0.28	0.24	0.03	0.00	0.00	0.56	0.72	0.73
GPF.R	10	0.26	0.18	0.28	0.19	0.19	0.14	0.06	0.00	0.00	0.65	0.60	0.47
IORB.L	10	0.24	0.24	0.34	0.10	0.37	0.24	0.04	0.17	0.14	0.84	0.49	0.80
IORB.R	10	0.33	0.20	0.34	0.21	0.30	0.21	0.10	0.08	0.00	0.65	0.63	0.80
NPF.L	10	0.12	0.11	0.23	0.24	0.21	0.19	0.00	0.00	0.00	0.38	0.71	0.60
NPF.R	10	0.11	0.12	0.28	0.27	0.23	0.18	0.00	0.00	0.00	0.36	0.85	0.60
MENT.L	10	0.22	0.15	0.24	0.17	0.25	0.14	0.08	0.07	0.00	0.60	0.52	0.40
MENT.R	10	0.23	0.14	0.15	0.10	0.14	0.13	0.08	0.03	0.00	0.50	0.29	0.40
Constructed Midline Landmarks													
Mid.EAM	10	0.25	0.15	0.12	0.05	0.18	0.09	0.04	0.05	0.03	0.50	0.24	0.31
Mid.GPF	10	0.13	0.07	0.19	0.16	0.21	0.16	0.05	0.00	0.00	0.24	0.54	0.57
Mid.IORB	10	0.20	0.17	0.27	0.13	0.26	0.21	0.03	0.08	0.10	0.50	0.49	0.80
Mid.MENT	10	0.17	0.10	0.18	0.10	0.19	0.10	0.08	0.02	0.00	0.41	0.37	0.30
Mid.NPF	10	0.09	0.07	0.21	0.22	0.22	0.18	0.00	0.00	0.00	0.23	0.78	0.60
Mid.OVAL	10	0.09	0.05	0.23	0.14	0.19	0.14	0.00	0.03	0.00	0.15	0.42	0.50
Mid.SPIN (= ELSA)	10	0.10	0.05	0.18	0.07	0.23	0.11	0.01	0.06	0.10	0.19	0.31	0.37

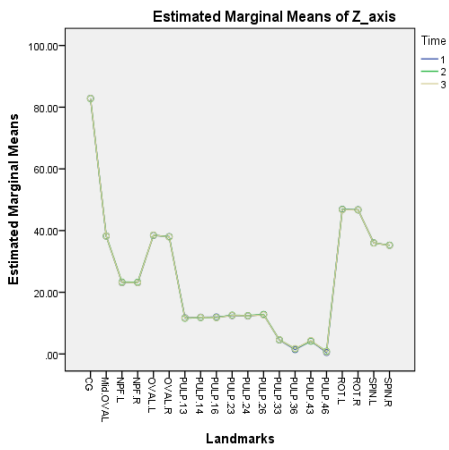
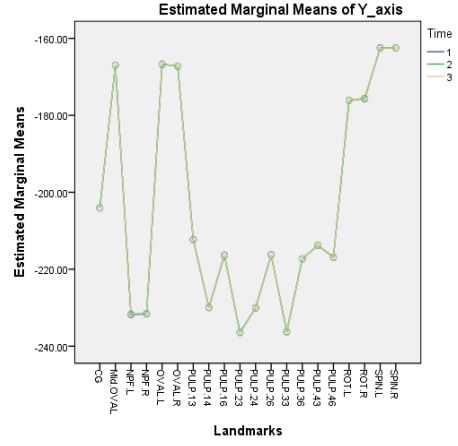
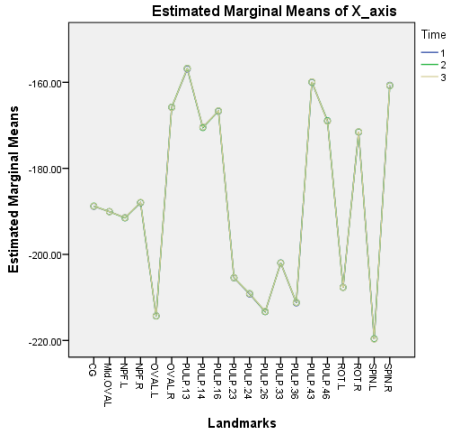
Appendix 5: Profile Plots of Estimated Marginal Means (in mm) of Intra-examiner reliability in X, Y, Z-axes (APEX.13 to AVBN 46)



Appendix 6: Profile Plots of Estimated Marginal Means (in mm) of Intra-examiner reliability in X, Y, Z-axes (MDFM to NPF)



Appendix 7: Profile Plots of Estimated Marginal Means (in mm) of Intra-examiner reliability in X, Y, Z-axes (CG to SPIN)



Appendix 8: Assessment of Accuracy between Cranial Base Landmarks based on Intra-class correlation coefficient (ICC), Mean differences and standard deviation (in mm).

Transverse Cranial Base Measurements		
Euclidean Distances	ICC	Mean difference \pm SD (mm)
PVID.R-PVID.L	1.00	0.28 \pm 0.22
OVAL.R-OVAL.L	0.99	0.47 \pm 0.30
SPIN.R-SPIN.L	0.99	0.53 \pm 0.37
OVAL.L-MID.SPIN	0.96	0.46 \pm 0.35
OVAL.R-MID.SPIN	0.89	0.60 \pm 0.63
EAM.R-EAM.L	0.98	0.70 \pm 0.37
HYPO.R-HYPO.L	0.95	0.51 \pm 0.43

Vertical/AP Cranial Base Measurements		
Euclidean Distances	ICC	Mean difference \pm SD (mm)
PVID.L-OVAL.L	1.00	0.46 \pm 0.31
Mid.Oval-MID.SPIN	0.98	0.28 \pm 0.21
Mid.PVID-MID.SPIN	1.00	0.45 \pm 0.29
PVID.L-MID.SPIN	0.99	0.68 \pm 0.47
PVID.R-MID.SPIN	0.97	0.70 \pm 0.65
MID.SPIN-CG	0.99	0.51 \pm 0.28
MID.SPIN-MDFM	1.00	0.49 \pm 0.30

Appendix 9: Assessment of Accuracy between Cranial Base Landmarks to CG & MDFM based on Intra-class correlation coefficient (ICC), Mean differences and standard deviation (in mm).

Cranial Base to Crista Galli (CG)		
Euclidean Distances	ICC	Mean difference \pm SD (mm)
MID.SPIN-CG	0.99	0.51 \pm 0.28
SPIN.R-CG	0.99	0.65 \pm 0.39
SPIN.L-CG	0.99	0.43 \pm 0.37
Mid.PVID-CG	0.99	0.39 \pm 0.30
PVID.R-CG	0.99	0.45 \pm 0.28
PVID.L-CG	0.99	0.48 \pm 0.24
Mid.OVAL-CG	1.00	0.37 \pm 0.26
OVAL.R-CG	0.99	0.52 \pm 0.37
OVAL.L-CG	1.00	0.32 \pm 0.25
Mid.EAM-CG	0.99	0.52 \pm 0.37
HYPO.R-CG	0.98	1.08 \pm 0.95
HYPO.L-CG	0.99	0.85 \pm 0.73
CG-MDFM	0.99	1.00 \pm 0.52

Cranial Base to Foramen Magnum (MDFM)		
Euclidean Distances	ICC	Mean difference \pm SD (mm)
MID.SPIN-MDFM	1.00	0.49 \pm 0.30
SPIN.R-MDFM	0.97	0.84 \pm 0.78
SPIN.L-MDFM	0.97	0.73 \pm 0.86
Mid.PVID- MDFM	1.00	0.51 \pm 0.47
PVID.R- MDFM	1.00	0.56 \pm 0.45
PVID.L- MDFM	1.00	0.62 \pm 0.52
Mid.OVAL-MDFM	1.00	0.84 \pm 0.78
OVAL.R-MDFM	0.98	0.81 \pm 0.89
OVAL.L-MDFM	1.00	0.49 \pm 0.30
Mid.AEM-MDFM	0.99	0.73 \pm 0.86
HYPO.R-MDFM	0.89	0.78 \pm 0.63
HYPO.L-MDFM	0.65	1.28 \pm 1.48

Appendix 10: Assessment of Accuracy for Maxillary and Mandibular Skeletal Landmarks.

Euclidean Distances	N	ICC	Mean ± SD (mm)	Min. (mm)	Max. (mm)
Maxillary Skeletal (Anterior to Posterior)					
GPF.L-NPF.L	10	0.92	0.82 ± 0.51	0.12	1.94
GPF.L- IORB.L	10	0.88	0.63 ± 0.46	0.11	1.41
IORB.L-MDFM	10	0.98	1.16 ± 1.04	0.34	3.55
IORB.R-MDFM	10	0.98	1.29 ± 1.27	0.16	4.71
MENT.L-MDFM	10	0.94	1.30 ± 1.35	0.04	4.92
MENT.R-MDFM	10	0.97	1.28 ± 1.33	0.11	4.20
Maxilla to Mandible (Vertical)					
MENT.L-GPF.L	10	0.99	0.51 ± 0.38	0.06	1.22
MENT.R-NPF.R	10	0.99	0.52 ± 0.34	0.07	1.11
MENT.R-IORB.R	10	0.99	0.55 ± 0.26	0.13	0.88
Skeletal to Skeletal (Transverse)					
GPF.R-GPF.L	10	0.98	0.52 ± 0.27	0.24	1.06
NPF.R-NPF.L	10	0.87	0.52 ± 0.34	0.07	1.03
IORB.R-IORB.L	10	0.96	0.69 ± 0.49	0.17	1.49
MENT.R-MENT.L	10	1.00	0.20 ± 0.15	0.02	0.42

Appendix 11: Assessment of Accuracy for Dental Landmarks in the Transverse dimension.

Euclidean Distances	ICC	Mean ± SD (mm)	Min. (mm)	Max. (mm)
Maxillary Teeth Pairings (Transverse)				
PULP.16-26	1.00	0.23 ± 0.23	0.08	0.86
PULP.14-24	0.99	0.27 ± 0.27	0.04	0.92
PULP.13-23	0.99	0.26 ± 0.17	0.05	0.47
APEX.16-26	0.95	0.48 ± 0.39	0.10	1.27
APEX.14-24	0.96	0.46 ± 0.35	0.06	1.15
APEX.13-23	0.99	0.22 ± 0.21	0.03	0.74
AVBN.16-26	0.95	0.67 ± 0.38	0.25	1.27
AVBN.14-24	0.98	0.35 ± 0.21	0.04	0.59
AVBN.13-23	0.98	0.55 ± 0.28	0.15	0.99

Euclidean Distances	ICC	Mean ± SD (mm)	Min. (mm)	Max. (mm)
Mandibular Teeth Pairings (Transverse)				
PULP.43-33	1.00	0.17 ± 0.12	0.05	0.43
PULP.46-36	0.97	0.23 ± 0.18	0.06	0.61
APEX.43-33	0.99	0.25 ± 0.19	0.02	0.64
APEX.46-36	0.99	0.26 ± 0.26	0.03	0.87
AVBN.43-33	0.97	0.51 ± 0.37	0.05	1.13
AVBN.46-36	0.92	0.68 ± 0.45	0.25	1.59

Appendix 12: Assessment of Accuracy for Dental Landmarks in the Vertical dimension.

Euclidean Distances	ICC	Mean ± SD (mm)	Min. (mm)	Max. (mm)
Maxillary Teeth to Crista Galli (CG)				
PULP.26-CG	1.00	0.41 ± 0.31	0.03	0.85
PULP.24-CG	0.99	0.73 ± 0.25	0.30	1.08
PULP.23-CG	0.99	0.74 ± 0.36	0.07	1.11
APEX.26-CG	0.99	0.40 ± 0.38	0.01	1.08
APEX.24-CG	1.00	0.28 ± 0.21	0.02	0.75
APEX.23-CG	0.99	0.66 ± 0.40	0.23	1.27
AVBN.26-CG	0.99	0.67 ± 0.37	0.07	1.17
AVBN.24-CG	0.99	0.57 ± 0.45	0.03	1.36
AVBN.23-CG	0.99	0.68 ± 0.47	0.04	1.43

Euclidean Distances	ICC	Mean ± SD (mm)	Min. (mm)	Max. (mm)
Mandibular Teeth to Crista Galli (CG)				
PULP.36-CG	0.99	0.71 ± 0.31	0.11	1.08
PULP.33-CG	0.99	0.69 ± 0.44	0.04	1.29
APEX.36-CG	1.00	0.46 ± 0.27	0.16	1.07
APEX.33-CG	1.00	0.59 ± 0.38	0.08	1.35
AVBN.33-CG	0.72	0.90 ± 0.71	0.09	2.21
AVBN.36-CG	1.00	0.46 ± 0.24	0.01	0.77

Appendix 13: Assessment of Accuracy for Dental Landmarks in the Antero-posterior dimension.

Euclidean Distances	ICC	Mean ± SD (mm)	Min. (mm)	Max. (mm)
Maxillary Teeth (Anterior-Posterior)				
PULP.26-24	0.97	0.22 ± 0.20	0.02	0.53
PULP.16-14	0.98	0.34 ± 0.11	0.19	0.51
PULP.24-23	0.94	0.24 ± 0.13	0.03	0.51
PULP.14-13	0.99	0.23 ± 0.22	0.01	0.75
APEX.26-24	0.94	0.54 ± 0.35	0.04	1.26
APEX.16-14	0.95	0.33 ± 0.51	0.01	1.62
APEX.24-23	0.94	0.34 ± 0.33	0.01	0.95
APEX.14-13	0.84	0.57 ± 0.49	0.04	1.41
AVBN.26-24	0.62	0.86 ± 0.78	0.09	2.39
AVBN.16-14	0.94	0.58 ± 0.30	0.11	1.19
AVBN.24-23	0.67	0.75 ± 0.70	0.04	2.28
AVBN.14-13	0.64	0.71 ± 0.42	0.07	1.34

Euclidean Distances	ICC	Mean ± SD (mm)	Min. (mm)	Max. (mm)
Mandibular Teeth (Anterior-Posterior)				
PULP.46-43	1.00	0.49 ± 0.50	0.01	1.75
PULP.36-33	0.90	0.50 ± 0.53	0.10	1.93
APEX.46-43	0.95	0.38 ± 0.39	0.04	1.37
APEX.36-33	0.99	0.22 ± 0.22	0.01	0.8
AVBN.46-43	0.96	0.38 ± 0.36	0.01	0.97
AVBN.36-33	0.91	0.59 ± 0.64	0.01	1.92

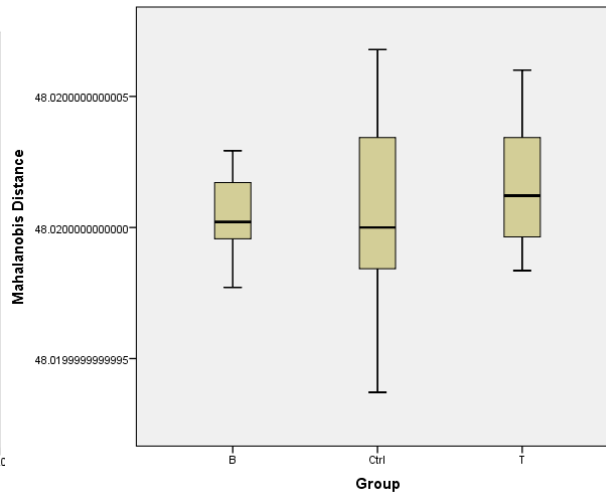
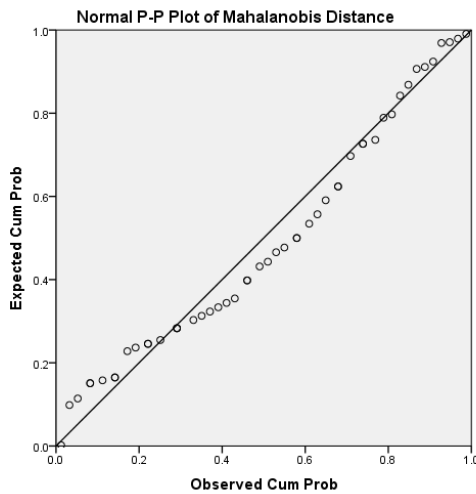
Appendix 14: Intra-class correlation coefficient (ICC), Mean differences & Standard deviation for Accuracy of the remaining Cranial Base Landmarks.

Crista Galli (CG) to Cranial Base		
Euclidean Distances	ICC	Mean difference \pm SD (mm)
Mid.EAM-CG	0.99	0.52 \pm 0.37
HYPO.R-CG	0.98	1.08 \pm 0.95
HYPO.L-CG	0.99	0.85 \pm 0.73
CG-MDFM	0.99	1.00 \pm 0.52

Foramen Magnum (MDFM) to Cranial Base		
Euclidean Distances	ICC	Mean difference \pm SD (mm)
Mid.AEM-MDFM	0.99	0.73 \pm 0.86
HYPO.R-MDFM	0.89	0.78 \pm 0.63
HYPO.L-MDFM	0.65	1.28 \pm 1.48

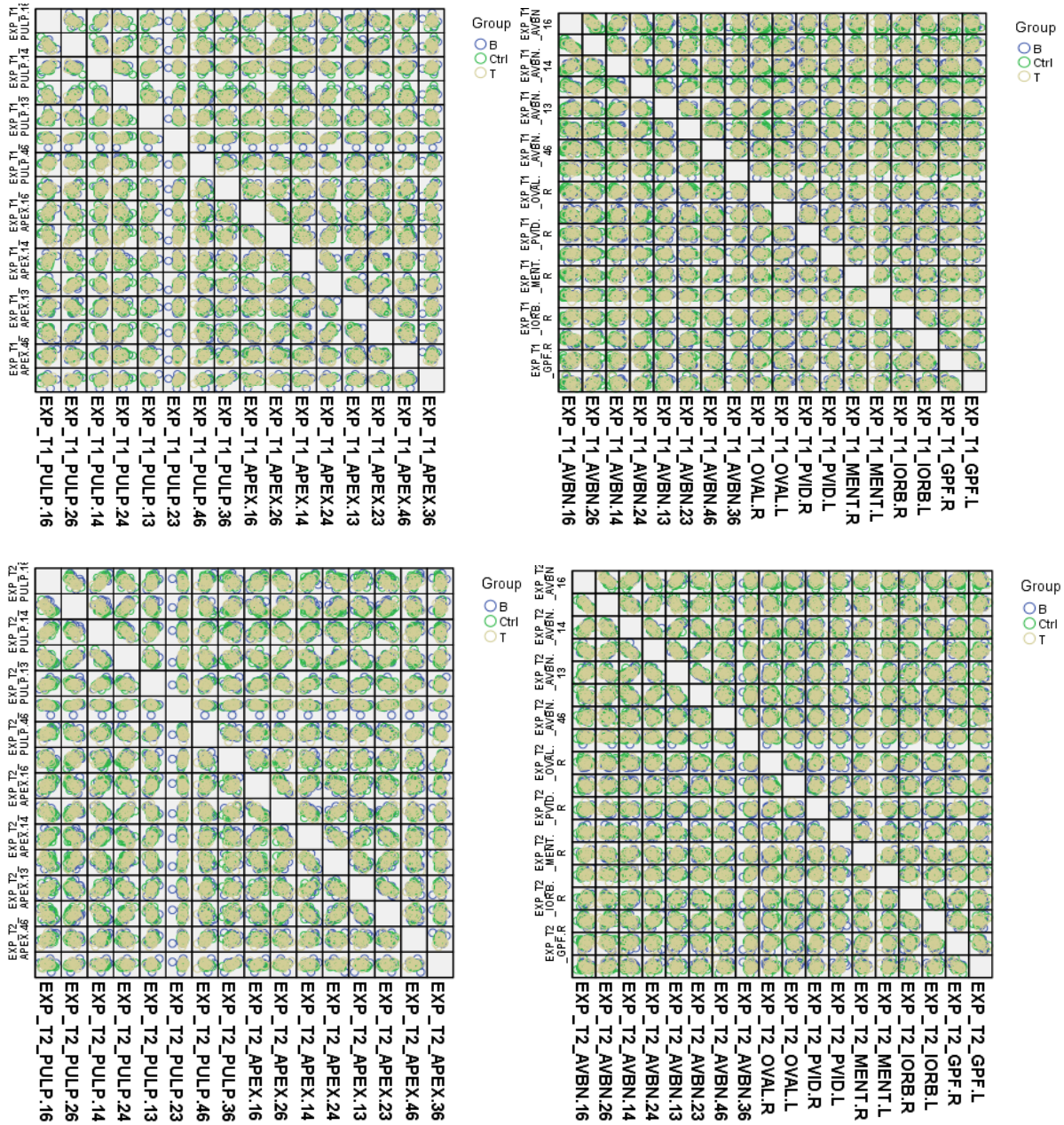
Appendix 15: A) P-P Plot (Left) and B) Box Plot (Right) Of the Mahalanobis Distance.

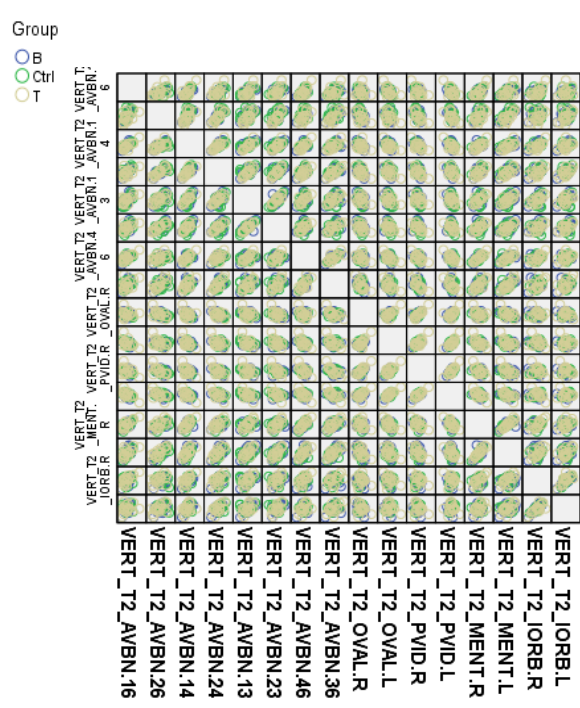
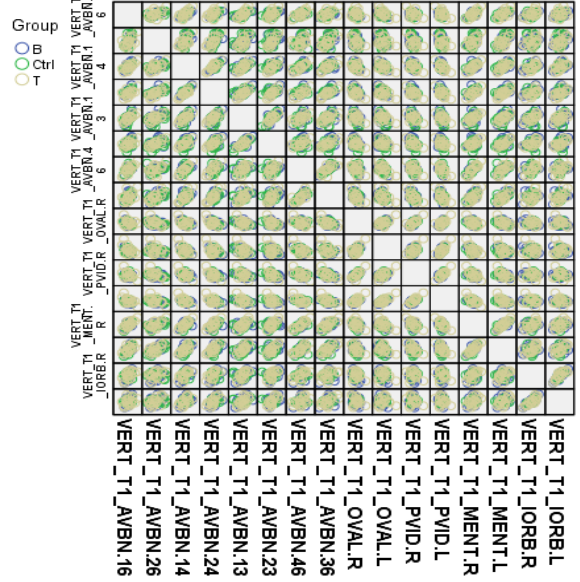
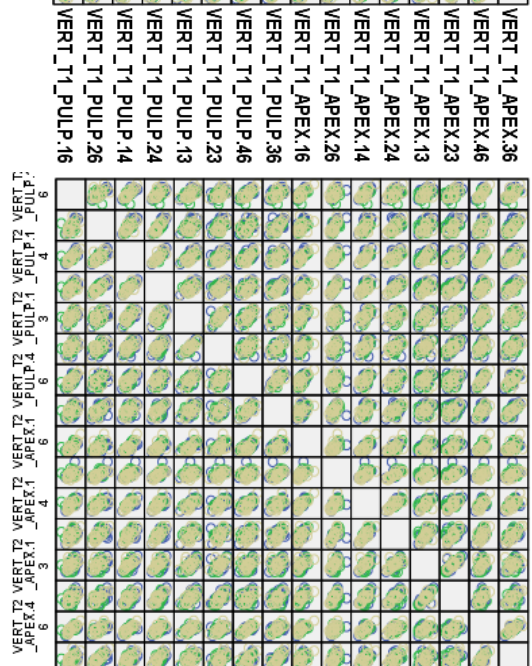
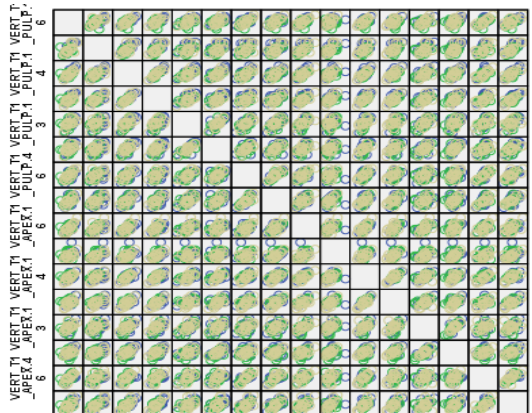
Multivariate outlier detection was performed using the Mahalanobis' distance.



Appendix 16: Bivariate Scatter Plots Of Measurements At T1 (Above) And T2 (Below).

A Maximum of 16 variables were included in each Scatter Plot, due to the limitation of SPSS in generating a readable table.

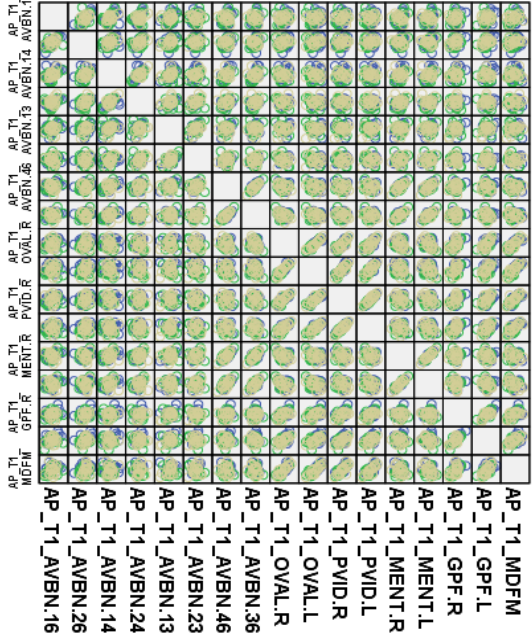




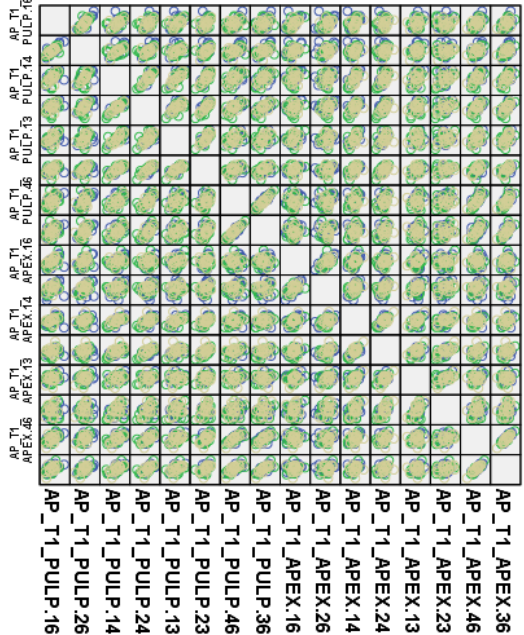
Group
 ● B
 ● Ctrl
 ● T

Group
 ● B
 ● Ctrl
 ● T

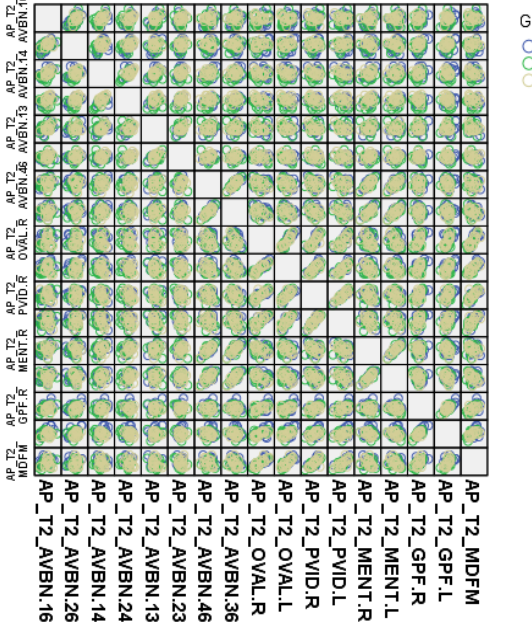
Group
 ● B
 ● Ctrl
 ● T



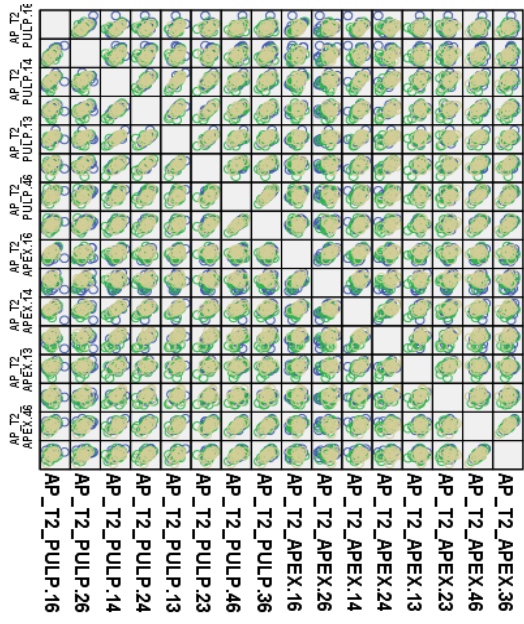
Group
 ● B
 ● Ctrl
 ● T



Group
 ● B
 ● Ctrl
 ● T



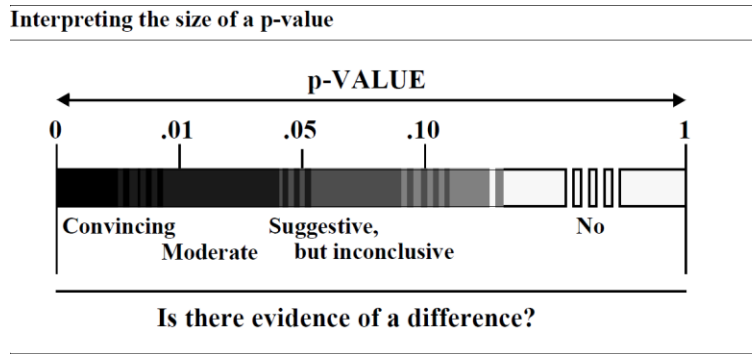
Group
 ● B
 ● Ctrl
 ● T



Appendix 17: Pearson Correlation For Age (Covariate) With T2-T1 Difference of Distances

Distance differences (T2-T1) indicated by Pearson correlation (*r*) was found to be < 0.5, for all dependent variables (for 468 distances). Age and Gender were not covariates.

Appendix 18: Interpretation of p-value



Appendix 19: Comparison of combined transverse changes (T2-T1), between all three groups.

T2-T1 Measure	Right-side - Left-side		Mean (mm)			Significance		
	Right-sided Landmarks	Left-sided Landmarks	B-RME	Ctrl	T-RME	B-RME vs. Ctrl	T-RME vs. Ctrl	T- vs. B-RME
IMW †	PULP.16	PULP.26	4.17	0.47	5.66	**	**	NS (TAD-side) ** (Imp-side)
IPW †	PULP.14	PULP.24	2.13	0.24	5.12	*	**	**
ICW †	PULP.13	PULP.23	1.19	0.56	2.44	NS	*	NS
IABW †	AVBN.16	AVBN.26	1.66	0.15	1.55	** (TAD-side) NS (Imp-side)	**	NS
GPFW †	GPF.R	GPF.L	1.79	0.48	1.75	** (TAD-side) NS (Imp-side)	**	NS
IORBW †	IORB.R	IORB.L	0.94	0.46	1.25	NS	NS	NS
IMENTW †	MENT.R	MENT.L	0.15	0.39	0.67	NS	NS	NS
ILW †	PULP.46	PULP.36	0.36	-0.08	0.60	NS	NS	NS

NS: not statistically significant, $p > 0.05$, *: statistically significant $p < 0.05$, **: statistically significant $p < 0.01$.

† **IMW**: Inter-upper-molar width (PULP. 16 to PULP.26); **IPW**: Inter-premolar width (PULP. 14 to PULP.24); **ICW**: Inter-canine width (PULP. 13 to PULP.23); **IABW**: Inter-Alveolar-Bone width (AVBN.16 to AVBN.26); **GPFW**: Inter-Greater-Palatine-Foramen width (GPF.R to GPF.L); **IORBW**: Inter-Infraorbital-Foramen width (IORB.R to IORB.L); **IMENTW**: Inter-Mental-Foramen width (MENT.R to MENT.L); **ILW**: Inter-lower-molar width (PULP. 46 to PULP.36); all relative to mid-sagittal plane.

Appendix 20: Percentage of Skeletal to Dental Change (T2-T1)

Percentage Change (T2-T1)	B-RME	Ctrl	T-RME
% Dental Expansion (IMW-GPFW-IABW) / IMW)	17.27%	-34.04%	41.70%
% Alveolar Bone Expansion (IABW / IMW)	39.81%	31.91%	27.39%
% Skeletal Expansion (GPFW / IMW)	42.93%	102.13%	30.92%
% Skeletal Expansion (IORBW / IMW)	22.54 %	97.87 %	22.08 %
Total Expansion (IMW+IABW+GPFW Expansion)	100.00%	100.00%	100.00%

† **GPFW**: Inter-Greater-Palatine-Foramen width (GPF.R to GPF.L); **IORBW**: Inter-Infraorbital-Foramen width (IORB.R to IORB.L); **IABW**: Inter-Alveolar-Bone width (AVBN.16 to AVBN.26); **IMW**: Inter-upper-molar width (PULP. 16 to PULP.26).

Appendix 21: Distribution of subjects by L-R difference > 1 mm relative to Mid-sagittal plane. Results were all not statistically significant (p=1.000).

Number of Symmetrical Cases across L-R Landmarks:	T1 (# of subjects)/(total subjects) (%)				T2-T1 change (# of subjects (%))		
	B-RME	Ctrl	T-RME	Total	B-RME	Ctrl	T-RME
Lower 6 crowns	5/17 (29%)	4/16 (25%)	8/17 (47%)	17/50 (24%)	+1 (+6%)	+1(+6%)	+1 (+10%)
Mental foramina	6/17 (35%)	3/16 (19%)	5/17 (29%)	14/50 (28%)	+2 (+12%)	+2 (+13%)	+3 (+18%)
Upper 6 crowns	5/17 (29%)	7/16 (44%)	9/17 (53%)	21/50 (42%)	+1 (+6%)	0 (+0%)	-1 (-6%)
Greater Palatine	7/16 (41%)	9/16 (56%)	11/17 (65%)	27/50 (68%)	+3 (+18%)	-1 (-6%)	+2 (+12%)
Upper 4 crowns	8/17 (47%)	5/16 (31%)	12/17 (71%)	25/50 (50%)	-1 (-6%)	+2 (+13%)	+2 (+12%)

Posterior Arch Symmetry

- No statistically significant differences (p=1.000) were found in any of the three groups at T1 or T2.

Appendix 22: Cranial Base Reference Landmark Changes (T2-T1)

Cranial base changes from T2-T1 (Appendix Tables: 22A, 22B, 22C, below), based on:

OVAL = Foramen Ovale

PVID = Posterior Vidian Canal

- During the 6 month observation period, mild of displacement of the reference landmark PVID was noted: ≤ 0.40 mm (transverse), ≤ 0.55 mm (antero-posterior), and ≤ 1.10 mm (vertical).
- During the 6 month observation period, mild of displacement of the reference landmark OVALE was noted: ≤ 0.40 mm (transverse and antero-posterior), and ≤ 0.55 mm and ≤ 0.70 mm in the vertical dimension respectively.
- This reflects statistically non-significant ($p>0.05$), amount of vertical growth, minimal transverse and antero-posterior cranial base growth changes during this 6 month observation period.

Appendix 22A: Between-Group Comparisons: Transverse treatment changes (T2-T1)

Variable	Group Mean \pm S.D. (in mm)			P-value for Group Differences		
	B-RME	Ctrl	T-RME	T-RME-B-RME	B-RME-Ctrl	T-RME-Ctrl
OVAL_R	-0.10 \pm 1.07	0.37 \pm 1.41	0.20 \pm 0.76	1.000	.680	1.000
OVAL_L	0.16 \pm 0.98	-0.18 \pm 1.22	0.08 \pm 0.73	1.000	.990	1.000
PVID_R	-0.05 \pm 0.90	0.37 \pm 0.93	0.01 \pm 1.07	1.000	.660	.870
PVID_L	0.20 \pm 0.93	-0.25 \pm 1.12	-0.02 \pm 1.10	1.000	.670	1.000

Appendix 22B: Between-Group Comparisons: Antero-posterior treatment changes (T2-T1)

Variable	Group Mean \pm S.D. (in mm)			P-value for Group Differences		
	B-RME	Ctrl	T-RME	T-RME-B-RME	B-RME-Ctrl	T-RME-Ctrl
OVAL_R	0.29 \pm 1.24	-0.13 \pm 1.57	0.37 \pm 1.63	1.000	1.000	1.000
OVAL_L	-0.14 \pm 1.31	-0.54 \pm 1.40	0.40 \pm 1.23	.710	1.000	.140
PVID_R	0.10 \pm 1.74	-0.33 \pm 2.25	0.44 \pm 1.26	1.000	1.000	.670
PVID_L	0.13 \pm 1.12	-0.46 \pm 1.29	0.07 \pm 1.25	1.000	.520	.650

Appendix 22C: Between-Group Comparisons: Vertical treatment changes (T2-T1)

Variable	Group Mean \pm S.D. (in mm)			P-value for Group Differences		
	B-RME	Ctrl	T-RME	T-RME-B-RME	B-RME-Ctrl	T-RME-Ctrl
OVAL_R	0.02 \pm 1.24	0.67 \pm 0.83	0.33 \pm 1.15	1.000	.250	1.000
OVAL_L	0.07 \pm 1.14	-0.32 \pm 1.32	0.27 \pm 1.19	1.000	1.000	.520
PVID_R	0.18 \pm 1.67	1.10 \pm 1.51	0.52 \pm 0.73	1.000	.180	.690
PVID_L	-0.36 \pm 1.39	-0.29 \pm 0.79	0.14 \pm 1.05	.590	1.000	.810

References

1. McNamara JA. Maxillary transverse deficiency. *American Journal of Orthodontics and Dentofacial Orthopedics* 2000;117:567-570.
2. Kutin G, Hawes RR. Posterior cross-bites in the deciduous and mixed dentitions. *American journal of orthodontics* 1969;56:491-504.
3. Thilander B, Myrberg N. The prevalence of malocclusion in Swedish schoolchildren. *European Journal of Oral Sciences* 1973;81:12-20.
4. Heikinheimo K, Salmi K, Myllärniemi S. Long term evaluation of orthodontic diagnoses made at the ages of 7 and 10 years. *The European Journal of Orthodontics* 1987;9:151-159.
5. Thilander B, Pena L, Infante C, Parada SS, de Mayorga C. Prevalence of malocclusion and orthodontic treatment need in children and adolescents in Bogota, Colombia. An epidemiological study related to different stages of dental development. *The European Journal of Orthodontics* 2001;23:153-168.
6. Keski-Nisula K, Lehto R, Lusa V, Keski-Nisula L, Varrela J. Occurrence of malocclusion and need of orthodontic treatment in early mixed dentition. *American Journal of Orthodontics and Dentofacial Orthopedics* 2003;124:631-638.
7. da Silva Filho OG, Santamaria Jr M, Filho LC. Epidemiology of posterior crossbite in the primary dentition. *Journal of Clinical Pediatric Dentistry* 2007;32:73-78.
8. Bishara SE, Staley RN. Maxillary expansion: clinical implications. *American Journal of Orthodontics and Dentofacial Orthopedics* 1987;91:3-14.
9. Lagravère MO, Heo G, Major PW, Flores-Mir C. Meta-analysis of immediate changes with rapid maxillary expansion treatment. *The Journal of the American Dental Association* 2006;137:44-53.
10. Bell RA. A review of maxillary expansion in relation to rate of expansion and patient's age. *American journal of orthodontics* 1982;81:32-37.
11. Kennedy DB, Osepchok M. Unilateral posterior crossbite with mandibular shift: a review. *Journal-Canadian Dental Association* 2005;71:569.
12. Haas AJ. Long-term posttreatment evaluation of rapid palatal expansion. *Angle Orthod* 1980;50:189-217.
13. Lagravere MO, Major PW, Flores-Mir C. Long-term dental arch changes after rapid maxillary expansion treatment: a systematic review. *The Angle orthodontist* 2005;75:155-161.
14. Lagravere MO, Major PW, Flores-Mir C. Long-term skeletal changes with rapid maxillary expansion: a systematic review. *The Angle orthodontist* 2005;75:1046-1052.
15. Sievers MM, Larson BE, Gaillard PR, Wey A. Asymmetry assessment using cone beam CT: A Class I and Class II patient comparison. *The Angle Orthodontist* 2011;82:410-417.
16. Sanders DA, Rigali PH, Neace WP, Uribe F, Nanda R. Skeletal and dental asymmetries in Class II subdivision malocclusions using cone-beam computed tomography. *American Journal of Orthodontics and Dentofacial Orthopedics* 2010;138:542. e541-542. e520.

17. Katsumata A, Fujishita M, Maeda M, Ariji Y, Ariji E, Langlais RP. 3D-CT evaluation of facial asymmetry. *Oral Surgery, Oral Medicine, Oral Pathology, Oral Radiology, and Endodontology* 2005;99:212-220.
18. Baek S-H, Cho I-S, Chang Y-I, Kim M-J. Skeletodental factors affecting chin point deviation in female patients with class III malocclusion and facial asymmetry: a three-dimensional analysis using computed tomography. *Oral Surgery, Oral Medicine, Oral Pathology, Oral Radiology, and Endodontology* 2007;104:628-639.
19. Jacobson A, RL J. *Radiographic Cephalometry: From Basics to 3-D Imaging*, (Book/CD-ROM set), Chapter 23. 2007.
20. Lagravère MO, Carey J, Toogood RW, Major PW. Three-dimensional accuracy of measurements made with software on cone-beam computed tomography images. *American Journal of Orthodontics and Dentofacial Orthopedics* 2008;134:112-116.
21. Scarfe WC, Farman AG, Sukovic P. Clinical applications of cone-beam computed tomography in dental practice. *Journal-Canadian Dental Association* 2006;72:75.
22. Yajima A, Otonari-Yamamoto M, Sano T, Hayakawa Y, Otonari T, Tanabe K et al. Cone-beam CT (CB Throne) applied to dentomaxillofacial region. *The Bulletin of Tokyo Dental College* 2006;47:133-141.
23. Mah JK, Huang JC, Choo H. Practical applications of cone-beam computed tomography in orthodontics. *The Journal of the American Dental Association* 2010;141:75-135.
24. Lagravère MO, Gordon JM, Guedes IH, Flores-Mir C, Carey JP, Heo G et al. Reliability of traditional cephalometric landmarks as seen in three-dimensional analysis in maxillary expansion treatments. *The Angle orthodontist* 2009;79:1047-1056.
25. de Moraes ME, Hollender LG, Chen CS, Moraes LC, Balducci I. Evaluating craniofacial asymmetry with digital cephalometric images and cone-beam computed tomography. *Am J Orthod Dentofacial Orthop* 2011;139:e523-531.
26. Lee K-M, Hwang H-S, Cho J-H. Comparison of transverse analysis between posteroanterior cephalogram and cone-beam computed tomography. *Angle Orthodontist* 2013;84:715-719.
27. Ghafari J, Cater PE, Shofer FS. Effect of film-object distance on posteroanterior cephalometric measurements: suggestions for standardized cephalometric methods. *American Journal of Orthodontics and Dentofacial Orthopedics* 1995;108:30-37.
28. Gateno J, Xia JJ, Teichgraber JF. Effect of facial asymmetry on 2-dimensional and 3-dimensional cephalometric measurements. *Journal of Oral and Maxillofacial Surgery* 2011;69:655-662.
29. Thiesen G, Gribel BF, Freitas MPM. Facial asymmetry: a current review. *Dental press journal of orthodontics* 2015;20:110-125.
30. Betts N, Vanarsdall R, Barber H, Higgins-Barber K, Fonseca R. Diagnosis and treatment of transverse maxillary deficiency. *The International journal of adult orthodontics and orthognathic surgery* 1994;10:75-96.
31. Chien P, Parks E, Eraso F, Hartsfield J, Roberts W, Ofner S. Comparison of reliability in anatomical landmark identification using two-dimensional digital cephalometrics and three-dimensional cone beam computed tomography in vivo. *Dentomaxillofacial Radiology* 2014.

32. Oz U, Orhan K, Abe N. Comparison of linear and angular measurements using two-dimensional conventional methods and three-dimensional cone beam CT images reconstructed from a volumetric rendering program in vivo. *Dentomaxillofac Radiol* 2011;40:492-500.
33. Lin L, Ahn H-W, Kim S-J, Moon S-C, Kim S-H, Nelson G. Tooth-borne vs bone-borne rapid maxillary expanders in late adolescence. *The Angle Orthodontist* 2014;85:253-262.
34. Lagravère MO, Carey J, Heo G, Toogood RW, Major PW. Transverse, vertical, and anteroposterior changes from bone-anchored maxillary expansion vs traditional rapid maxillary expansion: A randomized clinical trial. *American Journal of Orthodontics and Dentofacial Orthopedics* 2010;137:304.e301-304.e312.
35. Krebs A. Expansion of the midpalatal suture, studied by means of metallic implants. *Acta Odontologica Scandinavica* 1959;17:491-501.
36. Wehrbein H, Göllner P. Skeletal Anchorage in Orthodontics - Basics and Clinical Application. *Journal of Orofacial Orthopedics / Fortschritte der Kieferorthopädie* 2007;68:443-461.
37. Hansen L, Tausche E, Hietschold V, Hotan T, Lagravère M, Harzer W. Skeletally-anchored Rapid Maxillary Expansion using the Dresden Distractor. *Journal of Orofacial Orthopedics / Fortschritte der Kieferorthopädie* 2007;68:148-158.
38. Baydas B, Yavuz İ, Uslu H, Dagsuyu İM, Ceylan İ. Nonsurgical rapid maxillary expansion effects on craniofacial structures in young adult females: a bone scintigraphy study. *The Angle orthodontist* 2006;76:759-767.
39. Tausche E, Hansen L, Hietschold V, Lagravère MO, Harzer W. Three-dimensional evaluation of surgically assisted implant bone-borne rapid maxillary expansion: A pilot study. *American Journal of Orthodontics and Dentofacial Orthopedics* 2007;131:S92-S99.
40. Rakosi T, Graber T. *Orthodontic and Dentofacial Orthopedic Treatment*, Chapter 7 2009:155-176.
41. Hassan AH, AlGhamdi AT, Al-Fraidi AA, Al-Hubail A, Hajrassy MK. Unilateral cross bite treated by corticotomy-assisted expansion: two case reports. *Head & face medicine* 2010;6:1.
42. Hesse KL, Årtun J, Joondeph DR, Kennedy DB. Changes in condylar position and occlusion associated with maxillary expansion for correction of functional unilateral posterior crossbite. *American Journal of Orthodontics and Dentofacial Orthopedics* 1997;111:410-418.
43. Harrison JE, Ashby D. Orthodontic treatment for posterior crossbites. *The Cochrane Library* 2001.
44. Thilander B, Wahlund S, Lennartsson B. The effect of early interceptive treatment in children with posterior cross-bite. *The European Journal of Orthodontics* 1984;6:25-34.
45. Schröder U, Schröder I. Early treatment of unilateral posterior crossbite in children with bilaterally contracted maxillae. *The European Journal of Orthodontics* 1984;6:65-69.
46. O'Byrn BL, Sadowsky C, Schneider B, BeGole EA. An evaluation of mandibular asymmetry in adults with unilateral posterior crossbite. *American Journal of Orthodontics and Dentofacial Orthopedics* 1995;107:394-400.
47. Pirttiniemi P, Kantomaa T, Lahtela P. Relationship between craniofacial and condyle path asymmetry in unilateral cross-bite patients. *The European Journal of Orthodontics* 1990;12:408-413.

48. De Felipe NLO, Da Silveira AC, Viana G, Kusnoto B, Smith B, Evans CA. Relationship between rapid maxillary expansion and nasal cavity size and airway resistance: short-and long-term effects. *American Journal of Orthodontics and Dentofacial Orthopedics* 2008;134:370-382.
49. Rodrigues Ado P, Monini Ada C, Gandini LG, Jr., Santos-Pinto A. Rapid palatal expansion: a comparison of two appliances. *Braz Oral Res* 2012;26:242-248.
50. Myers DR, Barenie JT, Bell RA, Williamson EH. Condylar position in children with functional posterior crossbites: before and after crossbite correction. *Pediatr Dent* 1980;2:190-194.
51. Piancino MG, Talpone F, Dalmasso P, Debernardi C, Lewin A, Bracco P. Reverse-sequencing chewing patterns before and after treatment of children with a unilateral posterior crossbite. *The European Journal of Orthodontics* 2006;28:480-484.
52. Iodice G, Danzi G, Cimino R, Paduano S, Michelotti A. Association between posterior crossbite, skeletal, and muscle asymmetry: a systematic review. *The European Journal of Orthodontics* 2016:cjw003.
53. Ileri Z, Basciftci FA. Asymmetric rapid maxillary expansion in true unilateral crossbite malocclusion: A prospective controlled clinical study. *The Angle Orthodontist* 2015;85:245-252.
54. Baka ZM, Akin M, Ucar FI, Ileri Z. Cone-beam computed tomography evaluation of dentoskeletal changes after asymmetric rapid maxillary expansion. *American Journal of Orthodontics and Dentofacial Orthopedics* 2015;147:61-71.
55. Proffit W FH, Sarver D.,. *Contemporary orthodontics*. Mosby; 2013.
56. Davidovitch M, Efstathiou S, Sarne O, Vardimon AD. Skeletal and dental response to rapid maxillary expansion with 2-versus 4-band appliances. *American Journal of Orthodontics and Dentofacial Orthopedics* 2005;127:483-492.
57. Isaacson RJ, Wood JL, Ingram AH. Forces produced by rapid maxillary expansion: I. Design of the force measuring system. *The Angle Orthodontist* 1964;34:256-260.
58. Zimring JF, Isaacson RJ. Forces Produced By Rapid Maxillary Expansion. 3. Forces Present During Retention. *Angle Orthod* 1965;35:178-186.
59. Chaconas SJ, Caputo AA. Observation of orthopedic force distribution produced by maxillary orthodontic appliances. *Am J Orthod* 1982;82:492-501.
60. Garib DG, Henriques JFC, Janson G, de Freitas MR, Fernandes AY. Periodontal effects of rapid maxillary expansion with tooth-tissue-borne and tooth-borne expanders: a computed tomography evaluation. *American journal of orthodontics and dentofacial orthopedics* 2006;129:749-758.
61. Weissheimer A, de Menezes LM, Mezomo M, Dias DM, de Lima EMS, Rizzato SMD. Immediate effects of rapid maxillary expansion with Haas-type and hyrax-type expanders: a randomized clinical trial. *American Journal of Orthodontics and Dentofacial Orthopedics* 2011;140:366-376.
62. Garrett BJ, Caruso JM, Rungcharassaeng K, Farrage JR, Kim JS, Taylor GD. Skeletal effects to the maxilla after rapid maxillary expansion assessed with cone-beam computed

tomography. *American Journal of Orthodontics and Dentofacial Orthopedics* 2008;134:8.e1-8.e11.

63. Garib DG, Henriques JFC, Janson G, Freitas MR, Coelho RA. Rapid maxillary expansion-tooth tissue-borne versus tooth-borne expanders: a computed tomography evaluation of dentoskeletal effects. *The Angle orthodontist* 2005;75:548-557.

64. Bazargani F, Feldmann I, Bondemark L. Three-dimensional analysis of effects of rapid maxillary expansion on facial sutures and bones: a systematic review. *The Angle Orthodontist* 2013;83:1074-1082.

65. Langford S, Sims M. Root surface resorption, repair, and periodontal attachment following rapid maxillary expansion in man. *American journal of orthodontics* 1982;81:108-115.

66. Barber AF, Sims M. Rapid maxillary expansion and external root resorption in man: a scanning electron microscope study. *American journal of orthodontics* 1981;79:630-652.

67. Garib DG, Henriques JF, Janson G, de Freitas MR, Fernandes AY. Periodontal effects of rapid maxillary expansion with tooth-tissue-borne and tooth-borne expanders: a computed tomography evaluation. *Am J Orthod Dentofacial Orthop* 2006;129:749-758.

68. Ramieri GA, Spada MC, Austa M, Bianchi SD, Berrone S. Transverse maxillary distraction with a bone-anchored appliance: dento-periodontal effects and clinical and radiological results. *International Journal of Oral and Maxillofacial Surgery* 2005;34:357-363.

69. Parr JA, Garetto LP, Wohlford ME, Arbuckle GR, Roberts WE. Sutural expansion using rigidly integrated endosseous implants: an experimental study in rabbits. *The Angle orthodontist* 1997;67:283-290.

70. Shapiro P, Kokich V. Uses of implants in orthodontics. *Dental Clinics of North America* 1988;32:539-550.

71. Baccetti T, Franchi L, Cameron CG, McNamara Jr JA. Treatment timing for rapid maxillary expansion. *The Angle orthodontist* 2001;71:343-350.

72. Lee HK, Bayome M, Ahn CS, Kim S-H, Kim KB, Mo S-S et al. Stress distribution and displacement by different bone-borne palatal expanders with micro-implants: a three-dimensional finite-element analysis. *The European Journal of Orthodontics* 2012;cjs063.

73. MacGinnis M, Chu H, Youssef G, Wu KW, Machado AW, Moon W. The effects of micro-implant assisted rapid palatal expansion (MARPE) on the nasomaxillary complex—a finite element method (FEM) analysis. *Progress in orthodontics* 2014;15:1.

74. Zhou Y, Long H, Ye N, Xue J, Yang X, Liao L et al. The effectiveness of non-surgical maxillary expansion: a meta-analysis. *The European Journal of Orthodontics* 2013:cjt044.

75. Ferro F, Spinella P, Lama N. Transverse maxillary arch form and mandibular asymmetry in patients with posterior unilateral crossbite. *American Journal of Orthodontics and Dentofacial Orthopedics* 2011;140:828-838.

76. Marcotte MR. The use of the occlusogram in planning orthodontic treatment. *American journal of orthodontics* 1976;69:655-667.

77. Fiorelli G, Melsen B. The "3-D occlusogram" software. *Am J Orthod Dentofacial Orthop* 1999;116:363-368.

78. Canuto LFG, de Freitas MR, Janson G, de Freitas KMS, Martins PP. Influence of rapid palatal expansion on maxillary incisor alignment stability. *American Journal of Orthodontics and Dentofacial Orthopedics* 2010;137:164. e161-164. e166.
79. Moussa R, O'Reilly MT, Close JM. Long-term stability of rapid palatal expander treatment and edgewise mechanotherapy. *American Journal of Orthodontics and Dentofacial Orthopedics* 1995;108:478-488.
80. Alavi DG, BeGole EA, Schneider BJ. Facial and dental arch asymmetries in Class II subdivision malocclusion. *American Journal of Orthodontics and Dentofacial Orthopedics* 1988;93:38-46.
81. Mraiwa N, Jacobs R, Van Cleynenbreugel J, Sanderink G, Schutyser F, Suetens P et al. The nasopalatine canal revisited using 2D and 3D CT imaging. *Dentomaxillofac Radiol* 2004;33:396-402.
82. Grayson B, Cutting C, Bookstein FL, Kim H, McCarthy JG. The three-dimensional cephalogram: theory, techniques, and clinical application. *American Journal of Orthodontics and Dentofacial Orthopedics* 1988;94:327-337.
83. Swennen GR, Schutyser F, Barth E-L, De Groeve P, De Mey A. A new method of 3-D cephalometry Part I: the anatomic Cartesian 3-D reference system. *Journal of craniofacial surgery* 2006;17:314-325.
84. Kusayama M, Motohashi N, Kuroda T. Relationship between transverse dental anomalies and skeletal asymmetry. *American Journal of Orthodontics and Dentofacial Orthopedics* 2003;123:329-337.
85. Ricketts RM. Perspectives in the clinical application of cephalometrics: the first fifty years. *The Angle orthodontist* 1981;51:115-150.
86. Ludlow JB, Gubler M, Cevitanes L, Mol A. Precision of cephalometric landmark identification: cone-beam computed tomography vs conventional cephalometric views. *American Journal of Orthodontics and Dentofacial Orthopedics* 2009;136:312. e311-312. e310.
87. de Oliveira AEF, Cevitanes LHS, Phillips C, Motta A, Burke B, Tyndall D. Observer reliability of three-dimensional cephalometric landmark identification on cone-beam computerized tomography. *Oral Surgery, Oral Medicine, Oral Pathology, Oral Radiology, and Endodontology* 2009;107:256-265.
88. Mah J HD. Three-dimensional craniofacial imaging. *Am J Orthod Dentofacial Orthop* 2004;126:308-309.
89. Lagravere MO, Hansen L, Harzer W, Major PW. Plane orientation for standardization in 3-dimensional cephalometric analysis with computerized tomography imaging. *Am J Orthod Dentofacial Orthop* 2006;129:601-604.
90. Park S-H, Yu H-S, Kim K-D, Lee K-J, Baik H-S. A proposal for a new analysis of craniofacial morphology by 3-dimensional computed tomography. *American Journal of Orthodontics and Dentofacial Orthopedics* 2006;129:600.e623-600.e634.
91. Shibata M, Nawa H, Kise Y, Fuyamada M, Yoshida K, Katsumata A et al. Reproducibility of three-dimensional coordinate systems based on craniofacial landmarks. *The Angle Orthodontist* 2012;82:776-784.

92. Nelson SJ. Wheeler's dental anatomy, physiology and occlusion. Elsevier Health Sciences; 2014.
93. Hayashi K, Uechi J, Mizoguchi I. Three-Dimensional Analysis of Dental Casts Based on a Newly Defined Palatal Reference Plane. *The Angle Orthodontist* 2003;73:539-544.
94. Porto OCL, de Freitas JC, de Alencar A, Estrela C. The use of three-dimensional cephalometric references in dentoskeletal. *Dental Press J Orthod* 2014;19:78-85.
95. Lagravere MO, Major PW, Carey J. Sensitivity analysis for plane orientation in three-dimensional cephalometric analysis based on superimposition of serial cone beam computed tomography images. *Dentomaxillofac Radiol* 2010;39:400-408.
96. Naji P, Alsufyani NA, Lagravère MO. Reliability of anatomic structures as landmarks in three-dimensional cephalometric analysis using CBCT. *The Angle Orthodontist* 2013;84:762-772.
97. Lagravère MO, Gordon JM, Flores-Mir C, Carey J, Heo G, Major PW. Cranial base foramen location accuracy and reliability in cone-beam computerized tomography. *American Journal of Orthodontics and Dentofacial Orthopedics* 2011;139:e203-e210.
98. Arat ZM, Rübendüz M, Arman Akgül A. The displacement of craniofacial reference landmarks during puberty: a comparison of three superimposition methods. *The Angle orthodontist* 2003;73:374-380.
99. Trpkova B, Prasad NG, Lam EW, Raboud D, Glover KE, Major PW. Assessment of facial asymmetries from posteroanterior cephalograms: validity of reference lines. *American journal of orthodontics and dentofacial orthopedics* 2003;123:512-520.
100. Athanasiou AE. *Orthodontic cephalometry*. London ; Baltimore: : Mosby-Wolfe; 1995.
101. Major PW, Johnson DE, Hesse KL, Glover KE. Landmark identification error in posterior anterior cephalometrics. *The Angle orthodontist* 1994;64:447-454.
102. MIDTGÅRD J, BJÖRK G, Linder-Aronson S. Reproducibility of cephalometric landmarks and errors of measurements of cephalometric cranial distances. *The Angle orthodontist* 1974;44:56-61.
103. Jacobson A, RL J. *Radiographic Cephalometry: From Basics to 3-D Imaging*, (Book/CD-ROM set), Chapter 24; 2007: p. 293-299.
104. Baumrind S, Frantz RC. The reliability of head film measurements: 1. Landmark identification. *American journal of orthodontics* 1971;60:111-127.
105. Afrand M, Ling CP, Khosrotehrani S, Flores-Mir C, Lagravère-Vich MO. Anterior cranial-base time-related changes: A systematic review. *American Journal of Orthodontics and Dentofacial Orthopedics* 2014;146:21-32.e26.
106. Moss ML, Salentijn L. Differences between the functional matrices in anterior open-bite and in deep overbite. *American journal of orthodontics* 1971;60:264-280.
107. Keith A, Champion GG. A Contribution to the Mechanism of Growth of the Human Face. *International Journal of Orthodontia, Oral Surgery and Radiography* 1922;8:607-633.
108. Bidarkotimath S, Viveka S, Udyavar A. Vidian canal: radiological anatomy and functional correlations. *J Morpholl Sci* 2012;29:27-31.

109. Chen J, Xiao J. Morphological study of the pterygoid canal with high-resolution CT. *Int J Clin Exp Med* 2015;8:9484-9490.
110. Sayinsu K, Isik F, Traklyali G, Arun T. An evaluation of the errors in cephalometric measurements on scanned cephalometric images and conventional tracings. *Eur J Orthod* 2007;29:105-108.
111. Jacobson A, Jacobson RL. *Radiographic Cephalometry: From Basics to 3-D Imaging*, (Book/CD-ROM set) ,Chapter 7. 2007.
112. Gupta T. Localization of important facial foramina encountered in maxillo-facial surgery. *Clinical Anatomy* 2008;21:633-640.
113. Aggarwal A, Kaur H, Gupta T, Tubbs RS, Sahni D, Batra YK et al. Anatomical study of the infraorbital foramen: A basis for successful infraorbital nerve block. *Clin Anat* 2015;28:753-760.
114. Damstra J, Fourie Z, Slater JJH, Ren Y. Reliability and the smallest detectable difference of measurements on 3-dimensional cone-beam computed tomography images. *American journal of orthodontics and dentofacial orthopedics* 2011;140:e107-e114.
115. Weisstein EW. "Point-Plane Distance.". *MathWorld--A Wolfram Web Resource*. <http://mathworld.wolfram.com/Point-PlaneDistance.html>; 2016.
116. Portney L WM. *Foundations of clinical research: applications to practice.*: Prentice Hall, Upper Saddle River 2008.
117. Nagasaka S, Fujimura T, Segoshi K. Development of a non-radiographic cephalometric system. *Eur J Orthod* 2003;25:77-85.
118. Berge JK, Bergman RA. Variations in size and in symmetry of foramina of the human skull. *Clinical anatomy* 2001;14:406-413.
119. Marmary Y, Zilberman Y, Mirsky Y. Use of foramina spinosa to determine skull midlines. *The Angle Orthodontist* 1979;49:263-268.
120. Williamson PC, Major PW, Nebbe B, Glover KE, West K. Landmark identification error in submentovertex cephalometrics: a computerized method for determining the condylar long axis. *Oral Surgery, Oral Medicine, Oral Pathology, Oral Radiology, and Endodontology* 1998;86:360-369.
121. Madsen DP, Sampson WJ, Townsend GC. Craniofacial reference plane variation and natural head position. *The European Journal of Orthodontics* 2008;30:532-540.
122. Braun S, Hnat WP, Johnson BE. The curve of Spee revisited. *American journal of orthodontics and dentofacial orthopedics* 1996;110:206-210.
123. Damgaard C, Caspersen LM, Kjaer I. Maxillary sagittal growth evaluated on dry skulls from children and adolescents. *Acta Odontol Scand* 2011;69:274-278.
124. Sejrsen B, Jakobsen J, Kjær I. Human palatal growth evaluated on medieval crania using nerve canal openings as references. *American journal of physical anthropology* 1996;99:603-611.
125. Ikuta CRS, Cardoso CL, Ferreira-Júnior O, Lauris JRP, Souza PHC, Rubira-Bullen IRF. Position of the greater palatine foramen: an anatomical study through cone beam computed tomography images. *Surgical and Radiologic Anatomy* 2013;35:837-842.

126. Pinheiro-Neto CD, Fernandez-Miranda JC, Rivera-Serrano CM, Vaezi AE, Snyderman CH, Gardner PA. Endoscopic Anatomy of the Palatovaginal Canal (Palatosphenoidal Canal): A Landmark for Dissection of the Vidian Nerve during Endonasal Transpterygoid Approaches. *Skull Base* 2011;21:A045.
127. Mahboubi H, Wu EC, Jahanbakhshi R, Coale K, Rothholtz VS, Zardouz S et al. A novel method to determine standardized anatomic dimensions of the osseous external auditory canal. *Otol Neurotol* 2012;33:715-720.
128. Pancherz H, Gökbüget K. The reliability of the Frankfort horizontal in roentgenographic cephalometry. *The European Journal of Orthodontics* 1996;18:367-372.
129. Choi JW, Jung SY, Kim H-J, Lee S-H. Positional symmetry of porion and external auditory meatus in facial asymmetry. *Maxillofacial plastic and reconstructive surgery* 2015;37:1.
130. Periago DR, Scarfe WC, Moshiri M, Scheetz JP, Silveira AM, Farman AG. Linear accuracy and reliability of cone beam CT derived 3-dimensional images constructed using an orthodontic volumetric rendering program. *The Angle orthodontist* 2008;78:387-395.
131. Springate S. The effect of sample size and bias on the reliability of estimates of error: a comparative study of Dahlberg's formula. *The European Journal of Orthodontics* 2012;34:158-163.
132. Garib DG, Henriques JF, Carvalho PE, Gomes SC. Longitudinal effects of rapid maxillary expansion. *Angle Orthod* 2007;77:442-448.
133. Chang JY, McNamara JA, Jr., Herberger TA. A longitudinal study of skeletal side effects induced by rapid maxillary expansion. *Am J Orthod Dentofacial Orthop* 1997;112:330-337.
134. Brin I, Ben-Bassat Y, Blustein Y, Ehrlich J, Hochman N, Marmary Y et al. Skeletal and functional effects of treatment for unilateral posterior crossbite. *Am J Orthod Dentofacial Orthop* 1996;109:173-179.
135. Marshall SD, Southard KA, Southard TE. Early transverse treatment Seminars in Orthodontics: Elsevier; 2005: p. 130-139.